J. Physiol. (1952) 116, 424–448

MEASUREMENT OF CURRENT-VOLTAGE RELATIONS IN THE MEMBRANE OF THE GIANT AXON OF *LOLIGO*

BY A. L. HODGKIN, A. F. HUXLEY AND B. KATZ

From the Laboratory of the Marine Biological Association, Plymouth, and the Physiological Laboratory, University of Cambridge

(*Received* 24 *October* 1951)

The importance of ionic movements in excitable tissues has been emphasized by a number of recent experiments. On the one hand, there is the finding that the nervous impulse is associated with an inflow of sodium and an outflow of potassium (e.g. Rothenberg, 1950; Keynes & Lewis, 1951). On the other, there are experiments which show that the rate of rise and amplitude of the action potential are determined by the concentration of sodium in the external medium (e.g. Hodgkin & Katz, 1949*a*; Huxley & Stämpfli, 1951). Both groups of experiments are consistent with the theory that nervous conduction depends on a specific increase in permeability which allows sodium ions to move from the more concentrated solution outside a nerve fibre to the more dilute solution inside it. This movement of charge makes the inside of the fibre positive and provides a satisfactory explanation for the rising phase of the spike. Repolarization during the falling phase probably depends on an outflow of potassium ions and may be accelerated by a process which increases the potassium permeability after the action potential has reached its crest (Hodgkin, Huxley & Katz, 1949).

Outline of experiments

The general aim of this series of papers is to determine the laws which govern movements of ions during electrical activity. The experimental method was based on that of Cole (1949) and Marmont (1949), and consisted in measuring the flow of current through a definite area of the membrane of a giant axon from *Loligo*, when the membrane potential was kept uniform over this area and was changed in a stepwise manner by a feed-back amplifier. Two internal electrodes consisting of fine silver wires were thrust down the axis of the fibre for a distance of about 30 mm. One of these electrodes recorded the membrane potential, and the feed-back amplifier regulated the current entering the other electrode in such a way as to change the membrane potential suddenly and

hold it at the new level. Under these conditions it was found that the membrane current consisted of a nearly instantaneous surge of capacity current, associated with the sudden change of potential, and an ionic current during the period of maintained potential. The ionic current could be resolved into a transient component associated with movement of sodium ions, and a prolonged phase of 'potassium current'. Both currents varied with the permeability of the membrane to sodium or potassium and with the electrical and osmotic driving force. They could be distinguished by studying the effect of changing the concentration of sodium in the external medium.

The first paper of this series deals with the experimental method and with the behaviour of the membrane in a normal ionic environment. The second (Hodgkin & Huxley, 1952*a*) is concerned with the effect of changes in sodium concentration and with a resolution of the ionic current into sodium and potassium currents. Permeability to these ions may conveniently be expressed in units of ionic conductance. The third paper (Hodgkin & Huxley, 1952*b*) describes the effect of sudden changes in potential on the time course of the ionic conductances, while the fourth (Hodgkin & Huxley, 1952*c*) deals with the inactivation process which reduces sodium permeability during the falling phase of the spike. The fifth paper (Hodgkin & Huxley, 1952*d*) concludes the series and shows that the form and velocity of the action potential may be calculated from the results described previously.

A report of preliminary experiments of the type described here was given at the symposium on electrophysiology in Paris (Hodgkin *et al.* 1949).

Nomenclature

In this series of papers we shall regard the resting potential as a positive quantity and the action potential as a negative variation. V is used to denote displacements of the membrane potential from its resting value. Thus

$$V = E - E_r,$$

where E is the absolute value of the membrane potential and E_r is the absolute value of the resting potential, with signs taken in the sense outside potential minus inside potential. With this choice of signs it is logical to take $+I$ for inward current density through the membrane. These definitions make membrane current positive under an external anode and agree with the accepted use of the terms negative and positive after-potential. They conflict with the common practice of showing action potentials as an upward deflexion and are inconvenient in experiments in which an internal electrode measures potentials with respect to an external earth. Lower-case symbols (v_m) are employed when it is necessary to give potentials with respect to earth, but no confusion should arise since this usage is confined to the sections dealing with the experimental method.

Theory

Although the results described in this paper do not depend on any particular assumption about the electrical properties of the surface membrane, it may be helpful to begin by stating the theoretical assumption which determined the design and analysis of the experiments. This is that the membrane current may be divided into a capacity current which involves a change in ion density at the outer and inner surfaces of the membrane, and an ionic current which depends on the movement of charged particles through the membrane. Equation 1 applies to such a system, provided that the behaviour of the membrane capacity is reasonably close to that of a perfect condenser:

$$I = C_M \frac{\partial V}{\partial t} + I_i, \tag{1}$$

where I is the total current density through the membrane, I_i is the ionic current density, C_M is the membrane capacity per unit area, and t is time. In most of our experiments $\partial V/\partial t = 0$, so that the ionic current can be obtained directly from the experimental records. This is the most obvious reason for using electronic feed-back to keep the membrane potential constant. Other advantages will appear as the experimental results are described.

EXPERIMENTAL METHOD

The essential features of the electrode system are illustrated by Fig. 1. Two long silver wires, each 20 μ. in diameter, were thrust down the axis of a giant axon for a distance of 20–30 mm. The greater part of these wires was insulated but the terminal portions were exposed in the manner shown in Fig. 1. The axon was surrounded by a 'guard ring' system which contained the external electrodes. Current was applied between the current wire (*a*) and an earth (*e*), while the potential difference across the membrane could be recorded from the voltage wire (*b*) and an external electrode (*c*). The advantage of using two wires inside the nerve is that polarization of the current wire does not affect the potential recorded by the voltage wire. The current wire was exposed for a length which corresponded to the total height of the guard-system, while the voltage wire was exposed only for the height of the central channel. The guard system ensured that the current crossing the membrane between the partitions A_2 and A_3 flowed down the channel C. This component of the current was determined by recording the potential difference between the external electrodes *c* and *d*.

Internal electrode assembly

In practice it would be difficult to introduce two silver wires into an axon without using some form of support. Another requirement is that the electrode must be compact, since previous experience showed that axons do not survive well unless the width of an internal electrode is less than 150 μ. (Hodgkin & Huxley, 1945). After numerous trials the design shown in Fig. 4 was adopted. The first operation in making such an electrode was to push a length of the voltage wire through a 70 μ. glass capillary and twist it round the capillary in a spiral which started at the tip and proceeded toward the shank of the capillary. The spiral was wound by rotating the shank of the capillary in a small chuck attached to a long screw. During this process the free end of the wire was pulled taut by a weight while the capillary was supported, against the pull of the wire, by a fine glass hook. A second hook controlled the angle at which the wire left the capillary. When sufficient wire had been wound it was attached to the capillary by application of shellac solution,

cut close to the capillary and insulated with shellac in the appropriate regions (Fig. 4). The next operation was to wind on the current wire, starting from the shank and proceeding to the tip. Correct spacing of current and voltage wires was maintained by making small adjustments in the position of the second glass hook. When the current wire had been wound to the tip it was attached to the capillary, cut short and insulated as before. The whole operation was carried out under a binocular microscope. Shellac was applied as an alcoholic solution and was dried and hardened

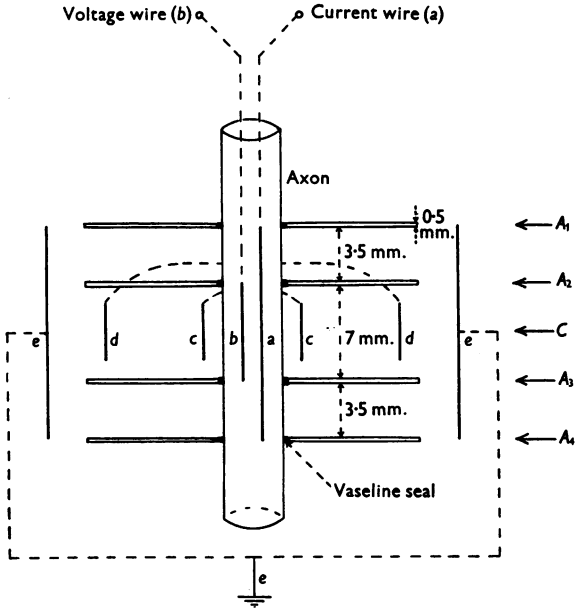

Fig. 1. Diagram illustrating arrangement of internal and external electrodes. A_1, A_2, A_3 and A_4 are Perspex partitions. *a*, *b*, *c*, *d* and *e* are electrodes. Insulated wires are shown by dotted lines. For sections through *A* and *C*, see Figs. 2 and 3.

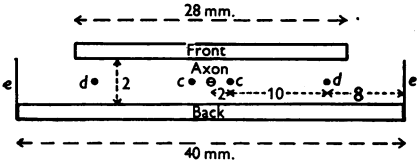

Fig. 2.

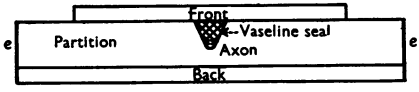

Fig. 3.

Fig. 2. Central channel of guard system. Section through *C*, Fig. 1. *c* and *d* are silver wires, *e* is a silver sheet. All dimensions are in mm.

Fig. 3. Partition of guard system. Section through A_1, A_2, A_3 or A_4, Fig. 1.

by baking for several hours under a lamp. Insulation between wires and across the shellac was tested so as to ensure that the film of shellac was complete and that the wires did not touch at any point. The exposed portion of the wires was then coated electrolytically with chloride. The electrode was first made an anode in order to deposit chloride and was then made a cathode in order to reduce some of the chloride and obtain a large surface of silver. This process was repeated a number of times ending with an application of current in the direction to deposit chloride. In this way an electrode of low polarization resistance was obtained.

In order to test the performance of the electrode it was immersed in salt solution and the current wire polarized by application of an electric current. In theory this should have caused no change in the potential difference between the voltage wire and the solution in which it was immersed. In practice we observed a very small change in potential which will be called 'mutual polarization'. Leakage between wires was a possible cause of this effect, but other explanations cannot be excluded.

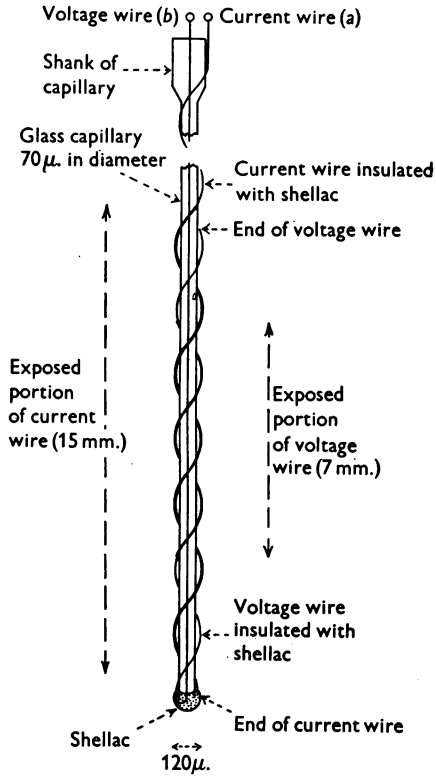

Fig. 4. Diagram of internal electrode (not to scale). The pitch of each spiral was 0·5 mm. The exposed portions of the wires are shown by heavy lines.

The general appearance of the electrode inside a giant axon is illustrated by Fig. 5. These photographs were obtained at an early stage of the investigation, and the axon was cleaned less carefully than in later experiments. The internal electrode differed from those finally employed in that both wires were wound from the shank of the electrode and that the pitch was somewhat greater.

Guard system

The general form of the guard system is shown in Figs. 1–3. It consisted of a flat box made out of Perspex which was divided into three compartments by two partitions A_2 and A_3 and closed with walls A_1 and A_4. The front of the box was removable and was made from a thin sheet of Perspex which could be sealed into position with vaseline. V-shaped notches were made in the two end walls and in the partitions. The partitions were greased and the notches filled with an oil-vaseline mixture in order to prevent leakage between compartments (Figs. 1 and 3). The guard ring assembly was mounted on a micromanipulator so that it could be manoeuvred into position after the electrode had been inserted. The outer electrode (*e*) was made from silver sheet while the

inner electrodes (*c*) and (*d*) were made from 0·5 mm. silver wire. Exposed portions of the electrodes were coated electrolytically with chloride and the wires connecting the electrodes with external terminals were insulated with shellac.

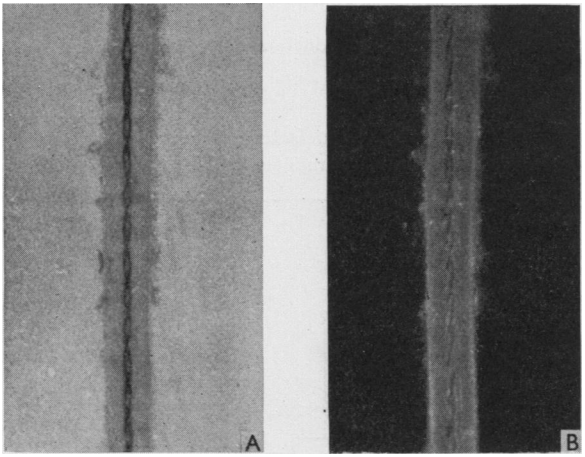

Fig. 5. Photomicrographs of giant axon and internal electrode. A, transmitted light; B, dark ground. The axon diameter was about 600 μ. The glass rod supporting the wires is not clearly seen.

Feed-back amplifier

A simplified diagram of the feed-back amplifier is shown in Fig. 6. It consisted of a differential d.c. amplifier with cathode follower input and output. The output of the amplifier was coupled to the input in such a way that negative feed-back was employed. This meant that any spontaneous change in membrane potential caused an output current to flow in a direction which restored the membrane potential to its original value. The level at which the potential was held constant was determined by the bias voltage v_3 and the control voltage v_4. v_3 was set so that no current passed through the nerve in the resting condition. This preliminary operation was carried out with the protective resistance R_f at its maximum value. This was important since an incorrect setting would otherwise have caused a large current to flow through the membrane. R_f was gradually reduced to zero; at the same time v_3 was adjusted to keep the membrane current zero. In order to change the membrane potential a rectangular pulse $\pm v_4$ was fed into the second stage of the amplifier. A large current then flowed into the membrane and changed its potential abruptly to a new level determined by

$$v_1 - v_2 = \beta v_4, \tag{2}$$

where v_1 and v_2 are the two input voltages and v_4 is the control voltage; β is a constant determined by resistance values and valve characteristics. Its value was of the order of 0·001. Any tendency to depart from Equation 2 was neutralized by a large output current which promptly restored the equilibrium condition defined by this relation.

In the majority of the experiments the slider of the potentiometer P was set to zero. Under these conditions the potential difference between the internal and external recording electrodes ($v_b - v_c$) was directly proportional to ($v_1 - v_2$). If α is the voltage gain of the cathode followers (about 0·9), then

$$v_b - v_c = \frac{2}{\alpha}(v_1 - v_2) = \frac{2\beta v_4}{\alpha}. \tag{3}$$

The performance of the feed-back amplifier was tested in each experiment by recording the time course of the potential difference between the internal and external electrodes. This showed that the recorded potential followed the control voltage with a time lag of about 1 μsec. and an

accuracy of 1–2%. It is therefore unnecessary to discuss the numerous approximations which have to be made in order to derive Equation 2.

The voltage gain of the feed-back amplifier and cathode followers was about 400 in the steady state. At high frequencies the gain was about 1200, since the condenser C_1 increased the gain under transient conditions. The mutual conductance of the feed-back system $\left[\frac{\partial i}{\partial (v_b - v_c)}\right]$ was about 1 mho in the steady state and 3 mhos at high frequencies. The maximum current that the amplifier could deliver was about 5 mA.

The method described would be entirely satisfactory if there were no resistance, apart from that of the membrane, between internal and external electrodes. In practice there was a small series

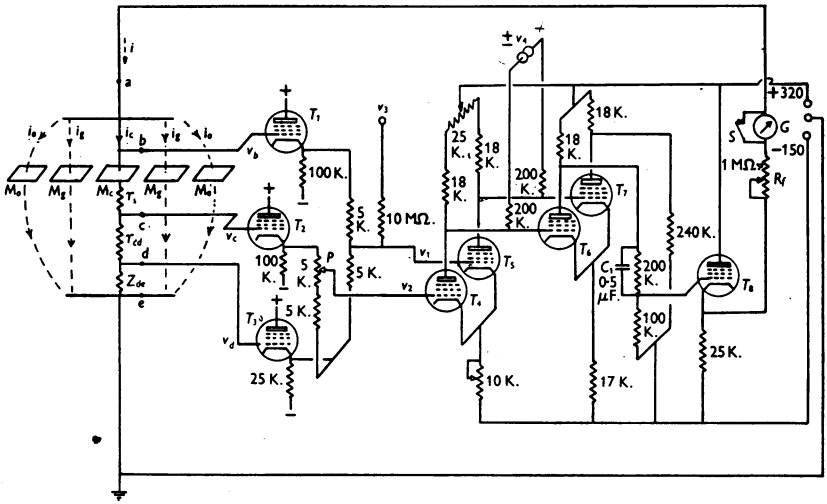

Fig. 6. Schematic diagram of feed-back amplifier. Screen resistances, grid stoppers and other minor circuit elements have been omitted. T_1, T_2, T_3 and T_8 are cathode followers; T_4, T_5, T_6 and T_7 are d.c. amplifiers. All valves were 6AK5 except T_1 and T_2 which were 1223. G is a microammeter used in setting-up. S is a switch for short-circuiting G. M_c is the membrane in the central section of the guard system. M_g, membrane in guard channels. M_o, membrane outside guard system. i_c, i_g and i_o are currents through these elements. r_{cd}, fluid-resistance used to measure current (74 Ω. at 20° C.). r_s, resistance in series with membrane (about 52 Ω. at 20° C.). z_{de}, impedance of large earthed electrode and sea water between d and e. Potentials are given with respect to earth.

resistance, represented by r_s in Fig. 6 and discussed further on p. 444. This meant that the true membrane potential was in error by the quantity $r_s i_c$. Thus

$$v_i - v_o = v_b - v_c - r_s i_c = 2\beta v_4/\alpha - r_s i_c, \tag{4}$$

where $v_i - v_o$ is the potential difference between the inner and outer surfaces of the membrane, r_s is the resistance in series with the membrane and i_c is the current flowing through the central area of membrane.

In principle the error introduced by r_s can be abolished by setting the potentiometer P to an appropriate value. All three cathode followers (T_1, T_2, T_3) had the same gain so that v_1 and v_2 were determined by the following equations:

$$v_1 = \tfrac{1}{2}\alpha\,(v_b + v_d), \tag{5}$$

$$v_2 = \tfrac{1}{2}\alpha\,[v_c + v_d + p\,(v_c - v_d)], \tag{6}$$

and

$$v_1 - v_2 = \tfrac{1}{2}\alpha\,[v_b - v_c - p\,(v_c - v_d)], \tag{7}$$

where p is proportional to the setting of the potentiometer P and varied between extremes of 0 and 1 and v_d is the potential of electrode d.

From Ohm's law

$$v_c - v_d = r_{cd} i_c, \tag{8}$$

where r_{cd} is the resistance of the central channel between electrodes c and d.

From Equations 4, 7 and 8

$$v_1 - v_2 = \tfrac{1}{2}\alpha\,[v_i - v_o + i_c\,(r_s - p r_{cd})]. \tag{9}$$

If $p = r_s/r_{cd}$

$$v_i - v_o = \frac{2}{\alpha}(v_1 - v_2) = \frac{2\beta v_4}{\alpha}. \tag{10}$$

The ratio r_s/r_{cd} was found to be about 0·7 and subsequent trials showed that a setting of $p = 0{\cdot}6$ could be used with safety. This procedure, which will be called compensated feed-back, was used successfully in seven of the later experiments. It had to be employed with considerable caution since a system of this type is liable to oscillate. Another difficulty is that if p is inadvertently made greater than r_s/r_{cd} the overall feed-back becomes positive and there is a strong probability that the membrane will be destroyed by the very large currents which the amplifier is capable of producing.

Auxiliary equipment

In addition to the feed-back amplifier we employed the following additional units: (1) A d.c. amplifier and cathode-ray oscillograph for recording membrane current and potential. (2) A voltage calibrator, with a built-in standard cell, giving ±110 mV. in steps of 1 mV. (3) A time calibrator consisting either of an electrically maintained 1 kcyc./sec. tuning fork, or a 4 kcyc./sec. fork with circuits to give pulses at 4, 2, 1 or 0·5 kcyc./sec. (4) Two units for producing rectangular pulses. These pulses were of variable amplitude (0–100 V.) and the circuits were arranged in such

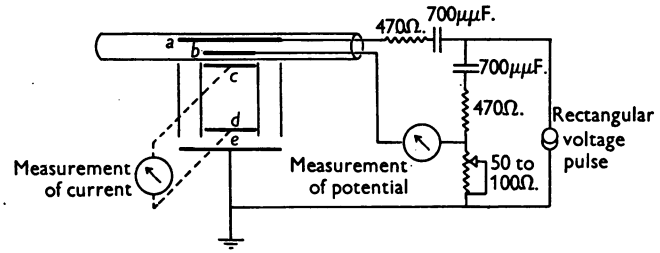

Fig. 7. Diagram of arrangement for recording response of membrane to short shock.

a way that the outputs of each generator were symmetrical with respect to earth. A single pulse generator was used in the early experiments, and its output was applied to the feed-back amplifier in the manner shown in Fig. 6. When required, the output of a second pulse generator was applied in parallel through a second pair of resistances. (5) An electrically operated refrigerator unit for cooling the preparation. All these items were of conventional design and need no detailed description.

Stimulation with brief currents

In the early stages of the work it was important to prove that the membrane was capable of giving an action potential of normal size. For this purpose we disconnected the feed-back amplifier and employed the arrangement shown in Fig. 7. A rectangular voltage step v_4 was applied to one internal electrode through a 700 μμF. condenser. The total area of membrane exposed to current flow from the electrode was about 0·3 cm.^{2} (1·5 cm. × π × 0·06 cm.). It therefore had a capacity of about 0·3 μF. When v_4 was suddenly changed by 10 V. the membrane potential was displaced by about 23 mV. (10 V. × 700/300,000). With this arrangement the membrane current consisted of very brief currents at the beginning and end of the voltage step. The size of the current could be varied by altering the size of the step, while the membrane current in the central channel of the guard-system could be measured by recording the potential difference

between electrodes *c* and *d*. The potential difference between the voltage wire (*b*) and the external electrode (*c*) was equal to the sum of the membrane potential and the potential difference across the ohmic resistance in series with the membrane. The second component was eliminated by the bridge circuit illustrated in Fig. 7.

Experimental procedure

Giant axons with a diameter of 400–800 μ. were obtained from the hindmost stellar nerve of *Loligo forbesi* and freed from all adherent tissue. Careful cleaning was important since the guard system did not operate satisfactorily if the axon was left with small nerve fibres attached to it. A further advantage in using cleaned axons was that the time required for equilibration in a test solution was greatly reduced by removing adherent tissue.

The axon was cannulated and mounted in the same type of cell as that described by Hodgkin & Huxley (1945) and Hodgkin & Katz (1949*a*). A conventional type of internal electrode, consisting of a long glass capillary, was thrust down the axon for a distance of 25–30 mm. This was then removed and the double wire electrode inserted in its place. Action potentials and resting potentials were recorded from the first electrode and the axon was rejected if these were not reasonably uniform over a distance of 20 mm. Another reason for starting with a conventional type of electrode was that the double wire electrode, in spite of the rigidity of its glass support, could not be inserted without buckling unless the axon had first been drilled with the glass capillary.

When the wire electrode was in position the guard system was brought into place by means of a micromanipulator. This operation was observed through a binocular microscope and care was taken to ensure that the central channel coincided exactly with the exposed portion of the internal voltage wire. The front of the guard-ring box was gently pressed into position and finally sealed by firm pressure with a pair of forceps. Before applying the front, spots of a vaseline-oil mixture were placed in such a position that they completed the seal round the axon when the front was pressed home (Figs. 1 and 3).

After the axon was sealed into position cold sea water (3–11° C.) was run into the cell and this temperature was maintained by means of a cooling coil which dipped into the cell. Air was bubbled through the cell in order to stir the contents and obtain a uniform temperature.

Before proceeding to study the behaviour of the axon under conditions of constant voltage its response to a short shock was observed. The experiment was discontinued if the action potential recorded in this way was less than about 85 mV. If the axon passed this test it was connected to the feed-back amplifier in the manner described previously.

Solutions were changed by running all the fluid from the cell and removing it from the guard-ring assembly with the aid of a curved capillary attached to a suction pump. A new solution was then run into the cell and was drawn into the guard rings by applying suction at appropriate places.

Calibration

The amplifier was calibrated at the end of each experiment, and all photographic records were analysed by projecting them on to a calibration grid. The readings obtained in this way were converted into current by dividing the potential difference between the two external electrodes *c* and *d* by the resistance between these electrodes (r_{cd}). This resistance was determined by blocking up the outer compartments of the guard-ring assembly and filling the central channel with sea water or with one of the standard test fluids. A silver wire was coated with silver chloride and inserted into the position normally occupied by the axon (Fig. 1). A known current was applied between the central wire and the outer electrode (*e*). The resistance between the two external electrodes *c* and *d* could then be obtained by measuring the change in potential difference resulting from a given application of current. It was found that the resistance between these electrodes was 74 Ω. when the central chamber was filled with sea water at 20° C. This value was close to that calculated from the dimensions of the system.

Membrane currents were converted to current densities by dividing them by the area of membrane exposed to current flow in the central compartment. The area was calculated from the measured axon diameter and the distance between the partitions A_2 and A_3 (Fig. 1).

RESULTS

Stimulation with brief currents

Before investigating the effect of a constant voltage it was important to establish that the membranes studied were capable of giving normal action potentials. This was done by applying a brief shock to one internal electrode and recording changes in membrane potential with the other. Details of the method are given on p. 431; typical results are shown in Fig. 8 (23° C.) and Fig. 9 (6° C.).

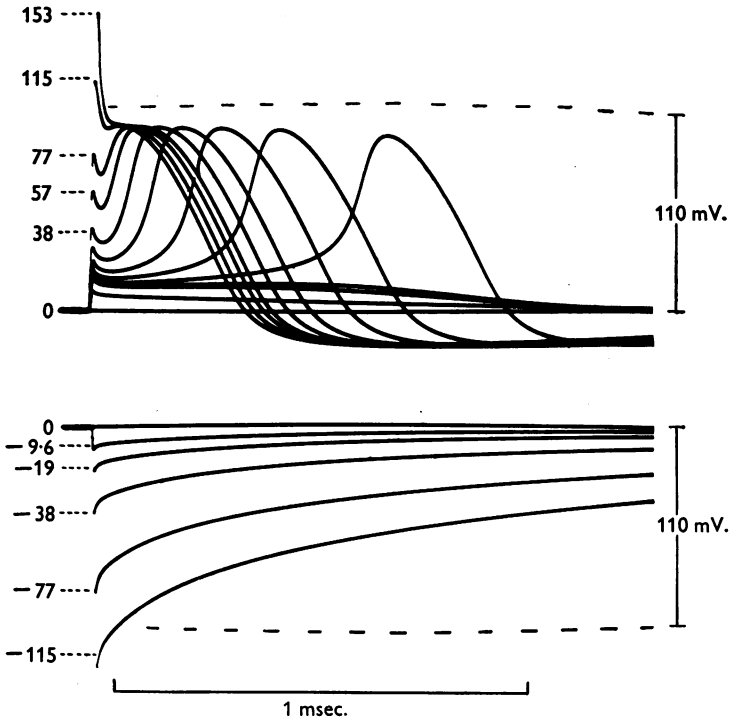

Fig. 8. Time course of membrane potential following a short shock at 23° C. Depolarizations shown upwards. Axon 18. The numbers attached to the curves give the strength of shock in mμcoulomb/cm.². Shock strengths for unlabelled curves are 29, 23, 19·2, 17·3, 16·7, 15·3, 9·6.

The shock used to displace the membrane potential was calibrated by recording the membrane current in the central channel (Fig. 7). This test showed that the current pulse consisted of a brief surge which was 95% complete in about 8 μsec. and reached a peak amplitude of about 50 mA./cm.² at the highest strengths. The total quantity of current passing through the central channel was evaluated by integrating the current record and was used to define the strength of the shock. The numbers attached to the records in Figs. 8 and 9 give the charge applied per unit area in mμcoulomb/cm.². It

will be seen that the initial displacement of membrane potential was proportional to the charge applied and that it corresponded to a membrane capacity of about 0·9 μF./cm.^{2}. Values obtained by this method are given in Table 1.

Although the initial charging process was linear, the subsequent behaviour of the membrane potential varied with the strength of shock in a characteristic

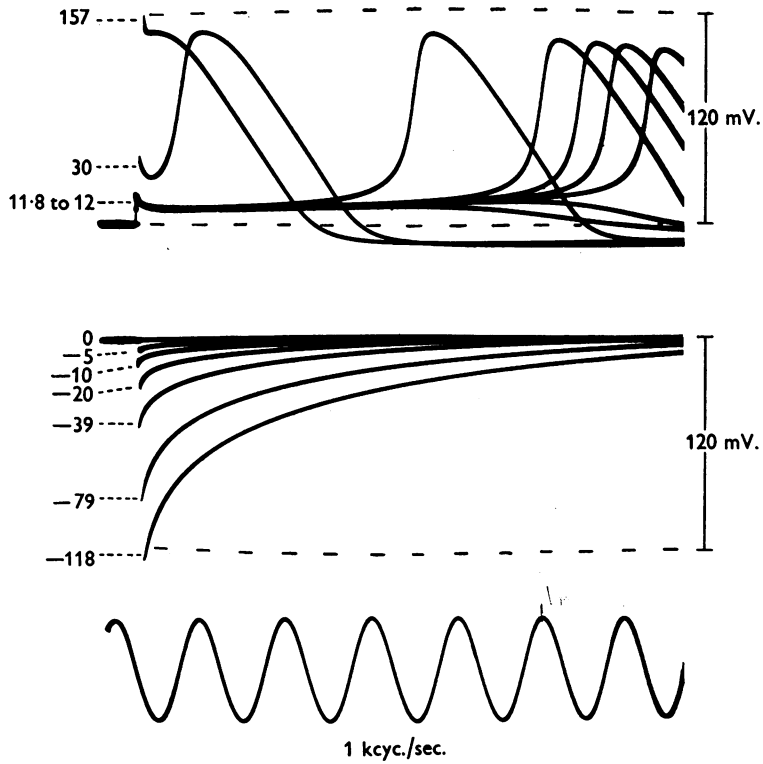

Fig. 9. Time course of membrane potential following a short shock at 6° C. Depolarization shown upwards. Axon 17. The numbers attached to the curves give the strength of shock in mμcoulomb/cm.^{2}. The initial displacement in the case of the uppermost curve cannot be seen; its value was about 200 mV.

manner. All the anodal records had the same general shape, but depolarizations of more than a few millivolts gave non-linear responses. If the depolarization was more than 15 mV. (Fig. 8) or 12 mV. (Fig. 9) the response became regenerative and produced an action potential of about 100 mV. If it was less than 12 or 15 mV. it was followed by a subthreshold response similar to that seen in most excitable tissues. If the potential was displaced to the threshold level it might remain in a state of unstable equilibrium for considerable periods of time. This is illustrated by Fig. 9 which shows the effect of a small variation of shock strength in the region of threshold.

Records such as those in Fig. 9 may be used to estimate the relation between membrane potential and ionic current. The total membrane current density (I) is negligible at times greater than 200 μsec. after application of the short

TABLE 1. Membrane capacities

Axon no.	Diameter (μ.)	Temperature (° C.)	Change in potential (mV.)	Membrane capacity (μF./cm.^{2}) Anodic	Cathodic	R_s (Ω.cm.^{2})	r_s (Ω.)	r_s/r_{cd}
			A. Voltage clamp					
13	520	9	+36 – 36	0·76	0·83	8·2	72	0·77
			+56 – 56	0·83	0·90			
			+98 – 98	0·83	0·96			
14	430	9	+36 – 34	0·81	0·83	5·8	61	0·65
17	588	7	+31 – 32	0·72	0·76	8·3	64	0·65
18	605	21	+30 – 31	0·92	0·91	5·5	41	0·57
19	515	8	+43 – 45	0·93	0·90	7·8	69	0·73
20	545	6	+42 – 43	0·88	0·86	9·1	76	0·77
21	533	9	+42 – 44	0·98	1·01	9·1	78	0·84
22	542	23	+40 – 41	1·01	1·03	4·0	34	0·50
25	603	8	+39 – 41	0·88	0·86	7·0	53	0·57
25*	603	7	+39 – 41	0·84*	0·82*	8·8*	66*	0·55*
26	675	20	+40 – 42	0·97	0·93	7·7	52	0·70
Average	—	—	—	0·88	0·90	7·3	60	0·68
				0·89				
			B. Short shock					
13	520	9	+58 – 50	1·07	1·11	—	—	—
17†	588	6	—	0·79†	0·74†	—	—	—
18†	605	23	—	0·85†	0·88†	—	—	—
Average	—	—	—	0·90	0·91	—	—	—
				0·91				
			C. Constant current					
29	540	21	—	—	1·49	6·4	42	0·57
41	585	4	—	—	0·78	11·9	92	0·88
Average	—	—	—	—	1·13	9·2	67	0·73
				1·13				
Average by all methods	—	—	—	0·91		7·6	61	0·68

* In this experiment choline was substituted for sodium in the external solution. The values obtained are excluded from the averages.

† In these experiments the shock strength was not measured directly but was obtained from the calibration for axon 13. The values for C_M are means obtained from a wide range of shock strengths.

shock. This means that the ionic current density (I_i) must be equal to the product of the membrane capacity per unit area (C_M) and the rate of depolarization. Thus if $I=0$, Equation 1 becomes

$$I_i = -C_M \frac{\partial V}{\partial t}. \tag{11}$$

Fig. 10 illustrates the relation between membrane potential and ionic current at a fixed time (290 μsec.) after application of the stimulus. It shows that

ionic current and membrane potential are related by a continuous curve which crosses the zero current axis at $V=0$, $V=-12$ mV. and $V=-110$ mV. Ionic current is inward over the regions -110 mV. $< V < -12$ mV. and $V>0$, and is outward for $V<-110$ mV. and -12 mV. $< V < 0$. $\partial I_i/\partial V$ is negative for -76 mV. $< V < -6$ mV. and is positive elsewhere.

A curve of this type can be used to describe most of the initial effects seen in Figs. 8 and 9. When the membrane potential is increased by anodal shocks the ionic current associated with the change in potential is in the inward direction. This means that the original membrane potential must be restored by an inward transfer of positive charge through the membrane. If the

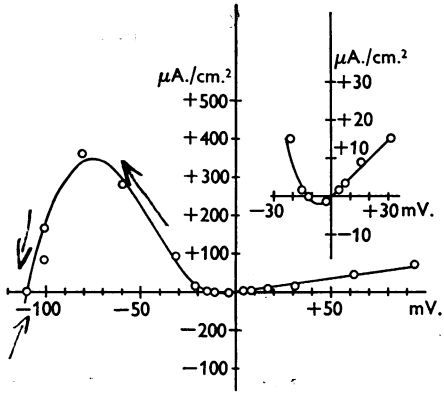

Fig. 10. Relation between ionic current density (I_i) and displacement of membrane potential (V). Abscissa: displacement of membrane potential from its resting value (anodal displacement shown positive). Ordinate: ionic current density obtained from $-C_M \frac{dV}{dt}$ (inward current shown positive). Inset: curve in region of origin drawn with tenfold increase in vertical scale. Axon 17; $C_M = 0{\cdot}74\,\mu$F./cm.^{2}; temperature 6·3° C. Measurements made 0·29 msec. after application of shock.

membrane potential is depolarized by less than 12 mV., ionic current is outward and again restores the resting condition by repolarizing the membrane capacity. At $V=-12$ mV., I_i is zero so that the membrane potential can remain in a state of unstable equilibrium. Between $V=-110$ mV. and $V=-12$ mV., I_i is inward so that the membrane continues to depolarize until it reaches $V=-110$ mV. If the initial depolarization is greater than 110 mV. I_i is outward which means that it will repolarize the membrane towards $V=-110$ mV. These effects are clearly seen in Figs. 8 and 9.

Membrane current under conditions of controlled potential

General description

The behaviour of the membrane under a 'voltage clamp' is illustrated by the pair of records in Fig. 11. These show the membrane current which flowed as a result of a sudden displacement of the potential from its resting value to

a new level at which it was held constant by electronic feed-back. In the upper record the membrane potential was increased by 65 mV.; in the lower record it was decreased by the same amount. The amplification was the same in both cases.

The first event in both records is a slight gap, caused by the surge of 'capacity current' which flowed when the membrane potential was altered suddenly. The surge was too rapid to be visible on these records, but was examined in other experiments in which low gain and high time base speed were employed (see p. 442). The ionic current during the period of constant potential was small when the membrane potential was displaced in the anodal direction, and is barely visible with the amplification used in Fig. 11. The top record in Fig. 12 gives the same current at higher amplification and shows

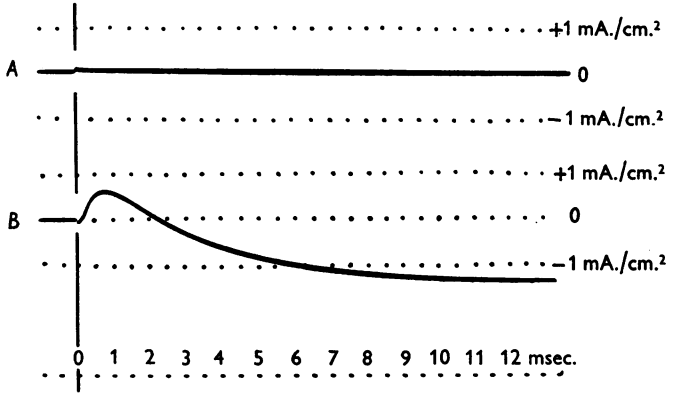

Fig. 11. Records of membrane current under a voltage clamp. At zero time the membrane potential was increased by 65 mV. (record *A*) or decreased by 65 mV. (record *B*); this level was then maintained constant throughout the record. Inward current is shown as an upward deflexion. Axon 41; diameter 585 μ. Temperature 3·8° C. Compensated feed-back.

that an increase of 65 mV. in the membrane potential was associated with an inward ionic current of about 30 μA./cm.^{2} which did not vary markedly with time. The sequence of events was entirely different when the membrane potential was reduced by 65 mV. (Fig. 11*B*). In this case the current changed sign during the course of the record and reached maximum amplitudes of +600 and −1300 μA./cm.^{2}. The initial phase of ionic current was inward and was therefore in the opposite direction to that expected in a stable system. If it had not been drawn off by the feed-back amplifier it would have continued to depolarize the membrane at a rate given by Equation 11. In this experiment C_M was 0·8 μF./cm.^{2} and I_i had a maximum value of 600 μA./cm.^{2}. The rate of depolarization in the absence of feed-back would therefore have been 750 V./sec., which is of the same general order as the maximum rate of rise of the spike (Hodgkin & Katz, 1949*a*, *b*). The phase of inward current was not maintained but changed fairly rapidly into a prolonged period of outward

current. In the absence of feed-back this current would have repolarized the membrane at a rate substantially greater than that observed during the falling phase of the spike. The outward current appeared to be maintained for an indefinite period if the membrane was not depolarized by more than 30 mV. With greater depolarization it declined slowly as a result of a polarization effect discussed on p. 445.

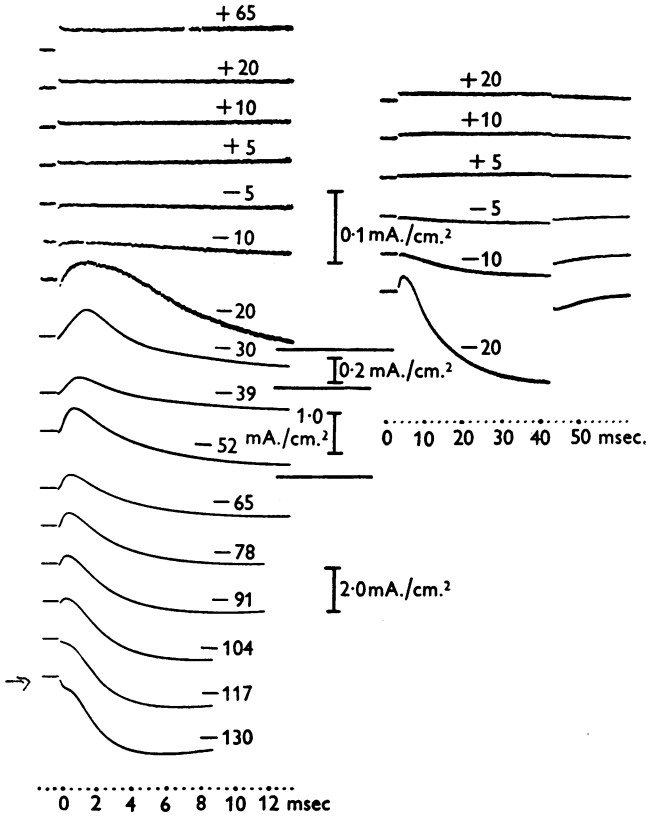

Fig. 12. Records of membrane current under a voltage clamp. The displacement of membrane potential (V) is given in millivolts by the number attached to each record. Inward current is shown as an upward deflexion. Six records at a lower time base speed are given in the right-hand column. Experimental details as in Fig. 11.

The features illustrated in Fig. 11 B were found over a wide range of voltages as may be seen from the complete family of curves in Fig. 12. An initial phase of inward current was conspicuous with depolarizations of 20–100 mV., while the delayed rise in outward current was present in all cathodal records. A convenient way of examining these curves is to plot ionic current density against membrane potential. This has been done in Fig. 13, in which the abscissa gives the displacement of membrane potential and the ordinate gives

the ionic current density at a short time (curve *A*) and in the 'steady state' (curve *B*). It will be seen that there is a continuous relation over the whole range, but that small changes in membrane potential are associated with large changes in current. At short times the relation between ionic current density

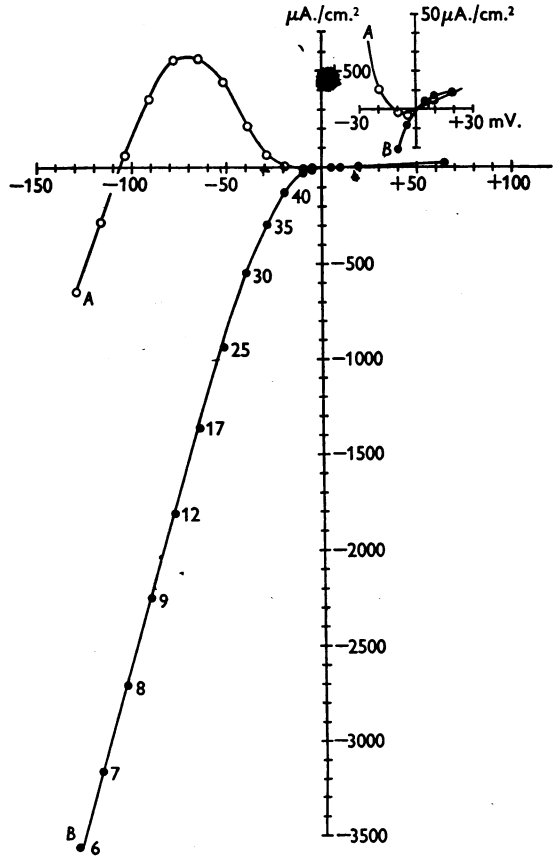

Fig. 13. Relation between membrane current density and membrane potential. Abscissa: displacement of membrane potential from its resting value in mV. Ordinate: membrane current density at 0·63 msec. after beginning of voltage step (curve *A*) and in 'steady state' (curve *B*). The numbers attached to curve *B* indicate the times in msec. at which the measurements were made. Inset: curves in region of origin drawn with a tenfold increase in the vertical scale. Inward current density is taken as positive and the membrane potential is given in the sense external potential minus the internal potential. Measurements were made from the records reproduced in Fig. 12 (3·8° C.).

and membrane potential is qualitatively similar to that obtained indirectly in Fig. 10. Ionic current is inward over the region -106 mV. $< V < -12$ mV. and for $V > 0$; it is outward for $V < -106$ mV. and for -12 mV. $< V < 0$. $\partial I_i/\partial V$ is negative for -70 mV. $< V < -7$ mV. and is positive elsewhere. More

quantitative comparisons are invalidated by the fact that the ionic current is a function of time as well as of membrane potential. At long times depolarization is invariably associated with an outward current and $\partial I_i/\partial V$ is always positive.

The electrical resistance of the membrane varied markedly with membrane potential. In Fig. 13, $\partial V/\partial I_i$ is about 2500 Ω.cm.^{2} for $V > 30$ mV. For $V = -110$ mV. it is 35 Ω.cm.^{2} (curve *A*) or 30 Ω.cm.^{2} (curve *B*). At $V = 0$, $\partial V/\partial I_i$ is 2300 Ω.cm.^{2} at short times and 650 Ω.cm.^{2} in the steady state. These results are comparable with those obtained by other methods (Cole & Curtis, 1939; Cole & Hodgkin, 1939).

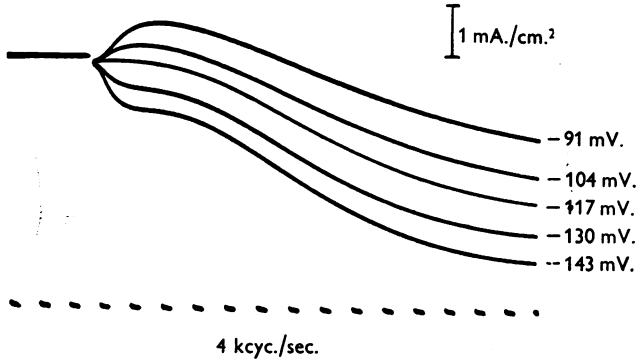

Fig. 14. Time course of membrane current during large depolarizations. Abscissa: time. Ordinate: inward current density. The numbers attached to the records give the displacement of membrane potential from its resting value. Axon 41; temperature 3·5° C. Compensated feed-back.

Fig. 14 illustrates the initial phase of ionic current at large depolarizations in greater detail. These records were obtained from the same axon as Fig. 12 but at an earlier stage of the experiment. They show that the initial 'hump' of ionic current changed sign at a potential of −117 mV. At −130 mV. the initial hump consists of outward current while it is plainly inward at −104 mV. The curve at −117 mV. satisfies the condition that $\partial I_i/\partial t = 0$ at short times and has no sign of the initial hump seen in the other records. It will be shown later that this potential probably corresponds to the equilibrium potential for sodium and that it varies with the concentration of sodium in the external medium (Hodgkin & Huxley, 1952*a*).

The effect of temperature

The influence of temperature on the ionic currents under a voltage clamp is illustrated by the records in Fig. 15. These were obtained from a pair of axons from the same squid. The first axon isolated was examined at 6° C. and gave the series of records shown in the left-hand column. About 5 hr. later the second axon, which had been kept at 5° C. in order to retard deterioration, was

examined in a similar manner at 22° C. Its physiological condition is likely to have been less normal than that of the first but the difference is not thought to be large since the two axons gave propagated action potentials of amplitude 107 and 103 mV. respectively, both measured at 22° C. The resting potentials were 55 mV. in both cases. The results obtained with the second axon are given in the right-hand column of Fig. 15. It will be seen that the general form and

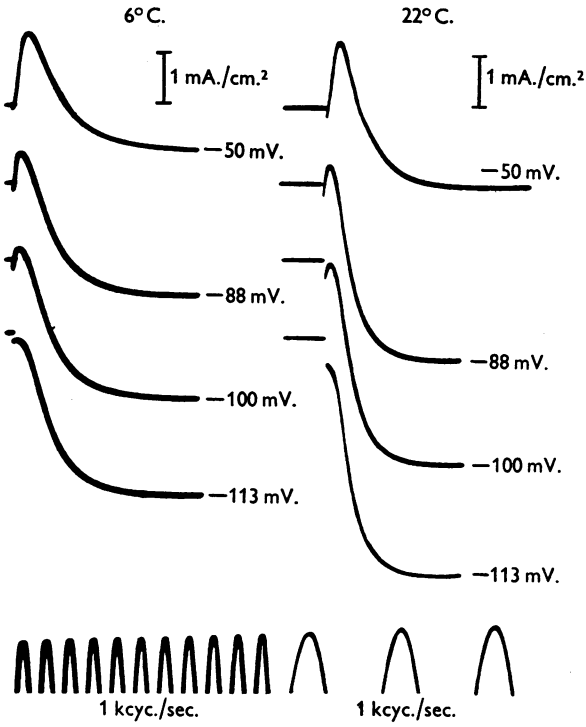

Fig. 15. Membrane currents at different temperatures. Axons 17 (6° C.) and 18 (22° C.), from the same squid. Inward current is shown as an upward deflexion. The numbers attached to each curve give the displacement of membrane potential. Uncompensated feed-back was employed.

amplitude of the two sets of records are similar but that the rate at which the ionic current changes with time was increased about sixfold by the rise in temperature of 16° C. It was found that the two families could be roughly superposed by assuming a Q_{10} of 3 for the rate at which ionic current changes with time. Values between 2·7 and 3·5 were found by analysing a number of experimental records obtained under similar conditions, but with different axons at different temperatures. In the absence of more precise information we shall use a temperature coefficient of 3 when it is necessary to compare rates measured at different temperatures.

The absolute magnitude of the current attained at any voltage probably varies with temperature, but much less than the time scale. In the experiment of Fig. 15 a rise of 16° C. increased the outward current about 1·5-fold, while the inward current at −50 mV. was approximately the same in the two records. Since the initial phase of inward current declined relatively rapidly as the axon deteriorated it is possible that a temperature coefficient of about 1·3 per 10° C. applies to both components of the current. Temperature coefficients of the order of 1·0–1·5 were also obtained by examining a number of results obtained with other axons.

The capacity current

The surge of current associated with the sudden change in membrane potential was examined by taking records at high time-base speed and low amplification. Tracings of a typical result are shown in Fig. 16. It will be seen

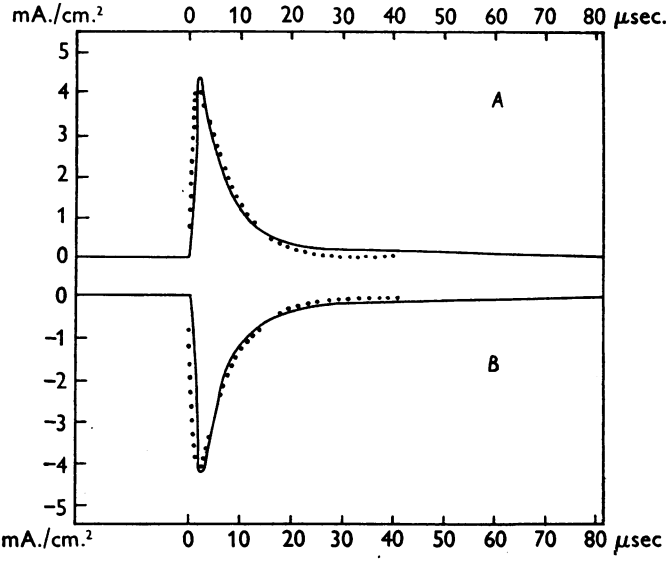

Fig. 16. Current through capacitative element of membrane during a voltage clamp. Abscissa: time in μsec. Ordinate: membrane current density (mA./cm.²) with inward current taken as positive. At $t=0$ the potential difference between external and internal electrodes was displaced +40 mV. in curve *A* or −40 mV. in curve *B*. The continuous curves were traced from experimental records. The dotted curves were calculated according to the equation

$$I^* = 6{\cdot}8\,[\exp(-0{\cdot}159t) - \exp(-t)],$$

where I^* is the current in mA./cm.² and t is time in μsec. This follows from the assumptions given in the text. Axon 25; temperature 8° C.

that the current records for anodal and cathodal changes are almost symmetrical and that the charging process is virtually complete in 50 μsec. In the anodal record the observed current declined from a peak of 4·5 mA./cm.² to a steady level of about 0·04 mA./cm.². The steady current is barely visible in the tracing

but could be seen more clearly at higher amplification and lower time-base speed; records taken under these conditions were similar to those in Fig. 12.

The membrane capacity was obtained from the change in potential and the area under the curves. A small correction was made for ionic current but the resting membrane conductance was sufficiently low for uncertainties here to be unimportant. In the experiment illustrated by Fig. 16*A* the charge entering the membrane capacity in 60 μsec. was 35 mμcoulomb/cm.^{2}, while the change in potential was 40 mV. Hence the membrane capacity per unit area was about 0·9 μF./cm.^{2}. Table 1 (p. 435) gives the results of other experiments of this kind. It also shows that replacement of all the sodium in sea water by choline had little effect on the membrane capacity and that there was no large change of capacity with temperature.

If a perfect condenser is short-circuited through zero resistance it loses its charge instantaneously. Fig. 16 suggests that the nerve capacity charged or discharged with a time constant of about 6 μsec. under a 'voltage clamp'. This raises the question whether the finite time of discharge was due to an imperfection in the membrane capacity or whether it arose from an imperfection in the method of holding the membrane potential constant. The records in Fig. 16 were obtained with uncompensated feed-back, which means that there was a small resistance in series with the capacitative element of the membrane. This clearly reduces the rate at which the membrane capacity can be discharged, and must be allowed for. It is also necessary to take account of the finite time constant of the recording amplifier (about 1 μsec. at this gain). Both effects have been considered in calculating the dotted lines in Fig. 16. These were drawn on the assumption that a 0·9 μF. condenser was charged to $\pm$40 mV. through a resistance of 7 Ω. and that the resulting pulses of current were recorded by an amplifier with an exponential time lag of 1 μsec. It will be seen that there is good agreement between the amplitude and general form of the two pairs of curves. Deviations at short times are not considered important since there was some uncertainty in the correction for amplifier delay.

At relatively long times ($>$25 μsec.) the current record shows a 'tail' which is not explained by the presence of a series resistance. This effect was present in all records and was larger at higher temperatures. It can be explained by supposing that the membrane capacity was not perfect but behaved in the manner described by Curtis & Cole (1938). The records in Fig. 16 are roughly consistent with a constant phase angle of 80°, while those at higher temperatures require somewhat lower values. These statements must be regarded as tentative since our experiments were not designed to measure the phase angle and do not give good data for quantitative analysis. For the time being the principal point to be emphasized is that the surge associated with a sudden

change in potential is adequately described by assuming that the membrane has a capacity of about 1 μF./cm.^{2} and a series resistance of about 7 Ω.cm.^{2}.

The surge of capacity current was larger in amplitude and occupied a shorter time when compensated feed-back was employed. These experiments were not suitable for analysis, since the charging current was oscillatory and could not be adequately recorded by the camera employed. All that could be seen in records of ionic current is a gap, as in Fig. 14.

Our values for the membrane capacity are in reasonable agreement with those obtained previously. Using transverse electrodes 5·6 mm. in length, Curtis & Cole (1938) obtained the following values in twenty-two experiments: average membrane capacity at 1 kcyc./sec., 1·1 μF./cm.^{2}, range 0·66 μF./cm.^{2} to 1·60 μF./cm.^{2}; average phase angle, 76°, range 64–85°.

The values for membrane capacity in the upper part of Table 1 were obtained by integrating the initial surge of current over a total time of about 50 μsec. If the phase angle is assumed to be 76° at all frequencies the average value of 0·89 μF./cm.^{2} obtained by this method is equivalent to one of 1·03 μF./cm.^{2} at 1 kcyc./sec. This is clearly in good agreement with the figures given by Curtis & Cole (1938), but is substantially less than the value of 1·8 μF./cm.^{2} mentioned in a later paper (Cole & Curtis, 1939). However, as Cole & Curtis point out, the second measurement is likely to be too large since the electrode length was only 0·57 mm. and no allowance was made for end-effects.

The series resistance

Between the internal and external electrodes there is a membrane with a resting resistance of about 1000 Ω.cm.^{2}. This resistance is shunted by a condenser with a capacity of about 1 μF./cm.^{2}. In series with the condenser, and presumably in series with the membrane as a whole, there is a small resistance which, in the experiment illustrated by Fig. 16, had an approximate value of 7 Ω.cm.^{2}. This 'series resistance' can be estimated without fitting the complete theoretical curve shown in that figure. A satisfactory approximation is to divide the time constant determining the decline of the capacitative curve by the measured value of the membrane capacity. This procedure was followed in calculating the values for the series resistance given in the upper part of Table 1. The symbol r_s gives the actual resistance in series with the central area of membrane, while R_s is the same quantity multiplied by the area of membrane exposed to current flow in the central channel of the guard system. The last column gives the ratio of r_s to the resistance (r_{cd}) between the current measuring electrodes, c and d. This ratio is of interest since it determined the potentiometer setting required to give fully compensated feed-back (pp. 430–1).

Another method of measuring the series resistance was to apply a rectangular pulse of current to the nerve and to record the potential difference (v_{bc}) between the internal electrode b and the external electrode c as a function of time. The current in the central channel of the guard system was also obtained by recording the potential difference (v_{cd}) between the external electrodes c and d. The two records were rounded to the same extent by amplifier delay so that the series resistance and the membrane capacity could be determined by fitting the record obtained from the internal electrode by the following equation

$$v_{bc} = \frac{r_s}{r_{cd}} v_{cd} + \frac{1}{r_{cd} c} \int_0^t v_{cd} \, dt,$$

where c is the capacity of the area of membrane exposed to current flow in the central channel.

This analysis was made with two axons and gave satisfactory agreement between observed and calculated values of v_{bc}, with values of r_s/r_{cd} and C_M which were similar to those obtained by the voltage clamp method (see Table 1).

The observed value of the series resistance ($r_s = 61\,\Omega$.) cannot be explained solely by convergence of current between the electrodes used to measure membrane potential. Only about 30% was due to convergence of current between electrode c and the surface of the nerve, while convergence between the membrane and the internal electrode should not account for more than 25%, unless the specific resistance of axoplasm was much greater than that found by Cole & Hodgkin (1939). The axons used in the present work were surrounded by a dense layer of connective tissue, 5–20 μ. in thickness, which adheres tightly and cannot easily be removed by dissection. According to Bear, Schmitt & Young (1937) the inner layer of this sheath has special optical properties and may be lipoid in nature. It seems reasonable to suppose that one or other of these external sheaths may have sufficient resistance to account for 45% of the series resistance. There was, in fact, some evidence that the greater part of the series resistance was external to the main barrier to ionic movement. Substitution of choline sea water for normal sea water increased r_{cd} by 23%, but it reduced r_s/r_{cd} by only 3·5% (Table 1, axon 25). This suggests that about 80% of r_s varied directly with the specific resistance of the external medium. Since the composition of axoplasm probably does not change when choline is substituted for sodium (Keynes & Lewis, 1951) it seems likely that most of the series resistance is located outside the main barrier to ionic movement. Further experiments are needed to establish this point and also to determine whether the resistive layer has any measurable capacity.

Accuracy of method

The effect of the series resistance. The error introduced by the series resistance (r_s) was discussed on p. 430. Its magnitude was assessed by comparing records obtained with uncompensated feed-back ($p = 0$) with those obtained with compensated feed-back ($p = 0{\cdot}6$). The effect of compensation was most conspicuous with a depolarization of about 30 mV. Fig. 17 shows typical curves in this region. A, B and C were obtained with uncompensated feed-back; α, β and γ with compensated feed-back. A gives the potential difference between external and internal electrodes. B is the potential difference between the external electrodes used to measure current and is equal to the product of the membrane current and the resistance r_{cd}. The true membrane potential differs from A by the voltage drop across r_s which is equal to $(r_s/r_{cd})\,B$. C shows the membrane potential calculated on the assumption that r_s/r_{cd} had its average value of 0·68. α, β and γ were obtained in exactly the same manner as A, B and C, except that the potentiometer setting (p) was increased from 0 to 0·6. It will be seen that this altered the form of the upper record in a manner which compensates for the effect of current flow. The error in C is about 20%, while γ deviates by only about 2·5%. Hence any error present in β is likely to be increased eightfold in B. Since the two records are not grossly different, β may be taken as a reasonably faithful record of membrane current under a voltage clamp.

Experiments of this type indicated that use of uncompensated feed-back introduced errors but that it did not alter the general form of the current record. Since the method of compensated feed-back was liable to damage axons it was not employed in experiments in which the preparation had to be kept in good condition for long periods of time.

Polarization effects. The outward current associated with a large and prolonged reduction of membrane potential was not maintained, but declined slowly as a result of a 'polarization effect'. The beginning of this decline can be seen in the lower records in Fig. 12. It occurred under conditions which had little physiological significance, for an axon does not normally remain with a membrane potential of -100 mV. for more than 1 msec. Nor does the total current through the membrane approach that in Fig. 12.

In order to explain the effect it may be supposed either: (1) that 'mutual polarization' of the electrode (p. 428) is substantially greater inside the axon than in sea water; (2) that currents may cause appreciable changes in ionic concentration near the membrane; (3) that some structure in series with the membrane may undergo a slow polarization. We were unable to distinguish

between these suggestions, but it was clear that the 'polarization effect' had little to do with the active changes, since it was also present in moribund axons and was little affected by temperature.

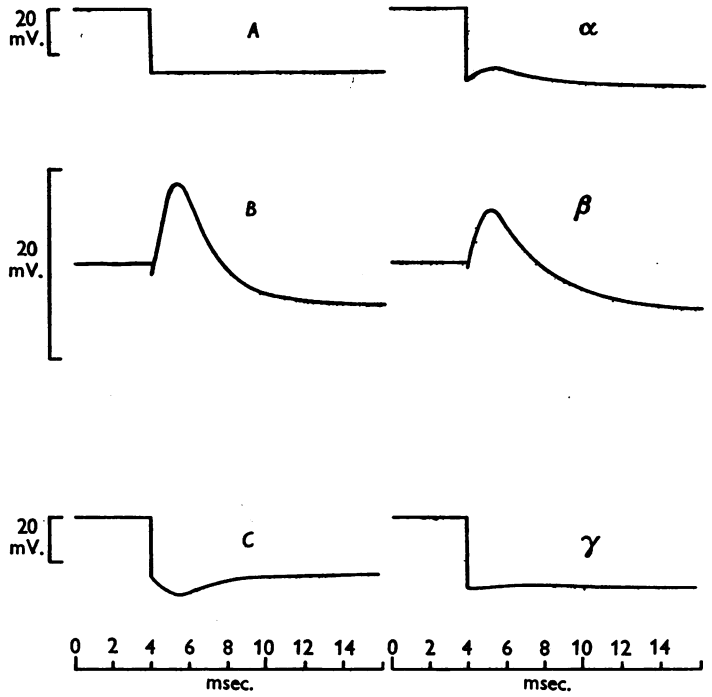

Fig. 17. Comparison of results obtained with uncompensated feed-back (A, B, C) and compensated feed-back (α, β, γ). A, α: potential difference between external and internal electrodes ($v_c - v_b$). B, β: potential difference between current measuring electrodes ($v_d - v_c$). C, γ: membrane potential calculated as $C = A - 0{\cdot}68B$, or $\gamma = \alpha - 0{\cdot}68\beta$. Records B and β may be converted into membrane current density by dividing by 11·9 Ω.cm.^{2}. Temperature 4° C. Axon 34.

SUMMARY

1. An experimental method for controlling membrane potential in the giant axon of *Loligo* is described. This depended on the use of an internal electrode consisting of two silver wires, a guard system for measuring membrane current and a 'feed-back' amplifier for clamping the membrane potential at any desired level.

2. Axons impaled with the double electrode gave 'all-or-nothing' action potentials of about 100 mV. when stimulated with a brief shock. The action potential had a well-defined threshold at a critical depolarization of about 15 mV. Depolarizations less than 10–15 mV. gave graded responses similar to those seen in other excitable tissues.

3. The feed-back amplifier was arranged to make the membrane potential undergo a sudden displacement to a new level at which it was held constant for

10–50 msec. Under these conditions the membrane current consisted of a brief surge of capacity current, associated with the sudden change in potential, and an ionic current during the period of maintained potential. The brief surge was proportional to the displacement of membrane potential and corresponded to the charging of a membrane with an average capacity of 0·9 μF./cm.^{2}. The sign and time course of the ionic current varied markedly with the membrane potential. Anodal displacements gave small currents which were always inward in direction. Depolarizations of less than 15 mV. gave outward currents which were small initially but increased markedly with time. Depolarizations of 15–110 mV. gave an initial phase of inward current which changed fairly rapidly into a large and prolonged outward current. The phase of inward current disappeared at about 110 mV. and was replaced by one of outward current. There was a continuous relation between ionic current and membrane potential. At short times this relation was similar to that derived from the rising phase of the action potential.

4. The maximum inward and outward ionic currents were little altered by temperature, but the rate at which the ionic current changed with time was increased about threefold for a rise of 10° C.

5. There was evidence of a small resistance in series with the capacitative element of the membrane. Errors introduced by this resistance were reduced by the use of compensated feed-back.

We wish to thank the Rockefeller Foundation for financial aid and the Director and staff of the Marine Biological Association for assistance at all stages of the experimental work.

REFERENCES

BEAR, R. S., SCHMITT, F. O. & YOUNG, J. Z. (1937). The sheath components of the giant nerve fibres of the squid. *Proc. Roy. Soc.* B, **123**, 496–529.

COLE, K. S. (1949). Dynamic electrical characteristics of the squid axon membrane. *Arch. Sci. physiol.* **3**, 253–258.

COLE, K. S. & CURTIS, H. J. (1939). Electric impedance of the squid giant axon during activity. *J. gen. Physiol.* **22**, 649–670.

COLE, K. S. & HODGKIN, A. L. (1939). Membrane and protoplasm resistance in the squid giant axon. *J. gen. Physiol.* **22**, 671–687.

CURTIS, H. J. & COLE, K. S. (1938). Transverse electric impedance of the squid giant axon. *J. gen. Physiol.* **21**, 757–765.

HODGKIN, A. L. & HUXLEY, A. F. (1945). Resting and action potentials in single nerve fibres. *J. Physiol.* **104**, 176–195.

HODGKIN, A. L. & HUXLEY, A. F. (1952*a*). Currents carried by sodium and potassium ions through the membrane of the giant axon of *Loligo*. *J. Physiol.* **116**, 449–472.

HODGKIN, A. L. & HUXLEY, A. F. (1952*b*). The components of membrane conductance in the giant axon of *Loligo*. *J. Physiol.* **116**, 473–496.

HODGKIN, A. L. & HUXLEY, A. F. (1952*c*). The dual effect of membrane potential on sodium conductance in the giant axon of *Loligo*. *J. Physiol.* **116**, 497–506.

HODGKIN, A. L. & HUXLEY, A. F. (1952*d*). A quantitative description of membrane current and its application to conduction and excitation in nerve. *J. Physiol.* (in the press).

HODGKIN, A. L., HUXLEY, A. F. & KATZ, B. (1949). Ionic currents underlying activity in the giant axon of the squid. *Arch. Sci. physiol.* **3**, 129–150.

HODGKIN, A. L. & KATZ, B. (1949*a*). The effect of sodium ions on the electrical activity of the giant axon of the squid. *J. Physiol.* **108**, 37–77.

HODGKIN, A. L. & KATZ, B. (1949*b*). The effect of temperature on the electrical activity of the giant axon of the squid. *J. Physiol.* **109**, 240–249.

HUXLEY, A. F. & STÄMPFLI, R. (1951). Effect of potassium and sodium on resting and action potentials of single myelinated nerve fibres. *J. Physiol.* **112**, 496–508.

KEYNES, R. D. & LEWIS, P. R. (1951). The sodium and potassium content of cephalod nerve fibres. *J. Physiol.* **114**, 151–182.

MARMONT, G. (1949). Studies on the axon membrane. *J. cell. comp. Physiol.* **34**, 351–382.

ROTHENBERG, M. A. (1950). Studies on permeability in relation to nerve function. II. Ionic movements across axonal membranes. *Biochim. biophys. acta*, **4**, 96–114.

J. Physiol. (1952) 116, 449–472

CURRENTS CARRIED BY SODIUM AND POTASSIUM IONS THROUGH THE MEMBRANE OF THE GIANT AXON OF *LOLIGO*

BY A. L. HODGKIN AND A. F. HUXLEY

From the Laboratory of the Marine Biological Association, Plymouth, and the Physiological Laboratory, University of Cambridge

(*Received* 24 *October* 1951)

In the preceding paper (Hodgkin, Huxley & Katz, 1952) we gave a general description of the time course of the current which flows through the membrane of the squid giant axon when the potential difference across the membrane is suddenly changed from its resting value, and held at the new level by a feed-back circuit ('voltage clamp' procedure). This article is chiefly concerned with the identity of the ions which carry the various phases of the membrane current.

One of the most striking features of the records of membrane current obtained under these conditions was that when the membrane potential was lowered from its resting value by an amount between about 10 and 100 mV. the initial current (after completion of the quick pulse through the membrane capacity) was in the inward direction, that is to say, the reverse of the direction of the current which the same voltage change would have caused to flow in an ohmic resistance. The inward current was of the right order of magnitude, and occurred over the right range of membrane potentials, to be the current responsible for charging the membrane capacity during the rising phase of an action potential. This suggested that the phase of inward current in the voltage clamp records might be carried by sodium ions, since there is much evidence (reviewed by Hodgkin, 1951) that the rising phase of the action potential is caused by the entry of these ions, moving under the influence of concentration and potential differences. To investigate this possibility, we carried out voltage clamp runs with the axon surrounded by solutions with reduced sodium concentration. Choline was used as an inert cation since replacement of sodium with this ion makes the squid axon completely inexcitable, but does not reduce the resting potential (Hodgkin & Katz, 1949; Hodgkin, Huxley & Katz, 1949).

METHOD

The apparatus and experimental procedure are fully described in the preceding paper (Hodgkin *et al.* 1952). 'Uncompensated feed-back' was employed.

Sea water was used as a normal solution. Sodium-deficient solutions were made by mixing sea water in varying proportions with isotonic 'choline sea water' of the following composition:

Ion	g. ions/kg. H_2O	Ion	g. ions/kg. H_2O
$Choline^+$	484	Mg^{++}	54
K^+	10	Cl^-	621
Ca^{++}	11	HCO_3^-	3

The mixtures are referred to by their sodium content, expressed as a percentage of that in sea water (30% Na sea water, etc.).

RESULTS

Voltage clamps in sodium-free solution

Fig. 1 shows the main differences between voltage clamp records taken with the axon surrounded by sea water and by a sodium-free solution. Each record gives the current which crossed the membrane when it was depolarized by 65 mV. After the top record was made, the sea water surrounding the axon was replaced by choline sea water, and the middle record was taken. The fluid was again changed to sea water, and the bottom record taken. The amplifier gain was the same in all three records, but a given deflexion represents a smaller current in the choline solution, since the current was detected by the potential drop along a channel filled with the fluid which surrounded the axon, and the specific resistance of the choline sea water was about 23% higher than that of ordinary sea water.

The most important features shown in Fig. 1 are the following: (1) When the external sodium concentration was reduced to zero, the inward current disappeared and was replaced by an early hump in the outward current. (2) The late outward current was only slightly altered, the steady level being 15–20% less in the sodium-free solution. (3) The changes were reversed when sea water was replaced. The currents are slightly smaller in the bottom record than in the top one, but the change is not attributable to an action of the choline since a similar drop occurred when an axon was kept in sea water for an equal length of time.

A series of similar records with different strengths of depolarization is shown in Fig. 2. The features described in connexion with Fig. 1 are seen at all strengths between -28 and -84 mV. At the weakest depolarization (-14 mV.) the early phase of outward current in the sodium-free record is too small to be detected. At the highest strengths the early current is outward even in sea water, and is then increased in the sodium-free solution.

These results are in qualitative agreement with the hypothesis that the inward current is carried by sodium ions which, as an early result of the decrease in membrane potential, are permitted to cross the membrane in both

directions under a driving force which is the resultant of the effects of the concentration difference and the electrical potential difference across the membrane. When the axon is in sea water, the concentration of sodium outside the membrane $[Na]_o$ is 5–10 times greater than that inside, $[Na]_i$. This tends to make the inward flux exceed the outward. The electrical potential

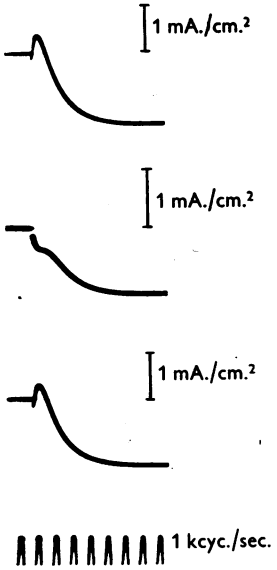

Fig. 1

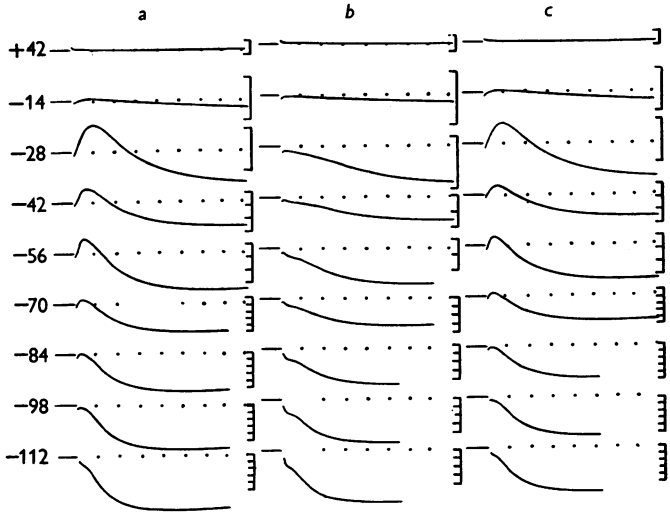

Fig. 2

Fig. 1. Records of membrane current during 'voltage clamps' in which membrane potential was lowered by 65 mV. Top record: axon in sea water. Centre record: axon in choline sea water. Bottom record: after replacing sea water. Axon no. 15; temperature 11° C. Inward current is shown upwards in this and all other figures.

Fig. 2. Records of membrane current during 'voltage clamps'. *a*, axon in sea water; *b*, axon in choline sea water; *c*, after replacing sea water. Displacement of membrane potential indicated in mV. Axon no. 21; temperature 8·5° C. Vertical scale: 1 division is 0·5 mA./cm.². Horizontal scale: interval between dots is 1 msec.

difference E also helps the inward and hinders the outward flux so long as it is positive, i.e. in the same direction as the resting potential. The net current carried by the positive charge of the sodium ions is therefore inward unless the depolarization is strong enough to bring E to a sufficiently large negative value to overcome the effect of the concentration difference. The critical value of E at which the fluxes are equal, and the net sodium current is therefore zero, will be called the 'sodium potential', E_{Na}. Its value should be given by the Nernst equation

$$E_{Na} = \frac{RT}{F} \log_e \frac{[Na]_i}{[Na]_o}. \qquad (1)$$

With values of E more negative than this, the net sodium flux is outward, causing the early phase of the outward current seen in the lowest record of the first and third columns of Fig. 2, where the axon was in sea water and was depolarized by 112 mV. A family of voltage clamp records which shows particularly well this transition from an initial rise to an initial fall as the strength of depolarization is increased is reproduced as Fig. 14 of the preceding paper.

When the axon is placed in a sodium-free medium, such as the 'choline sea water', there can be no inward flux of sodium, and the sodium current must always be outward. This will account for the early hump on the outward current which is seen at all but the lowest strength of depolarization in the centre column of Fig. 2.

Voltage clamps with reduced sodium concentration

The results of reducing the sodium concentration to 30 and 10% of the value in sea water are shown in Figs. 3 and 4 respectively. These figures do not show actual records of current through the membrane. The curves are graphs of ionic current against time, obtained by subtracting the current through the capacity from the recorded total current. The initial surge in an anodal record was assumed to consist only of capacity current, and the capacity current at other strengths was estimated by scaling this in proportion to the amplitude of the applied voltage change.

As would be expected, the results are intermediate between those shown in Fig. 2 for an axon in sea water and in choline sea water. Inward current is present, but only over a range of membrane potentials which decreases with the sodium concentration, and within that range, the strength of the current is reduced. A definite sodium potential still exists beyond which the early hump of ionic current is outward, but the strength of depolarization required to reach it decreases with the sodium concentration. Thus, in the first column of Fig. 3, with the axon in 30% sodium sea water, the sodium potential is almost exactly reached by a depolarization of 79 mV. In the second column, with sea water surrounding the axon, the sodium potential is just exceeded by a depolarization of 108 mV. In column 3, after re-introducing 30% sodium sea water, the sodium potential is slightly exceeded by a depolarization of 79 mV. Similarly, in Fig. 4, the sodium potentials are almost exactly reached by depolarizations of 105, 49 and 98 mV. in the three columns, the axon being in sea water, 10% sodium sea water and sea water respectively. The sequence of changes in the form of the curves as the sodium potential is passed is remarkably similar in all cases.

The external sodium concentration and the 'sodium potential'

Estimation of the 'sodium potential' in solutions with different sodium concentrations is of particular importance because it leads to a quantitative

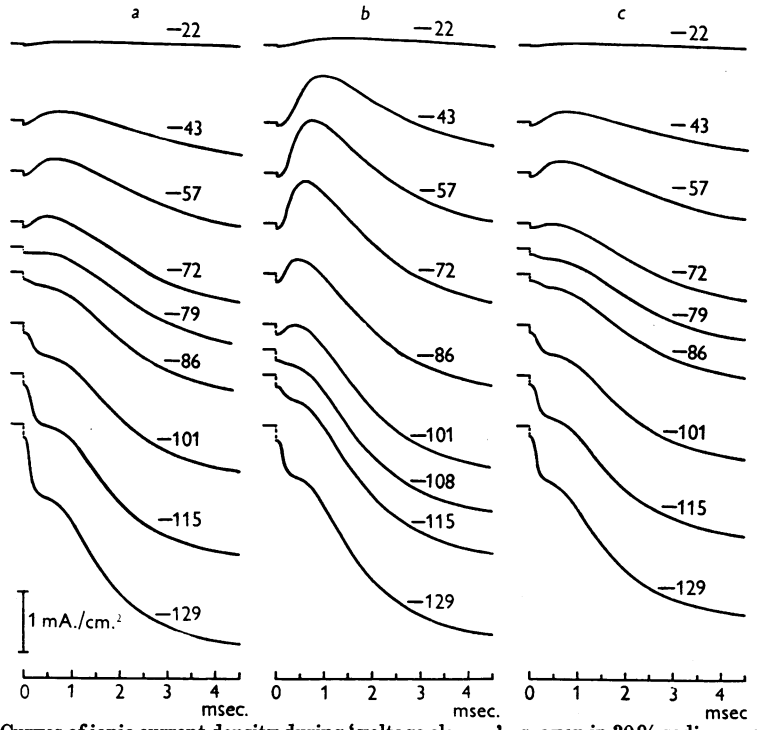

Fig. 3. Curves of ionic current density during 'voltage clamps'. *a*, axon in 30% sodium sea water; *b*, axon in sea water; *c*, after replacing 30% sodium sea water. Displacement of membrane potential indicated in millivolts. Axon no. 20; temperature 6·3° C.

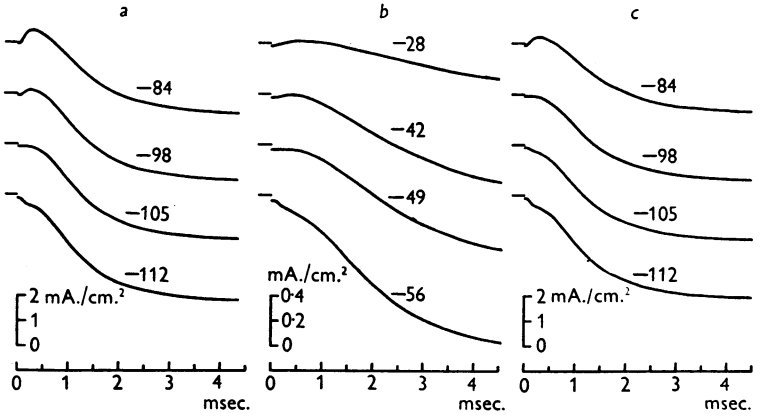

Fig. 4. Curves of ionic current density during voltage clamps in neighbourhood of sodium potential. *a*, axon in sea water; *b*, axon in 10% sodium sea water; *c*, after replacing sea water. Note that ordinate scale is larger in *b* than in *a* and *c*. Displacement of membrane potential in millivolts indicated for each curve. Axon no. 21; temperature 8·5° C.

test of our hypothesis. Equation (1) gives the sodium potential in sea water (E_{Na}), and the corresponding quantity (E'_{Na}) when the external sodium concentration is reduced to $[Na]'_o$ is given by

$$E'_{Na} = \frac{RT}{F} \log_e \frac{[Na]_i}{[Na]'_o}.$$

Hence $$E'_{Na} - E_{Na} = \frac{RT}{F}\left\{\log_e \frac{[Na]_i}{[Na]'_o} - \log_e \frac{[Na]_i}{[Na]_o}\right\} = \frac{RT}{F} \log_e \frac{[Na]_o}{[Na]'_o}. \quad (2)$$

The displacements of membrane potential, V, corresponding to these values are $V_{Na} = E_{Na} - E_r$ and $V'_{Na} = E'_{Na} - E'_r$, where E_r and E'_r are the values of the resting potential in sea water and in the test solution respectively. Hence

$$(V'_{Na} - V_{Na}) + (E'_r - E_r) = \frac{RT}{F} \log_e \frac{[Na]_o}{[Na]'_o}. \quad (3)$$

Each term in this equation can be determined experimentally, and data were obtained in four experiments on two axons. The results are given in Table 1, where the observed shift in sodium potential is compared with that predicted from the change in sodium concentration by Equation (3). It will be

TABLE 1. Comparison of observed and theoretical change in sodium potential when the fluid surrounding an axon is changed from sea water to a low sodium solution. Observed change: $E'_{Na} - E_{Na} = (V'_{Na} - V_{Na}) + (E'_r - E_r)$; theoretical change $= \frac{RT}{F} \log_e \frac{[Na]_o}{[Na]'_o}$.

Axon no.	Temp. (° C.)	$\frac{[Na]'_o}{[Na]_o}$	V_{Na} (mV.)	V'_{Na} (mV.)	$(E'_r - E_r)$ (mV.)	Sodium potential shift: Observed (mV.)	Sodium potential shift: Theoretical (mV.)
20	6·3	0·3	−105	−78	+3	+30	+28·9
20	6·3	0·1	−96	−45	+4	+55	+55·3
21	8·5	0·1	−100	−48	+4	+56	+55·6
21	8·5	0·1	−95	−45	+4	+54	+55·6

seen that there is good agreement, providing strong evidence that the early rise or fall in the recorded ionic current is carried by sodium ions, moving under the influence of their concentration difference and of the electric potential difference across the membrane.

Details of the estimation of the quantities which enter into Equation (3) are given in the following paragraphs.

Determination of V_{Na}. At the sodium potential there is neither inward sodium current, shown by an initial rise in the ionic current, nor outward sodium current, shown by an early hump in the outward current. It was found that these two criteria did in fact define the sodium potential very sharply, i.e. a hump appeared as soon as the ionic current showed an initial fall. It was therefore permissible to take as V_{Na} the strength of depolarization which gave an ionic current curve which started horizontally. This criterion was much more convenient to apply than the absence of a hump, since records were taken at fairly wide intervals of V (usually 7 mV.) and an interpolation procedure was necessary in order to estimate V_{Na} to the nearest 0·5 mV.

Change in resting potential. Experiments with ordinary capillary internal electrodes showed that the resting potential increased on the average by 4 mV. when the sea water surrounding the axon was replaced by choline sea water (a correction of 1·5 mV. for junction potentials in the external solutions is included in this figure). With intermediate sodium concentrations, the change in resting potential was assumed to be proportional to the change in sodium concentration. For instance, the resting potential in 30% sodium sea water was taken as 2·8 mV. higher than that in sea water.

Slow change in condition of axon. When an axon is kept in sea water, its sodium content rises (Steinbach & Spiegelman, 1943; Keynes & Lewis, 1951) and its resting potential falls. Both of these effects bring E_r and E_{Na} closer together, diminishing the absolute magnitude of V_{Na}. In comparing V_{Na} in two solutions, it was therefore necessary to determine V_{Na} first in one solution, then in the other and finally in the first solution again. The second value of V_{Na} was then compared with the mean of the first and third.

The internal sodium concentration and the sodium potential

In freshly mounted fibres the average difference between the sodium potential and the resting potential was found to be -109 mV. (ten axons with a range of -95 to -119 mV. at an average temperature of 8° C.). The average resting potential in these fibres was 56 mV. when measured with a microelectrode containing sea water. By the time the sodium potential was measured the resting potential had probably declined by a few millivolts and may be taken as 50 mV. Allowing 10–15 mV. for the junction potential between sea water and axoplasm (Curtis & Cole, 1942; Hodgkin & Katz, 1949) this gives an absolute resting potential of 60–65 mV. The absolute value of the sodium potential would then be -45 to -50 mV. The sodium concentration in sea water is about 460 m.mol./kg. H_2O (Webb, 1939, 1940) so that the internal concentration of sodium would have to be 60–70 m.mol./kg. H_2O in order to satisfy Equation 1. This seems to be a very reasonable estimate since the sodium concentration in freshly dissected axons is about 50 m.mol./kg. H_2O while that in axons kept for 2 or 3 hr. is about 100 m.mol./kg. H_2O (Steinbach & Spiegelman, 1943; Keynes & Lewis, 1951; Manery, 1939, for fraction of water in axoplasm).

Outward currents at long times

So far, this paper has been concerned with the earliest phases of the membrane current that flows during a voltage clamp. The only current which has the opposite sign from the applied voltage pulse is the inward current which occurs over a certain range of depolarizations when the surrounding medium contains sodium ions. This inward current is always transient, passing over into outward current after a time which depends on the strength of depolarization and on the temperature. The current at long times resembles that in an ohmic resistance in having the same sign as the applied voltage change, but differs in that the outward current due to depolarization rises with a delay to a density which may be 50–100 times greater than that associated with a similar increase in membrane potential. Figs. 1–3 show that this late current

is not greatly affected by the concentration of sodium in the fluid surrounding the axon.

An outward current which arises with a delay after a fall in the membrane potential is clearly what is required in order to explain the falling phase of the action potential. The outward currents reached in a voltage clamp may considerably exceed the maximum which occurs in an action potential; this may well be because the duration of an action potential is not sufficient to allow the outward current to reach its maximum value. These facts suggest that the outward current associated with prolonged depolarization is the same current which causes the falling phase of the action potential. The evidence (reviewed by Hodgkin, 1951) that the latter is caused by potassium ions leaving the axon is therefore a suggestion that the former is also carried by potassium ions. Direct evidence that such long-continued and outwardly directed membrane currents are carried by potassium ions has now been obtained in *Sepia* axons by a tracer technique (unpublished experiments). We shall therefore assume that this delayed outward current is carried by potassium ions, and we shall refer to it as 'potassium current', I_K. Since it is outward, it is not appreciably affected by the external potassium concentration, and evidence for or against potassium being the carrier cannot easily be obtained by means of experiments analogous to those which have just been described with altered external sodium concentration.

I_K in sea water and choline. As has been mentioned, the later part of the current record during a constant depolarization is much the same whether the axon is surrounded by sea water or by one of the solutions with reduced sodium concentration. There are, however, certain differences. For a given strength of depolarization, the maximum outward current is smaller by some 10 or 20% in the low-sodium solution, and at the higher strengths where the outward current is not fully maintained, the maximum occurs earlier in the low-sodium solution. Part of the difference in amplitude is explained by the difference of resting potential. Since the resting potential is greater in the low-sodium medium, a higher strength of depolarization is needed to reach a given membrane potential during the voltage clamp. This difference can be allowed for by interpolation between the actual strengths employed in one of the solutions. In most cases, this procedure did not entirely remove the difference between the amplitudes. There are, however, two other effects which are likely to contribute. In the first place, the effect of not using 'compensated feed-back' is probably greater in the low-sodium solution (see preceding paper, p. 445). This further reduces the amplitude of the voltage change which actually occurs across the membrane. In the second place, the fact that the current reached its maximum earlier suggests that 'polarization' (preceding paper, p. 445) had a greater effect in the low-sodium solution. We do not know enough about either of these effects to estimate the amount by

which they may have reduced the potassium current. It does seem at least possible that they account for the whole of the discrepancy, and we therefore assume provisionally that substituting choline sea water for sea water has no direct effect on the potassium current.

Separation of ionic current into I_{Na} and I_K

The results so far described suggest that the ionic current during a depolarization consists of two more or less independent components in parallel, an early transient phase of current carried by sodium ions, and a delayed long-lasting phase of current carried by potassium ions. In each case, the direction of the current is determined by the gradient of the electro-chemical potential of the ion concerned. It will clearly be of great interest if it is possible to estimate separately the time courses of these two components. There is enough information for doing this in data such as are presented in Fig. 2, if we make certain assumptions about the effect of changing the solution around the axon. If we compare the currents when the axon is in the low-sodium solution with those in sea water, the membrane potential during the voltage clamp being the same in both cases, then our assumptions are:

(1) The time course of the potassium current is the same in both cases.

(2) The time course of the sodium current is similar in the two cases, the amplitude and sometimes the direction being changed, but not the time scale or the form of the time course.

(3) $\frac{dI_K}{dt}=0$ initially for a period about one-third of that taken by I_{Na} to reach its maximum.

The first two of these assumptions are the simplest that can be made, and do not conflict with any of the results we have described, while the third is strongly suggested by the form of records near the sodium potential, as pointed out on p. 454. These points are sufficient reason for trying this set of assumptions first, but their justification can only come from the consistency of the results to which they lead. The differences between the effects of lack of compensation, and of the polarization phenomenon, in the two solutions, referred to at the end of the last section, will of course lead to certain errors in the analysis in the later stages of the ionic current.

The procedure by which we carried out this analysis was as follows:

(1) Three series of voltage clamp records at a range of strengths were taken, the first with the axon in one of the solutions chosen for the comparison, the second with the axon in the other solution, and the third with the first solution again. Such a set of records is reproduced in Fig. 2.

(2) Each record was projected on to a grid in which the lines corresponded to equal intervals of time and current, and the current was measured at a series of time intervals after the beginning of the voltage change.

(3) The time course of the initial pulse of current through the membrane capacity was determined from anodal records as described on p. 452 above, and subtracted from the measured total currents. Different corrections were needed in the two solutions, because the capacity current had a slower time course in the low sodium solutions, perhaps as a result of their lower conductivity. This procedure yielded a family of curves of ionic current against time such as is shown in Fig. 3.

(4) Each pair of curves in the first and third series at the same strength was averaged, in order to allow for the slow deterioration in the condition of the axon that took place during the experiment.

(5) The difference in resting potential was allowed for by interpolating between consecutive curves in either the second series or the series of averaged curves.

(6) We have now obtained curves of ionic current against time in the two solutions, with strengths of depolarization which reach the same membrane potential during the voltage clamp. The ionic current will be called I_i in sea water and I'_i in the low-sodium solution. The components carried by sodium and potassium in the two cases will be called I_{Na}, I'_{Na}, I_K and I'_K respectively. The next step was to plot I'_i against I_i, and to measure the initial slope k of the resulting graph (corresponding to the beginning of the voltage clamp).

Since we assume that initially $dI_K/dt=0$, and that I_{Na} and I'_{Na} have similar time courses, $k=I'_{Na}/I_{Na}$. Further, since we assume that $I_K=I'_K$,

$$I_i-I'_i=I_{Na}-I'_{Na}=I_{Na}(1-k).$$

Hence
$$I_{Na}=(I_i-I'_i)/(1-k), \tag{4}$$

$$I'_{Na}=k(I_i-I'_i)/(1-k), \tag{5}$$

and
$$I_K=I'_K=I_i-I_{Na}=(I'_i-kI_i)/(1-k). \tag{6}$$

These equations give the values of the component currents at any time in terms of the known quantities I_i and I'_i at that time. Curves of I_{Na} and I_K against time could therefore be constructed by means of these equations.

This procedure is illustrated in Fig. 5, which shows two pairs of ionic current curves together with the deduced curves of I_{Na}, I'_{Na} and I_K against time. The complete family of I_K curves from this experiment is shown in Fig. 6*b*, while Fig. 6*a* shows the family derived by the same procedure from another experiment. A satisfactory feature of these curves, which is to some extent a check on the validity of the assumptions, is that the general shape is the same at all strengths. If the time courses of I_{Na} and I'_{Na} had not been of similar form, Equation (6) would not have removed sodium current correctly. It would then have been unlikely that the curve of potassium current at a potential away from the sodium potential would have been similar to that at the sodium potential, where the sodium current is zero and Equation (6) reduces to $I_K=I_i$ because $k=\infty$.

On the other hand, it is clearly inconsistent that the I_{Na} and I'_{Na} curves in the lower part of Fig. 5 reverse their direction at 2 msec. after the beginning of the pulse. This is a direct consequence of the fact, discussed on p. 456 above, that the late outward current is somewhat greater in sea water than in the low-sodium solutions, even when allowance is made for the resting potential shift.

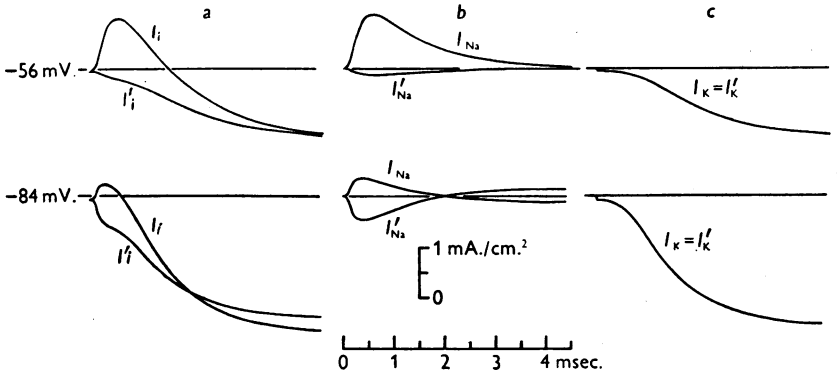

Fig. 5. Curves illustrating separation of ionic current into I_{Na} and I_K. Upper part of figure. *a*, ionic currents: I_i, axon in sea water, membrane potential lowered by 56 mV.; I'_i, axon in 10% sodium sea water, membrane potential lowered by 60 mV. (average of curves taken before and after I_i). *b*, sodium currents: I_{Na}, sodium current in sea water; I'_{Na}, sodium current in 10% sodium sea water. *c*, potassium current, same in both solutions. Lower part of figure. Same, but membrane potential lowered by 84 mV. in sea water and 88 mV. in 10% sodium sea water. Current and time scales same for all curves. Axon no. 21; temperature 8·5° C.

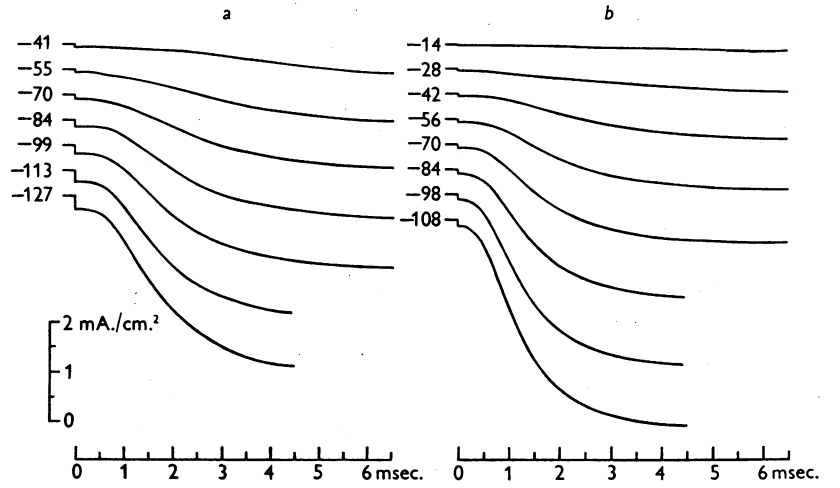

Fig. 6. Curves of potassium current against time for various strengths of depolarization. Displacement of membrane potential when axon is in sea water is indicated for each curve, in millivolts. *a*, derived from voltage clamps with axon in 30% sodium sea water, sea water and 30% sodium sea water. Axon no. 20; temperature 6·3° C. *b*, derived from voltage clamps with axon in 10% sodium sea water, sea water and 10% sodium sea water. Axon no. 21; temperature 8·5° C.

It was pointed out there that the difference may well be due to lack of compensation and to 'polarization'. Until these effects can be eliminated, estimates of sodium current at the longer times will be quite unreliable, and the corresponding estimates of potassium current will be somewhat reduced by these errors.

All the sodium current curves agree in showing that I_{Na} rises to a peak and then falls. With weak depolarizations (less than 40 mV.) the steady state value is definitely in the same direction as the peak, but at higher strengths the measured I_{Na} tends to a value which may have either direction. Since the sources of error mentioned in the last paragraph can cause an apparent reversal of I_{Na} during the pulse, it is possible that if these errors were larger than we suppose the whole of the apparent drop of I_{Na} from its peak value might also be spurious. At the time that an account of preliminary work with this technique was published (Hodgkin *et al.* 1949) we were unable to decide this point, and assumed provisionally that I_{Na} did not fall after reaching its maximum value. We are now convinced that this fall is genuine: (1) because of improvements in technique; (2) because of further experiments of other kinds which are described in the next two papers of this series (Hodgkin & Huxley, 1952*a*, *b*); and (3) because we occasionally observed records of the kind shown in Fig. 7. This is a record of membrane current during a voltage clamp in which an axon in choline sea water was depolarized by 84 mV. It will be seen that the early hump of outward current (due to sodium ions) was so marked that the total current reached a maximum at about 0·2 msec. and then fell before finally rising to the plateau attributable to movement of potassium ions. Unless we make the quite unwarrantable assumption that I_K itself has this double-humped form, this curve can only be explained by supposing that I_{Na} (outward in this case) falls after passing through a maximum value. The fact that such a clear maximum was not regularly observed was no doubt due to I_{Na} usually being smaller in relation to I_K than in this case.

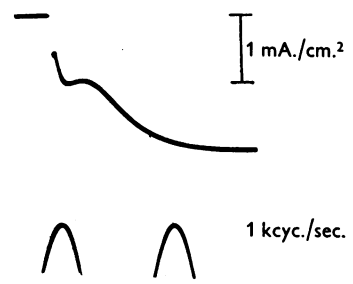

Fig. 7. Record of membrane current during a voltage clamp with axon in choline sea water, showing early maximum of outward current. Displacement of membrane potential during clamp = −84 mV. Axon no. 24; temperature 20° C.

We do not present a family of I_{Na} curves here, because the sequence of the curves is interrupted at the sodium potential. For this reason, the information is better given in the curves of 'sodium conductance' which are derived later in this paper (pp. 461–2 and Fig. 8). The variation of peak sodium current with strength of depolarization is shown in Fig. 13 for axons both in sea water and in low-sodium solutions.

Current carried by other ions. It seems to be possible to account for the variation of current with time during the voltage clamp by variations in the currents carried across the membrane by two ions, namely sodium and potassium. If, however, the membrane allowed constant fluxes of one or more other ion species, the current carried by these would form part of the 'I_K' which is deduced by our procedure, since this current would be independent both of time and of sodium concentration, and I_K is defined by its satisfying these criteria during the earliest part of the pulse. Reasons will be given in the next paper (Hodgkin & Huxley, 1952*a*) for supposing that the current carried by other ions is appreciable, though not of great importance except when the membrane potential is near to or above its resting value. Each of the I_K curves in Figs. 5 and 6 therefore includes a small constant component carried by other ions. This component probably accounts for much of the step in 'I_K' at the beginning of the voltage pulse.

Expression of ionic currents in terms of conductances

General considerations. The preceding sections have shown that the ionic current through the membrane is chiefly carried by sodium and potassium ions, moving in each case under a driving force which is the resultant of the concentration difference of the ion on the two sides of the membrane, and of the electrical potential difference across the membrane. This driving force alone determines the direction of the current carried by each ionic species, but the magnitude of the current depends also on the freedom with which the membrane allows the ions to pass. This last factor is a true measure of the 'permeability' of the membrane to the ion species in question. As pointed out by Teorell (1949*a*), a definition of permeability which takes no account of electrical forces is meaningless in connexion with the movements of ions, though it may well be appropriate for uncharged solutes.

The driving force for a particular ion species is clearly zero at the equilibrium potential for that ion. The driving force may therefore be measured as the difference between the membrane potential and the equilibrium potential. Using the same symbols as in Equations (1)–(3), the driving force for sodium ions will be $(E-E_{Na})$, which is also equal to $(V-V_{Na})$. The permeability of the membrane to sodium ions may therefore be measured by $I_{Na}/(E-E_{Na})$. This quotient, which we denote by g_{Na}, has the dimensions of a conductance (current divided by potential difference), and will therefore be referred to as the sodium conductance of the membrane. Similarly, the permeability of the membrane to potassium ions is measured by the potassium conductance g_K, which is defined as $I_K/(E-E_K)$. Conductances defined in this way may be called chord conductances and must be distinguished from slope conductances (G) defined as $\partial I/\partial E$.

These definitions are valid whatever the relation between I_{Na} and $(E-E_{Na})$,

or between I_K and $(E-E_K)$, but the usefulness of the definitions, and the degree to which they measure real properties of the membrane, will clearly be much increased if each of these relations is a direct proportionality, so that g_{Na} and g_K are independent of the strength of the driving force under which they are measured. It will be shown in the next paper (Hodgkin & Huxley, 1952*a*) that this is the case, for both sodium and potassium currents, in an axon surrounded by sea water, when the measurement is made so rapidly that the condition of the membrane has no time to change.

Application to measured sodium and potassium currents. The determination of sodium current, potassium current and sodium potential have been described in earlier sections of the present paper. The method by which the potassium potential, E_K, was found is described in the next paper (Hodgkin & Huxley, 1952*a*), and the values used here are taken from that paper. We have

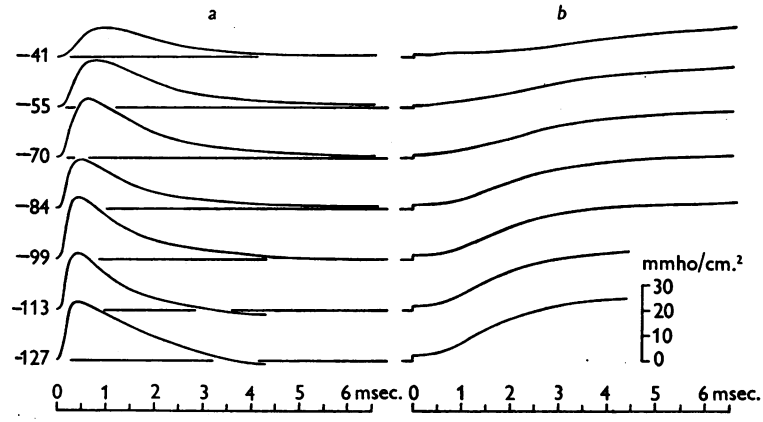

Fig. 8. Curves of sodium conductance (*a*) and potassium conductance (*b*). Displacement of membrane potential (millivolts) when axon was in sea water is indicated on each curve. Curves of I_i and I_K in same experiment are shown in Figs. 3 and 6*a* respectively. Axon no. 20; temperature 6·3° C.

therefore sufficient data to estimate g_{Na} and g_K as functions of time during a voltage clamp. Families of g_{Na} and g_K curves, for various strengths of depolarization, are shown in Fig. 8. The sodium conductances are calculated from the sodium currents in sea water, divided by the difference between membrane potential and sodium potential in sea water. If the same procedure had been applied to the corresponding quantities in the low-sodium solution, a similar family would have been obtained, but the relative amplitudes of the members of the family would have been slightly different. The values obtained from the sea water figures are the more interesting, both because they refer to a more normal condition, and because it is only in this case that the instantaneous relation between sodium current and voltage is linear

(Hodgkin & Huxley, 1952*a*). The corresponding distinction does not arise with g_K, since both I_K and E_K are the same in both solutions.

The shapes of individual curves in Fig. 8 are of course similar to those of curves of I_{Na} or I_K, such as are shown in Figs. 5 and 6, since the driving force for each ion is constant during any one voltage clamp. The change of amplitude of the curves with strength of depolarization is, however, less marked than with the current curves. For potassium, this can be seen by comparing Figs. 6*a* and 8*b*, which refer to the same experiment. For sodium, it is clear from Fig. 8*a* that the conductance curves undergo no marked change at the sodium potential, while the current curves reverse their direction at this point.

Membrane potential and magnitude of conductance. The effect of strength of depolarization on the magnitude of the conductances is shown in Figs. 9 and 10. For each experiment, the maximum values of g_{Na} and g_K reached in a voltage clamp of strength about 100 mV. are taken as unity, and the maximum values at other strengths are expressed in terms of these. Values of g_{Na} are available only from the four experiments in which there were enough data in sea water and in a low-sodium solution for the complete analysis to be carried out. The maximum values of g_K were also estimated in two other experiments. This was possible without complete analysis because the late current was almost entirely carried by potassium when the axon was in choline sea water.

The two curves are very similar in shape. At high strengths they become flat, while at low strengths they approach straight lines. Since the ordinate is plotted on a logarithmic scale, this means that peak conductance increases exponentially with strength of depolarization. The asymptote approached by the sodium conductances is probably steeper than that of the potassium data; the peak sodium conductances increase e-fold for an increase of 4 mV. in strength of depolarization; for potassium the corresponding figure is 5 mV.

The values of conductance at a depolarization of 100 mV., which are represented as unity in Figs. 9 and 10, are given in Table 2. In all these cases where enough measurements were made to construct a curve, the axon had been used for other observations before we took the records on which the analysis is based. In several cases, it was possible to estimate one or two values of sodium and potassium peak conductance at the beginning of the same experiment, and these were considerably higher than the corresponding values in Table 2, which must therefore be depressed by deterioration of the fibres.

More representative values of the peak g_K and g_{Na} at high strengths were estimated at the beginning of experiments on several fibres. Potassium current at long times can be estimated without difficulty, since I_{Na} is then negligible, especially at these depolarizations which are near the sodium potential. Nine fibres at 3–11° C. gave peak values of g_K at -100 mV. ranging from 22 to 41 m.mho/cm.^{2}, with a mean of 28; five fibres at 19–23° C. gave a range of

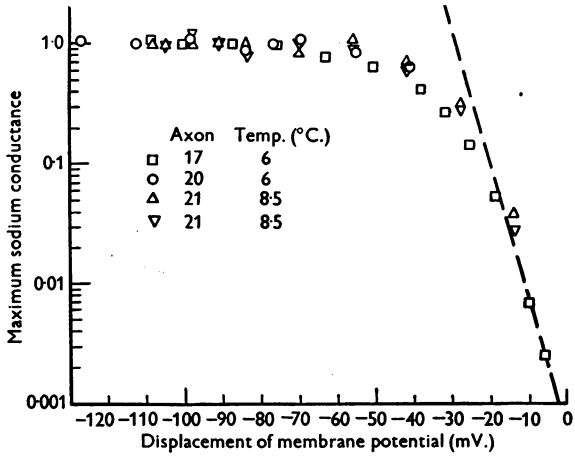

Fig. 9. Maximum sodium conductance reached during a voltage clamp. Ordinate: peak conductance relative to value reached with depolarization of 100 mV., logarithmic scale. Abscissa: displacement of membrane potential from resting value (depolarization negative).

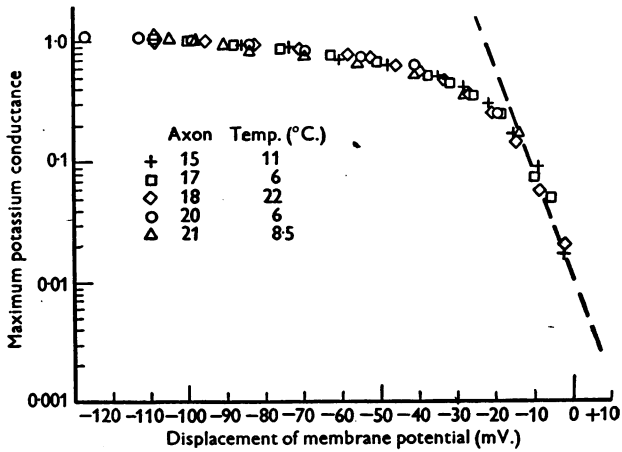

Fig. 10. Maximum potassium conductance reached during a voltage clamp. Ordinate: maximum conductance relative to value reached with depolarization of 100 mV., logarithmic scale. Abscissa: displacement of membrane potential from resting value (depolarization negative).

TABLE 2. Peak values of sodium and potassium conductance at a depolarization of 100 mV. Same experiments as Figs. 9 and 10. In each case, the value given in this table is represented as unity in Fig. 9 or Fig. 10.

		Peak conductances at −100 mV.	
Axon no.	Temp. (° C.)	Sodium (m.mho/cm.²)	Potassium (m.mho/cm.²)
15	11	—	21
17	6	18	20
18	21	—	28
20	6	22	23
21	8·5	23	31
21	8·5	17	—
		Mean 20	25

33–37 m.mho/cm.^{2}, mean 35. Values of the peak sodium conductance were obtained by measuring the peak inward current at a depolarization of about 60 mV. and dividing by the corresponding value of $(V - V_{Na})$. They are probably 10–20% low because current carried by potassium and other ions makes the peak inward current less than the peak sodium current, and because the peak conductance at 60 mV. depolarization is slightly less than that reached at 100 mV. Five fibres at 3–9° C. gave values ranging from 22 to 48 m.mho/cm.^{2}, mean 30; a single fibre at 22° C. gave 24 m.mho/cm.^{2}.

These results show that both g_K and g_{Na} can rise considerably higher than the values for the fully analysed experiments given in Table 2. They may be summarized by saying that on the average a freshly mounted fibre gives maximum conductances of about 30–35 m.mho/cm.^{2} both for sodium and for potassium, corresponding to resistances of about 30 Ω. for 1 cm.^{2} of membrane. This value may be compared with the resting resistance of about 1000 Ω. cm.^{2} (Cole & Hodgkin, 1939), and the resistance at the peak of an action potential, which is about 25 Ω. cm.^{2} (Cole & Curtis, 1939).

Membrane potential and rate of rise of conductance. It is evident from Fig. 8 that the strength of depolarization affects not only the maximum values attained by g_{Na} and g_K during a voltage clamp, but also the rates at which these maxima are approached. This is well shown by plotting the maximum rate of rise of conductance against displacement of membrane potential. This has been done for sodium conductance in Fig. 11 and for potassium conductance in Fig. 12. The data for g_K were taken from a fully analysed run, but in the case of sodium it is sufficient to take the maximum rate of rise of total ionic current, with the axon in sea water, and divide by $(V - V_{Na})$. The maximum rate of rise occurs so early that dI_K/dt is still practically zero, so that $dI_i/dt = dI_{Na}/dt$.

These graphs show that the rates of rise of both conductances continue to increase as the strength of the depolarization is increased, even beyond the point where the maximum values reached by the conductances themselves have become practically constant.

DISCUSSION

Only two aspects of the results described in this paper will be discussed at this stage. The first is the relationship between sodium current and external sodium concentration; the second is the application of the results to the interpretation of the action potential. Further discussion will be reserved for the final paper of this series (Hodgkin & Huxley, 1952*c*).

Sodium current and external sodium concentration

General considerations and theory. We have shown in the earlier parts of this paper that there is good reason for believing that the component of membrane

current that we refer to as I_{Na} is carried by sodium ions which move down their own electrochemical gradient, the speed of their movement, and therefore the magnitude of the current, being also determined by changes in the freedom

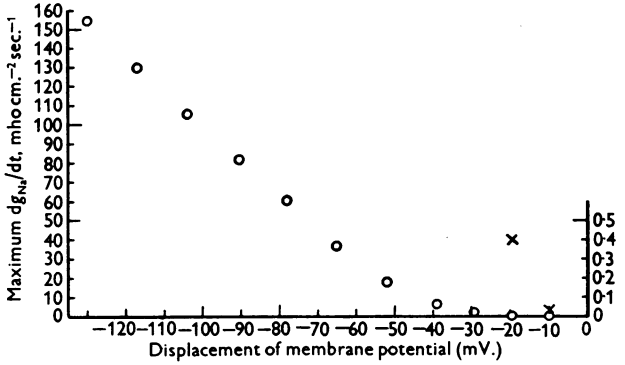

Fig. 11. Maximum rates of rise of sodium conductance during voltage clamps plotted against displacement of membrane potential. Circles are to be read with the scale on the left-hand side. The two lowest points are also re-plotted as crosses on 100 times the vertical scale, and are to be read with the scale on the right-hand side. The peak sodium conductance reached at high strengths of depolarization was 16 m.mho/cm.^{2}. Axon no. 41; temperature 3·5° C. Compensated feed-back.

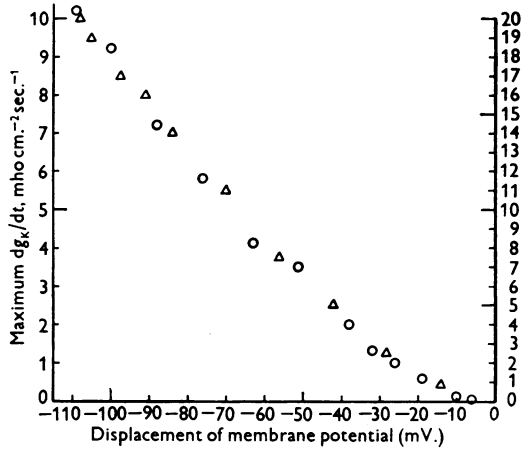

Fig. 12. Maximum rates of rise of potassium conductance during voltage clamps, plotted against displacement of membrane potential. Circles, left-hand scale: axon no. 17; temperature 6° C. Triangles, right-hand scale: axon no. 21; temperature 8·5° C. At −100 mV. the maximum potassium conductance was 20 m.mho/cm.^{2} for axon no. 17 and 31 m.mho/cm.^{2} for axon no. 21.

with which they are permitted to cross the membrane under this driving force. If this is in fact the case, we should expect that sodium ions would cross the membrane in both directions, the observed I_{Na} being the difference between the opposing currents carried by these two fluxes. At the sodium potential

the fluxes would be equal, making I_{Na} zero; as the membrane potential is increased from this value, the ratio of inward to outward flux would increase, making I_{Na} positive, and vice versa.

By making certain very general assumptions about the manner in which ions cross the membrane it is possible to derive an equation which predicts the effect of sodium concentration on sodium current. The theory on which this equation depends is closely connected with those of Behn (1897), Teorell (1949*b*) and Ussing (1949), but differs from them, both in the assumptions from which it is derived and in the range of cases to which it applies.

We assume only that the chance that any individual ion will cross the membrane in a specified interval of time is independent of the other ions which are present. The inward flux M_1 of any ion species will therefore be proportional to the concentration c_1 of that ion in the external fluid, and will not be affected by c_2, its concentration inside the axon. We may therefore write

$$M_1 = k_1 c_1, \tag{7}$$

where k_1 is a constant which depends on the condition of the membrane and on the potential difference across it. Similarly, the outward flux M_2 is given by

$$M_2 = k_2 c_2, \tag{8}$$

where k_2 is another constant, determined by the same factors as k_1 but in general different from it. Hence

$$M_1/M_2 = k_1 c_1/k_2 c_2. \tag{9}$$

The condition for equilibrium is that $M_1 = M_2$, so that

$$k_2/k_1 = c_1^*/c_2,$$

where c_1^* is the external concentration that would be in equilibrium with the (fixed) internal concentration, under the existing value of E, the membrane potential.

Substituting for k_1/k_2 in (9), we have

$$M_1/M_2 = c_1/c_1^*. \tag{10}$$

Now $c_1^*/c_2 = \exp(-EF/RT)$ and $c_1/c_2 = \exp(-E^*F/RT)$, where E^* is the equilibrium potential for the ion under discussion, so that

$$c_1/c_1^* = \exp(E - E^*)\, F/RT$$

and

$$M_1/M_2 = \exp(E - E^*)\, F/RT. \tag{11}$$

We now have in Equations (7), (8) and (11) three simple relations between M_1, M_2, c_1 and E. The effect of membrane potential on either of the fluxes alone is not specified by these equations, but is immaterial for our purpose.

If we wish to compare the sodium currents when the axon is immersed first in sea water, with sodium concentration $[Na]_o$, and then in a low-sodium

solution with sodium concentration $[Na]'_o$, the membrane potential having the same value E in both cases, we have:

$$\frac{I'_{Na}}{I_{Na}} = \frac{M'_{Na_1} - M'_{Na_2}}{M_{Na_1} - M_{Na_2}}.$$

From (7), $M'_{Na_1}/M_{Na_1} = [Na]'_o/[Na]_o$ and from (8) $M'_{Na_2} = M_{Na_2}$. Using these relations and Equation (11)

$$\frac{I'_{Na}}{I_{Na}} = \frac{([Na]'_o/[Na]_o)\exp(E - E_{Na})F/RT - 1}{\exp(E - E_{Na})F/RT - 1}. \tag{12}$$

Strictly, activities should have been used instead of concentrations throughout. In the final Equation (12), however, concentrations appear only in the ratio of the sodium concentrations in sea water and the sodium-deficient solution. The total ionic strength was the same in these two solutions, so that the ratio of activities should be very close to the ratio of concentrations. The activity coefficient in axoplasm may well be different, but this does not affect Equation (12).

Equation (11) is equivalent to the relation deduced by Ussing (1949) and is a special case of the more general equation derived by Behn (1897) and Teorell (1949*b*). All these authors start from the assumption that each ion moves under the influence of an electric field, a concentration gradient and a frictional resistance proportional to the velocity of the ion in the membrane. This derivation is more general than ours in the respect that it is still applicable if, for instance, a change in c_1 alters the form of the electric field in the membrane and therefore alters M_2; in this case, Equations (8) and therefore (12) are not obeyed. On the other hand, it is more restricted than our derivation in that it specifies the nature of the resistance to movement of the ions.

Agreement with experimental results. Equation (12) is tested against experimental results in Fig. 13. Section (*a*) shows data from the experiment illustrated in Figs. 3 and 6*a*. The values of the sodium current in sea water (I_{Na}) and in 30% Na sea water (I'_{Na}) were derived by the procedure described in the 'Results' section. The crosses are the peak values of I_{Na}, plotted against V, the displacement of membrane potential during the voltage clamp. A smooth curve has been fitted to them by eye. V_{Na} was taken as the position at which the axis of V was cut by this curve. Since

$$V = E - E_r, \quad (E - E_{Na}) = (V - V_{Na}),$$

and, for each point on the smoothed curve of I_{Na} against V, a corresponding value of I'_{Na} was calculated by means of Equation (12). These values are plotted as curve B. The experimentally determined peak values of I'_{Na} are shown as circles. These are seen to form a curve of shape similar to B, but of greater amplitude. They are well fitted by curve C, which was obtained from B by multiplying all ordinates by the factor 1·20.

Fig. 13*b*, *c* were obtained in the same way from experiments in which the low-sodium solutions were 10% Na sea water and choline sea water respectively. In each case, the peak values of I'_{Na} are well fitted by the values predicted by means of Equation (12), after multiplying by constant factors of 1·333 and 1·60 in (*b*) and (*c*) respectively.

These constant factors appear at first sight to indicate a disagreement with the theory, but they are explained quantitatively by an effect which is described in the fourth paper of this series (Hodgkin & Huxley, 1952*b*). The

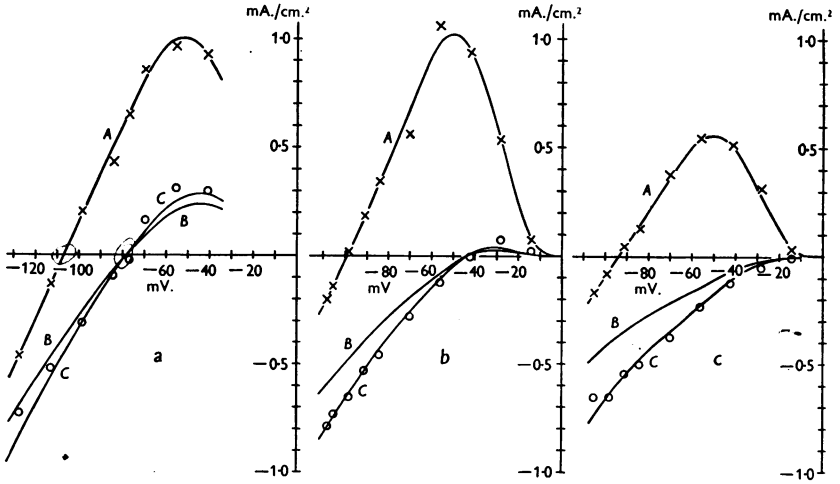

Fig. 13. Test of 'independence principle'. Three experiments. Crosses: peak sodium current density during voltage clamp; axon in sea water. Curve *A* fitted by eye. Circles: peak sodium current density during voltage clamp; axon in low sodium sea water. Curve *B*: peak sodium current density in low sodium sea water, predicted from curve *A* by Equation (12). Curve *C*: as curve *B*, but all ordinates multiplied by a factor *f*. Abscissa: membrane potential measured from resting potential in sea water. (*a*) Axon no. 20; temperature 6° C. Data from voltage clamps in (1) 30% sodium sea water, (2) sea water, (3) 30% sodium sea water. Circles are average values from runs (1) and (3). Value of V_{Na} inserted in Equation (12): −106·8 mV. Factor $f=1{\cdot}20$. (*b*) Axon no. 21; temperature 8·5° C. Data from voltage clamps in (1) 10% sodium sea water, (2) sea water, (3) 10% sodium sea water. Circles are average values from runs (1) and (3). $V_{Na}=-98{\cdot}8$ mV., $f=1{\cdot}333$. (*c*) Axon no. 21; temperature 8·5° C. Data from voltage clamps in (1) sea water, (2) choline sea water, (3) sea water, taken later than (*b*). Crosses are average values from runs (1) and (3). $V_{Na}=-93{\cdot}8$ mV., $f=1{\cdot}60$.

resting potential was higher in the low-sodium solutions than in sea water, and it is shown in that paper that increasing the membrane potential by current flow allows a subsequent depolarization to produce greater sodium currents than it would otherwise have done. The factor by which the sodium currents are thus increased is greater the lower the sodium concentration, and the poorer the condition of the fibre. The first of these effects explains why the factor is greater in (*b*) than in (*a*), while the second explains why it is greater in (*c*) than in (*b*). The experiments in Fig. 13*b*, *c* were performed on the same

fibre, and the deterioration between the experiments is shown by the fact that the I_{Na} values are only about half as great in (*c*) as in (*b*).

We can therefore say that, within experimental error, the sodium currents in sea water and in low-sodium solutions are connected by Equation (12), suggesting that the 'independence principle' from which this equation was derived is applicable to the manner in which the ions cross the membrane. This does not tell us much about the physical mechanism involved, since the 'independence' relations would be obeyed by several quite different systems. Examples are the 'constant field' system discussed by Goldman (1943), where the electric field through the membrane is assumed to be uniform and unaffected by the concentrations of ions present; and any system involving combination with carrier molecules in the membrane, so long as only a small proportion of the carrier is combined with the ion at any moment.

Origin of the action potential

The main conclusions that were drawn from the analysis presented in the 'Results' section of this paper may be summarized as follows. When the membrane potential is suddenly reduced (depolarization), the initial pulse of current through the capacity of the membrane is followed by large currents carried by ions (chiefly sodium and potassium), moving down their own electrochemical gradients. The current carried by sodium ions rises rapidly to a peak and then decays to a low value; that carried by potassium ions rises much more slowly along an S-shaped curve, reaching a plateau which is maintained with little change until the membrane potential is restored to its resting value.

These two components of the membrane current are enough to account qualitatively for the propagation of an action potential, the sequence of events at each point on the nerve fibre being as follows: (1) Current from a neighbouring active region depolarizes the membrane by spread along the cable structure of the fibre ('local circuits'). (2) As a result of this depolarization, sodium current is allowed to flow. Since the external sodium concentration is several times greater than the internal, this current is directed inwards and depolarizes the membrane still further, until the membrane potential reverses its sign and approaches the value at which sodium ions are in equilibrium. (3) As a delayed result of the depolarization, the potassium current increases and the ability of the membrane to pass sodium current decreases. Since the internal potassium concentration is greater than the external, the potassium current is directed outwards. When it exceeds the sodium current, it repolarizes the membrane, raising the membrane potential to the neighbourhood of the resting potential, at which potassium ions inside and outside the fibre are near to equilibrium.

The further changes which restore the membrane to a condition in which it

can propagate another impulse have also been studied by the 'voltage clamp' technique and are described in subsequent papers (Hodgkin & Huxley, 1952*a*, *b*). In the final paper of the series (Hodgkin & Huxley, 1952*c*), we show that an action potential can be predicted quantitatively from the voltage clamp results, by carrying through numerically the procedure which has just been outlined.

SUMMARY

1. The effect of sodium ions on the current through the membrane of the giant axon of *Loligo* was investigated by the 'voltage-clamp' method.

2. The initial phase of inward current, normally associated with depolarizations of 10–100 mV., was reversed in sign by replacing the sodium in the external medium with choline.

3. Provided that sodium ions were present in the external medium it was possible to find a critical potential above which the initial phase of ionic current was inward and below which it was outward. This potential was normally reached by a depolarization of 110 mV., and varied with external sodium concentration in the same way as the potential of a sodium electrode.

4. These results support the view that depolarization leads to a rapid increase in permeability which allows sodium ions to move in either direction through the membrane. These movements carry the initial phase of ionic current, which may be inward or outward, according to the difference between the sodium concentration and the electrical potential of the inside and outside of the fibre.

5. The delayed outward current associated with prolonged depolarization was little affected by replacing sodium ions with choline ions. Reasons are given for supposing that this component of the current is largely carried by potassium ions.

6. By making certain simple assumptions it is possible to resolve the total ionic current into sodium and potassium currents. The time course of the sodium or potassium permeability when the axon is held in the depolarized condition is found by using conductance as a measure of permeability.

7. It is shown that the sodium conductance rises rapidly to a maximum and then declines along an approximately exponential curve. The potassium conductance rises more slowly along an S-shaped curve and is maintained at a high level for long periods of time. The maximum sodium and potassium conductances were normally of the order of 30 m.mho/cm.^{2} at a depolarization of 100 mV.

8. The relation between sodium concentration and sodium current agrees with a theoretical equation based on the assumption that ions cross the membrane independently of one another.

REFERENCES

BEHN, U. (1897). Ueber wechselseitige Diffusion von Elektrolyten in verdünnten wässerigen Lösungen, insbesondere über Diffusion gegen das Concentrationsgefälle. *Ann. Phys., Lpz.*, N.F. **62**, 54–67.

COLE, K. S. & CURTIS, H. J. (1939). Electric impedance of the squid giant axon during activity. *J. gen. Physiol.* **22**, 649–670.

COLE, K. S. & HODGKIN, A. L. (1939). Membrane and protoplasm resistance in the squid giant axon. *J. gen. Physiol.* **22**, 671–687.

CURTIS, H. J. & COLE, K. S. (1942). Membrane resting and action potentials from the squid giant axon. *J. cell. comp. Physiol.* **19**, 135–144.

GOLDMAN, D. E. (1943). Potential, impedance, and rectification in membranes. *J. gen. Physiol.* **27**, 37–60.

HODGKIN, A. L. (1951). The ionic basis of electrical activity in nerve and muscle. *Biol. Rev.* **26**, 339–409.

HODGKIN, A. L. & HUXLEY, A. F. (1952*a*). The components of membrane conductance in the giant axon of *Loligo*. *J. Physiol.* **116**, 473–496.

HODGKIN, A. L. & HUXLEY, A. F. (1952*b*). The dual effect of membrane potential on sodium conductance in the giant axon of *Loligo*. *J. Physiol.* **116**, 497–506.

HODGKIN, A. L. & HUXLEY, A. F. (1952*c*). A quantitative description of membrane current and its application to conduction and excitation in nerve. *J. Physiol.* (in the press).

HODGKIN, A. L., HUXLEY, A. F. & KATZ, B. (1949). Ionic currents underlying activity in the giant axon of the squid. *Arch. Sci. physiol.* **3**, 129–150.

HODGKIN, A. L., HUXLEY, A. F. & KATZ, B. (1952). Measurement of current-voltage relations in the membrane of the giant axon of *Loligo*. *J. Physiol.* **116**, 424–448.

HODGKIN, A. L. & KATZ, B. (1949). The effect of sodium ions on the electrical activity of the giant axon of the squid. *J. Physiol.* **108**, 37–77.

KEYNES, R. D. & LEWIS, P. R. (1951). The sodium and potassium content of cephalopod nerve fibres. *J. Physiol.* **114**, 151–182.

MANERY, J. F. (1939). Electrolytes in squid blood and muscle. *J. cell. comp. Physiol.* **14**, 365–369.

STEINBACH, H. B. & SPIEGELMAN, S. (1943). The sodium and potassium balance in squid nerve axoplasm. *J. cell. comp. Physiol.* **22**, 187–196.

TEORELL, T. (1949*a*). *Annu. Rev. Physiol.* **11**, 545–564.

TEORELL, T. (1949*b*). Membrane electrophoresis in relation to bio-electrical polarization effects. *Arch. Sci. physiol.* **3**, 205–218.

USSING, H. H. (1949). The distinction by means of tracers between active transport and diffusion. *Acta physiol. scand.* **19**, 43–56.

WEBB, D. A. (1939). The sodium and potassium content of sea water. *J. exp. Biol.* **16**, 178–183.

WEBB, D. A. (1940). Ionic regulation in *Carcinus maenas*. *Proc. Roy. Soc.* B, **129**, 107–135.

J. Physiol. (1952) 116, 473–496

THE COMPONENTS OF MEMBRANE CONDUCTANCE IN THE GIANT AXON OF *LOLIGO*

BY A. L. HODGKIN AND A. F. HUXLEY

From the Laboratory of the Marine Biological Association, Plymouth, and the Physiological Laboratory, University of Cambridge

(*Received* 24 *October* 1951)

The flow of current associated with depolarizations of the giant axon of *Loligo* has been described in two previous papers (Hodgkin, Huxley & Katz, 1952; Hodgkin & Huxley, 1952). These experiments were concerned with the effect of sudden displacements of the membrane potential from its resting level ($V=0$) to a new level ($V=V_1$). This paper describes the converse situation in which the membrane potential is suddenly restored from $V=V_1$ to $V=0$. It also deals with certain aspects of the more general case in which V is changed suddenly from V_1 to a new value V_2. The experiments may be conveniently divided into those in which the period of depolarization is brief compared to the time scale of the nerve and those in which it is relatively long. The first group is largely concerned with movements of sodium ions and the second with movements of potassium ions.

METHODS

The apparatus and method were similar to those described by Hodgkin *et al.* (1952). The only new technique employed was that on some occasions two pulses, beginning at the same moment but lasting for different times, were applied to the feed-back amplifier in order to give a wave form of the type shown in Fig. 6. The amplitude of the shorter pulse was proportional to $V_1 - V_2$, while the amplitude of the longer pulse was proportional to V_2. The resulting changes in membrane potential consisted of a step of amplitude V_1, during the period when the two pulses overlap, followed by a second step of amplitude V_2.

RESULTS

Experiments with relatively brief depolarizations

Discontinuities in the sodium current

The effect of restoring the membrane potential after a brief period of depolarization is illustrated by Fig. 1. Record *A* gives the current associated with a maintained depolarization of 41 mV. As in previous experiments, this consisted of a wave of inward current followed by a maintained phase of

outward current. Only the beginning of the second phase can be seen at the relatively high time base speed employed. At 0·85 msec. the ionic current reached a value of 1·4 mA./cm.^{2}. Record *B* shows the effect of cutting short the period of depolarization at this time. The sudden change in potential was associated with a rapid surge of capacity current which is barely visible on the time scale employed. This was followed by a 'tail' of ionic current which

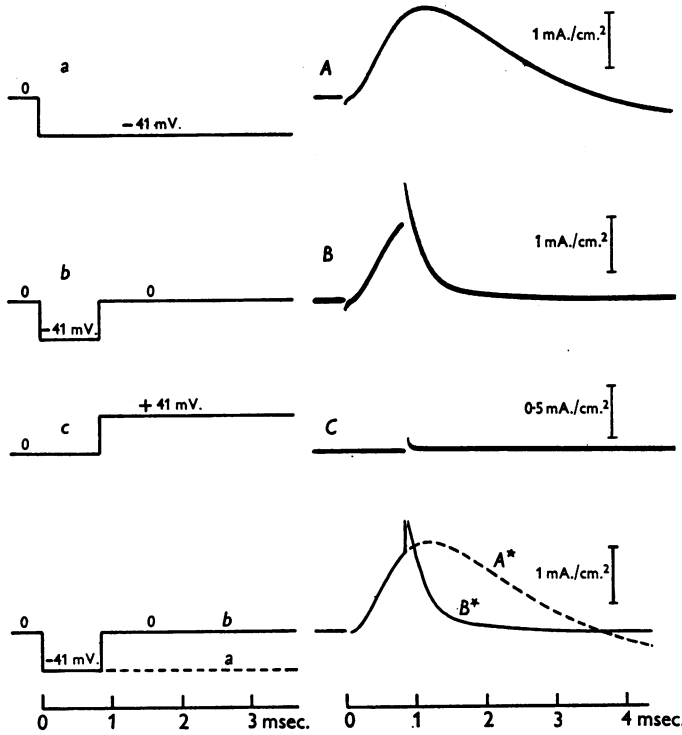

Fig. 1. Left-hand column: *a*, *b*, *c*, time course of potential difference between external and internal electrode. Right-hand column: *A*, *B*, *C*, records of membrane current associated with changes in membrane potential shown in left-hand column. (The amplification in *C* was 90% greater than that in *A* and *B*.) *A**, *B**, time course of ionic currents obtained by subtracting capacity current in *C* from *A* and *B*. Axon 25; temperature 5° C.; uncompensated feed-back. Inward current is shown upward in this and all other figures except Fig. 13.

started at about 2·2 mA./cm.^{2} and declined to zero with a time constant of 0·27 msec. The residual effects of the capacitative surge were small and could be eliminated by subtracting the record obtained with a corresponding anodal displacement (*C*). Curves corrected by this method are shown in *A** and *B**.

The first point which emerges from this experiment is that the total period of inward current is greatly reduced by cutting short the period of depolarization. This suggests that the process underlying the increase in sodium permeability is reversible, and that repolarization causes the sodium current to

fall more rapidly than it would with a maintained depolarization. Further experiments dealing with this phenomenon are described on p. 482. At present our principal concern is with the discontinuity in ionic current associated with a sudden change of membrane potential. Fig. 2*D* illustrates the discontinuity in a more striking manner. In this experiment the nerve was depolarized nearly to the sodium potential, so that the ionic current was relatively small during the pulse.

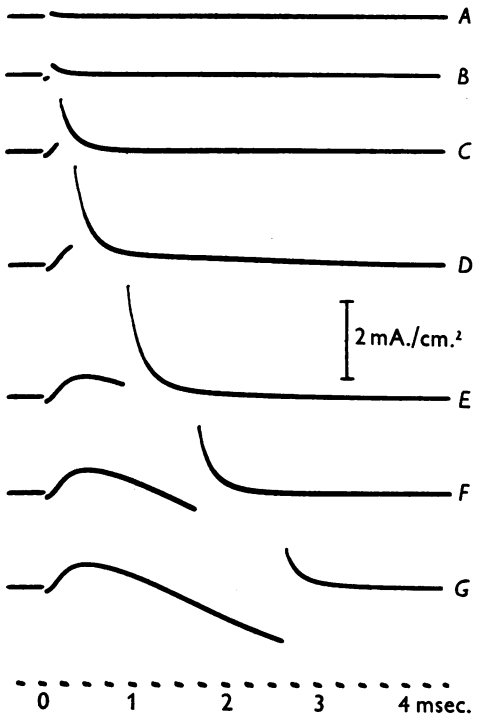

Fig. 2. Records of membrane current associated with depolarization of 97·5 mV. lasting, 0·05, 0·08, 0·19, 0·32, 0·91, 1·6 and 2·6 msec. The time and current calibration apply to all records. Axon 41; temperature 3·5° C.; compensated feed-back.

The other records in Fig. 2 illustrate the effect of altering the duration of the pulse. The surge of ionic current was small when the pulse was very short; it reached a maximum at a duration of 0·5 msec. and then declined with a time constant of about 1·4 msec. For durations less than 0·3 msec. the surge of ionic current was roughly proportional to the inward current at the end of the pulse. Since previous experiments suggest that this inward current is carried by sodium ions (Hodgkin & Huxley, 1952), it seems likely that the tail of inward current after the pulse also consists of sodium current. Fig. 3 illustrates an experiment to test this point. In *A*, the membrane was initially depolarized to the sodium potential. The ionic current was very small during the pulse but

the usual tail followed the restoration of the resting potential. The sequence of events was entirely different when choline was substituted for the sodium in the external fluid (Fig. 3*B*). In this case there was a phase of outward current during the pulse but no tail of ionic current when the membrane potential was restored. The absence of ionic current after the pulse is proved by the fact that the capacitative surges obtained with anodal and cathodal displacements were almost perfectly symmetrical (records *B* and *C*). These effects are explained quite simply by supposing that sodium permeability rises when the membrane is depolarized and falls exponentially after it has been repolarized.

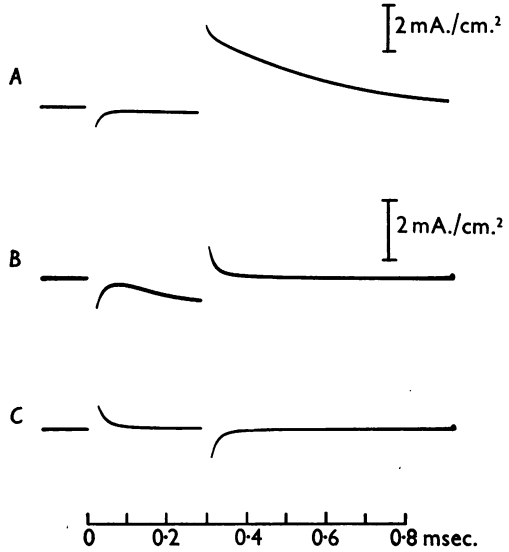

Fig. 3. *A*, membrane current associated with depolarization of 110 mV. lasting 0·28 msec.; nerve in sea water. *B*, same, but with nerve in choline sea water. *C*, membrane currents associated with an increase of 110 mV. in membrane potential; nerve in choline sea water. Axon 25; temperature 5° C.; uncompensated feed-back.

In record *A* the increase in permeability did not lead to any current during the pulse, since inward and outward movements of sodium are equal at the sodium potential. After the pulse the tendency of external sodium ions to enter the fibre is very much greater than that of internal sodium ions to leave. This means that there must be a large inward current after the pulse unless the sodium permeability reverts instantaneously to a low value. Record *B* is different because there were no external sodium ions to carry the current in an inward direction. The increase in sodium permeability therefore gave a substantial outward current during the period of depolarization but no inward current after the pulse. One might expect to see a 'tail' of outward current in *B* corresponding to the tail of inward current in *A*. However, the tendency of the internal sodium ions to leave the fibre against the resting

potential difference would be so small that the resulting outward current would be indistinguishable from the capacitative surge. According to the 'independence principle' (Hodgkin & Huxley, 1952, equation 12), the outward current in *B* should be only 1/97 of the inward current in *A*.

Continuity of sodium conductance

Discontinuities such as those in Figs. 1, 2 and 3*A* disappear if the results are expressed in terms of the sodium conductance (g_{Na}). This quantity was defined previously by the following equation:

$$g_{Na} = I_{Na}/(V - V_{Na}), \quad (1)$$

where V is the displacement of the membrane potential from its resting value and V_{Na} is the difference between the equilibrium potential for sodium ions and the resting potential (Hodgkin & Huxley, 1952).

The records in Fig. 4 allow g_{Na} to be estimated as a function of time. Curves α and *A* give the total ionic current for a nerve in sea water. Curve α was obtained with a maintained depolarization of 51 mV. and *A* with the same depolarization cut short at 1·1 msec. Curves β and *B* are a similar pair with the nerve in choline sea water. Curves γ and *C* give the sodium current obtained from the two previous curves by essentially the method used in the preceding paper (see Hodgkin & Huxley, 1952). In this experiment the depolarization was 51 mV. and the sodium potential was found to be −112 mV. To convert sodium current into sodium conductance the former must therefore be divided by 61 mV. during the depolarization or by 112 mV. after the pulse. Curves δ and *D* were obtained by this procedure and show that the conductance reverts to its resting level without any appreciable discontinuity at the end of the pulse. Fig. 5 illustrates the results of a similar analysis using the records shown in Fig. 2. In this experiment no tests were made in choline sea water, but the early part of the curve of sodium current was obtained by assuming that sodium current was zero initially and that the contribution of other ions remained at the level observed at the beginning of the pulse. Records made at the sodium potential (−117 mV.) indicated that the error introduced by this approximation should not exceed 5% for pulses shorter than 0·5 msec.

The instantaneous relation between ionic current and membrane potential

The results described in the preceding section suggest that the membrane obeys Ohm's law if the ionic current is measured immediately after a sudden change in membrane potential. In order to establish this point we carried out the more complicated experiment illustrated by Fig. 6. Two rectangular pulses were fed into the feed-back amplifier in order to produce a double step of membrane potential of the type shown inset in Fig. 6. The first step had a duration of 1·53 msec. and an amplitude of −29 mV. The second step was relatively long and its amplitude was varied between −60 mV. and +30 mV.

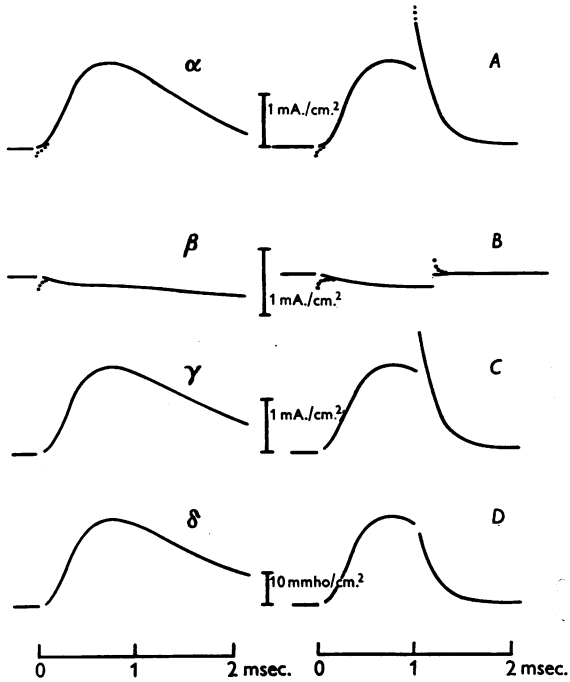

Fig. 4. α, ionic current in sea water associated with maintained depolarization of 51 mV. applied at $t=0$. (The dotted line shows the form of the original record before correcting for capacity current.) β, same in choline sea water. γ, sodium current estimated as $(\alpha-\beta)\times 0{\cdot}92$. δ, sodium conductance estimated as $\gamma/61$ mV. A, B, same as α and β respectively, but with depolarization lasting about 1·1 msec. C, sodium current estimated as $(A-B)\times 0{\cdot}92$ during pulse or $(A-B)\times 0{\cdot}99$ after pulse. D, sodium conductance estimated as $C/61$ mV. during pulse or $C/112$ mV. after pulse. The factors 0·92 and 0·99 allow for the outward sodium current in choline sea water and were obtained from the 'independence principle'. Axon 17; temperature 6° C.; V_{Na} in sea water $=-112$ mV.; uncompensated feed-back.

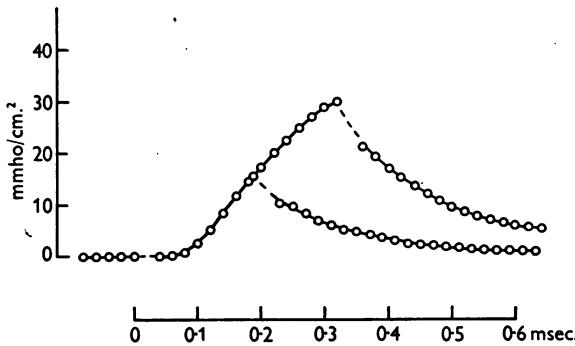

Fig. 5. Time course of sodium conductance estimated from records C and D (Fig. 2) by method described in text. At zero time the membrane potential was reduced by 97·5 mV. and was restored to its resting value at 0·19 msec. (lower curve) or 0·32 msec. (upper curve). The broken part of the curve has been interpolated in the region occupied by the capacitative surge. Axon 41; temperature 3·5° C.; compensated feed-back; $V_{Na}=-117$ mV.

The ordinate (I_2) is the ionic current at the beginning of the second step and the abscissa (V_2) is the potential during the second step. Measurement of I_2 depends on the extrapolation shown in Fig. 6*A*. This should introduce little error over most of the range but is uncertain for $V_2 > 0$, since the ionic current then declined so rapidly that it was initially obscured by capacity current. There was some variation in the magnitude of the current observed during the first pulse. This arose partly from progressive changes in the condition of the

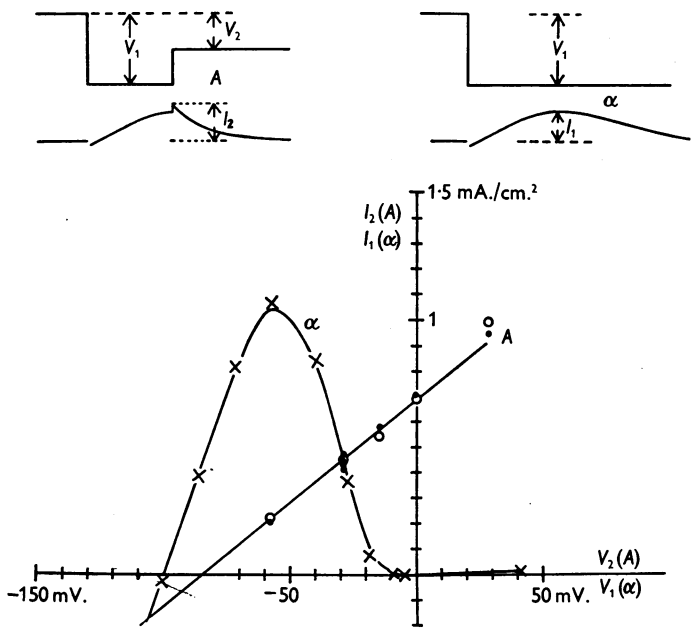

Fig. 6. Line *A*, instantaneous current-voltage relation. The first step had an amplitude of −29 mV. and a duration of 1·53 msec. The abscissa (V_2) gives the amplitude of the second step. The ordinate (I_2) is the ionic current at the beginning of the second step. The dots are observed currents. Hollow circles are these currents multiplied by factors which equalize the currents at the end of the first step. Inset *A*, method of measuring V_2 and I_2. Curve α and crosses, relation between maximum inward current (I_1) and membrane potential using single pulse of amplitude V_1. Inset α, method of measuring V_1 and I_1. Axon 31; temperature 4° C.; uncompensated feed-back.

nerve and partly from small changes in V_1 which cause large variations in current in the region of $V = -29$ mV. Both effects were allowed for by scaling all records so that the current had the same amplitude at the end of the first step. This procedure is justified by the fact that records made with $V_2 = 0$ show that the amplitude of the current immediately after the step was directly proportional to the current immediately before it.

The results are plotted in curve *A* and show that the relation between I_2 and V_2 is approximately linear. This is in striking contrast to the extremely non-

linear relation obtained when the current is measured at longer intervals. An example of the second type is provided by curve α which shows how the maximum inward current varied with membrane potential in the same axon. In this case only a single pulse of variable amplitude was employed and current was measured at times of 0·5–2·0 msec. Under these conditions the sodium conductance had time to reach the value appropriate to each depolarization and the current-voltage relation is therefore far from linear.

The line A and the curve α intersect at -29 mV. since the two methods of measurement are identical if $V_2 = V_1$. A second intersection occurs at -106 mV. which is close to the sodium potential in this fibre.

A similar pair of curves obtained with a larger initial depolarization is shown by A and α in Fig. 7. In this case the nerve was depolarized to the sodium potential so that one would expect the line A to be tangential to the curve α. This is approximately true, although any exact comparison is invalidated by the fact that the two curves could not be obtained at exactly the same time.

The instantaneous current-voltage relation in sodium-free solution

The measurements described in the preceding section indicate that the instantaneous behaviour of the membrane is linear when the nerve is in sea water. The conclusion cannot be expected to apply for all sodium concentrations. The method of defining a chord conductance breaks down altogether if there is no sodium in the external medium. In this case $V_{Na} = \infty$ and g_{Na} must be zero if the sodium current is to be finite. This condition could not be realized in practice but the theoretical possibility of its existence indicates that the concept of sodium conductance must be used with caution.

The lower part of Fig. 7 illustrates an attempt to determine the instantaneous current-voltage relation in a sodium-free solution. The upper curves (A and α) were measured in sea water and have already been described. The crosses in the lower part of the figure give the instantaneous currents in choline sea water, determined in the same way as the circles which give the corresponding relation in sea water. The effect of the change in resting potential has been allowed for by shifting the origin to the right by 4 mV. (see Hodgkin & Huxley, 1952). The series of records from which these measurements were made was started shortly after replacing normal sea water by choline sea water and was continued, in the order shown, with an interval of about 40 sec. between records. On analysis it was found that the earliest records (e.g. 1) showed a small inward current, whereas records taken later (e.g. 11 or 15) gave no such effect. It is evident that the series was started before all the sodium had diffused away from the nerve and that only the later records (e.g. 6–15) can be regarded as representative of a nerve in a sodium-free solution. Nevertheless, it is clear that the instantaneous current-voltage relation shows a marked curvature and is quite different from the linear relation in sea water.

The results are, in fact, reasonably close to those predicted by the 'independence principle'. This is illustrated by a comparison of the crosses in Fig. 7 with the theoretical curves *B* and *C* which were calculated from *A* on the assumption that the independence principle holds and that the sodium

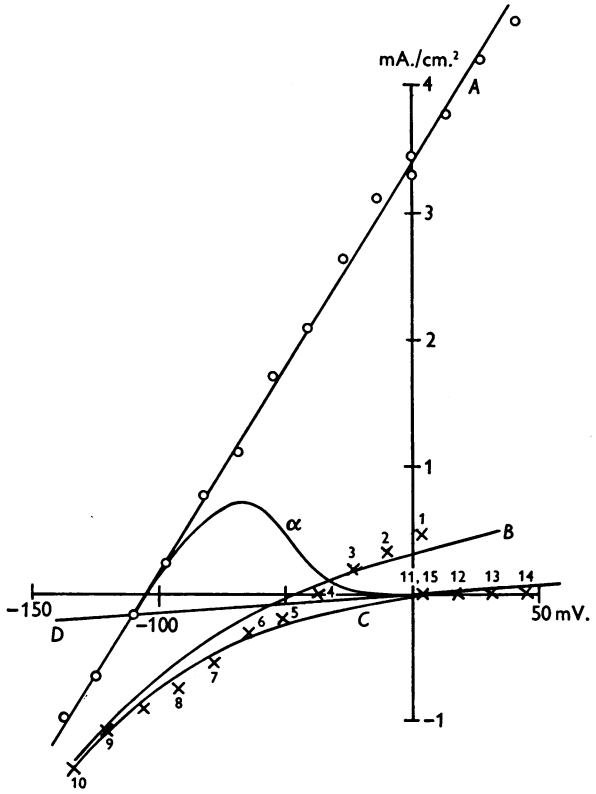

Fig. 7. Current-voltage relations in sea water and choline sea water. Ordinate: current density. Abscissa: displacement of membrane potential from resting potential in sea water. Line *A* and curve α were obtained in sea water in the same way as in Fig. 6, except that the current for α was not measured at the maximum but at a fixed time (0·28 msec.) after application of a single step. The initial depolarization for *A* was 110 mV. and the duration of the first step was 0·28 msec. The crosses give the instantaneous currents in choline sea water, determined in the same way as the circles in *A*. The numbers show the order in which the measurements were made. *B* and *C*, instantaneous current in 10% sodium sea water and in choline sea water respectively, derived from *A* by means of the 'independence principle' using the equations

$$\frac{(I_{Na})_B}{(I_{Na})_A} = \frac{0{\cdot}1 \exp{(V - V_{Na})/24} - 1}{\exp{(V - V_{Na})/24} - 1}$$

and

$$\frac{(I_{Na})_C}{(I_{Na})_A} = \frac{-1}{\exp{(V - V_{Na})/24} - 1},$$

V_{Na} = sodium potential in sea water = −110 mV. Sodium currents measured from the line *D* which passes through the origin and the point for the small current observed at the sodium potential in sea water. Axon 25; temperature 5° C.; uncompensated feed-back.

concentrations in the external solution were 10% (*B*) and 0% (*C*) of that in *A*. It will be seen that there is general agreement between calculated and observed results, although the change in external sodium and the possibility of progressive changes invalidates any exact comparison. In the preceding paper it was shown that the observed sodium currents in a choline solution were usually larger than those calculated from the independence principle. This deviation is not seen here, probably because the measurements in choline were made later than those in sea water and no attempt was made to correct for deterioration, which is likely to have reduced the currents by 30% between the sea water and choline runs.

The experiment described in the preceding paragraph indicates that the linear relation between current and voltage observed in sea water is not a general property of the membrane since it fails in sodium-free solutions. This does not greatly detract from the usefulness of the result, for the primary concern of this paper is to determine the laws governing ionic movements under conditions which allow a normal action potential to be propagated.

The reversible nature of the change in sodium conductance

The results described in the first part of this paper show that the sodium conductance reverts rapidly to a low value when the membrane potential is restored to its resting value. Figs. 2 and 5 suggest that this is true at all stages of the response and that the rate at which the conductance declines is roughly proportional to the value of the conductance. A rate constant (b_{Na}) can be defined by fitting a curve of the form $\exp(-b_{Na}t)$ to the experimental results. Values obtained by this method are given in Table 1.

In order to investigate the effect of repolarizing the membrane to different levels on the rate of decline of sodium conductance we carried out the experiment illustrated by Fig. 8. The curves in the left-hand column are tracings of the membrane current while those on the right give the sodium conductance, calculated on the assumption that the contribution of ions other than sodium is negligible (records made in a solution containing 10% of the normal sodium concentration show that the error introduced by this approximation should not exceed 5% of the maximum current). The initial depolarization was 29 mV. and the sodium conductance reached its maximum value in 1·53 msec. When the membrane potential was restored to its resting level the conductance fell towards zero with a rate constant of about 4·3 msec.$^{-1}$ (curve γ). If V_2 was made +28 mV. the rate constant increased to about 10 msec.$^{-1}$ and a further increase to 15 msec.$^{-1}$ occurred with $V_2 = +57$ mV. On the other hand, if V_2 was reduced to −14 mV. the conductance returned with a rate constant of only 1·6 msec.$^{-1}$. When $V_2 = -57$ mV. the conductance no longer fell but increased towards an 'equilibrium' value which was greater than that attained at −29 mV. (The curve cannot be followed beyond about 2 msec.

TABLE 1. Apparent values of rate constant determining decline of sodium conductance following repolarization to resting potential

Axon	Membrane potential during pulse (mV.)	Duration of pulse (msec.)	Temperature (° C.)	Average rate constant (msec.$^{-1}$)	Rate constant at 6° C. (msec.$^{-1}$)
15	−32	0·4–1·1	11	9·4	5·4
15	−91	0·1–0·5	11	9·0	5·2
17	−32	0·7–1·6	6	5·9	5·8
17	−51	0·2–1·0	6	6·7	6·6
24	−42	0·2	20	18·5	4·1
24	−84	0·1	20	17·2	3·9
25	−41	1·0	4	3·8	4·8
25	−110	0·3	4	3·3	4·0
31	−100	0·3	4	3·0	3·8
31	−29	1·5	4	4·2	5·3
32	−116	0·2	5	6·3*	6·9*
32	−67	0·7	5	6·3*	6·8*
41	−98	0·1–4	3	7·1*	9·6*
41	−117	0·1–3	3	7·7*	10·5*

Results marked with an asterisk were obtained with compensated feed-back. The last column is calculated on the assumption that the temperature coefficient (Q_{10}) of the rate constant is 3.

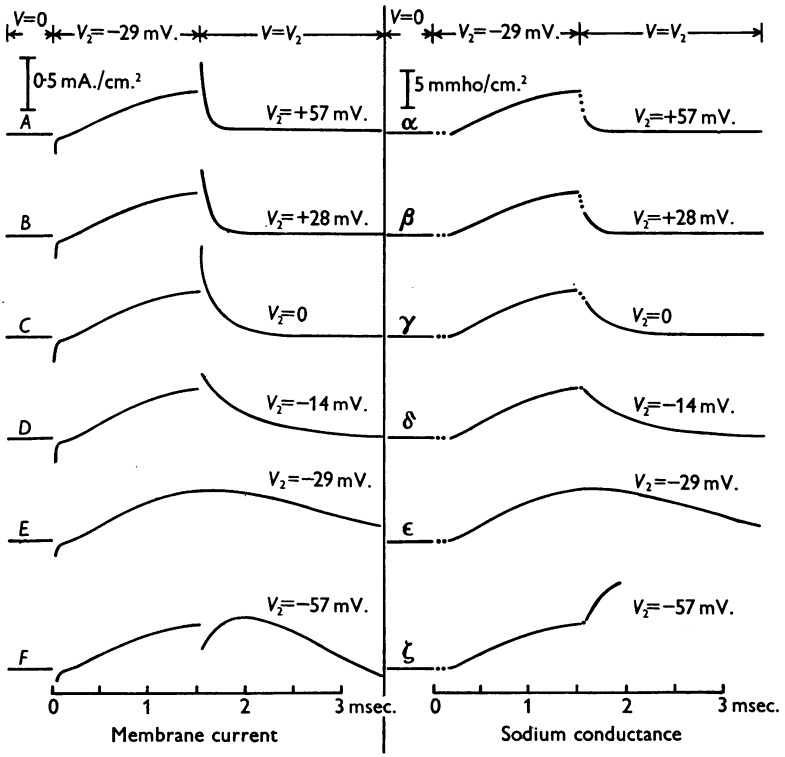

Fig. 8. *A–F*, time course of membrane current associated with change in membrane potential shown at top of figure. α–ζ; time course of sodium conductance obtained by dividing *A–F* by $V+100$ mV. Axon 31; temperature 4° C.; uncompensated feed-back.

because the contribution of potassium ions soon becomes important at large depolarizations.) The whole family of curves suggests that the conductance reached at any depolarization depends on the balance of two processes occurring at rates which vary in opposite directions with membrane potential.

The observation that the rate constant increases with membrane potential does not depend on the details of the method used to estimate sodium conductance, for the tracings of current in the left-hand column of Fig. 8 show exactly the same phenomenon. Similar results were obtained in all the experiments of this type, and are plotted against V_2 in Fig. 9. It will be seen that there is good agreement between different experiments, and that a tenfold increase of rate constant occurs between $V_2 = -20$ and $+50$ mV.

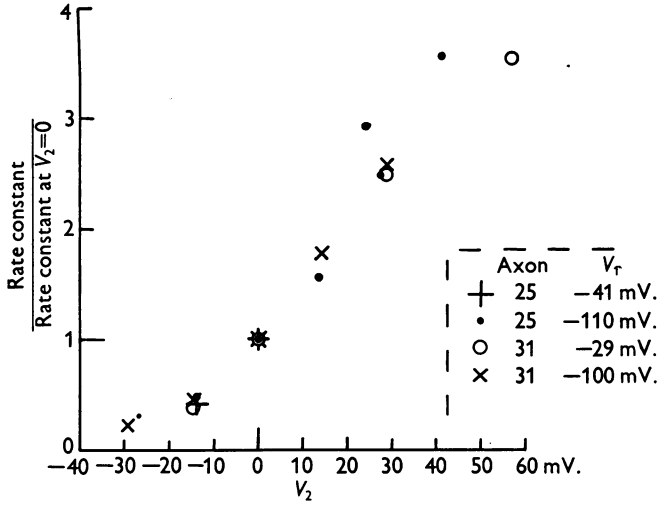

Fig. 9. Relation between rate constant determining decline of sodium conductance and potential to which membrane is repolarized. Abscissa: membrane potential during second step (V_2). Ordinate: relative value of rate constant.

Errors due to the series resistance

Most of the experiments in this paper were obtained with uncompensated feed-back and must therefore have been somewhat affected by the small resistance in series with the membrane (Hodgkin *et al.* 1952). The linearity of the relation between current and voltage illustrated by Figs. 6 and 7 can clearly stand, for the effect of a series resistance would simply be to change the slope of the straight line and not to introduce any curvature. From our estimates of the value of the series resistance it can be shown that the true slopes in these two figures should be 7 and 30% greater than those shown. A more serious error is introduced in the measurement of the rate constant. In Fig. 8 the total current at the beginning of the record was about 0·5 mA./cm.^{2}. This means that the true membrane potential was not zero but about -4 mV. At this potential the rate of return of membrane conductance would be slowed by about 8%. In some of the experiments used in compiling Table 1 this error may be as great as 50%. However, it should be small in axons 32 and 41 which were examined with compensated feed-back. We are also uncertain about the extent to which the rate of return of sodium conductance can be regarded as exponential. Axon 41, which was in excellent condition and was examined with compensated feed-back, showed clear depar-

tures from exponential behaviour in that the initial fall of conductance was too rapid (see Figs. 2 and 5). In all other experiments the curves of current against time were reasonably close to exponentials, but in many cases this may have been due to an error introduced by the series resistance.

Errors due to polarization effects

If the membrane was maintained in the depolarized condition for long periods of time the outward current declined as a result of a 'polarization effect' (Hodgkin *et al.* 1952). At the end of such a pulse a phase of inward current was observed and was found to be roughly proportional to the amount of 'polarization'. This was quite distinct from the inward current described in the preceding sections, since it only appeared with long pulses and was unaffected by removing external sodium. With the possible exception of Fig. 2*G*, the results described in the preceding sections are unlikely to have been affected by polarization since the duration of the pulse was always kept short.

The time course of the sodium conductance during a maintained depolarization

In a previous paper we showed that the time course of the sodium conductance could be obtained from records of membrane current in solutions of different sodium concentration (Hodgkin & Huxley, 1952). An alternative method of calculating these curves is illustrated by Fig. 10. The method

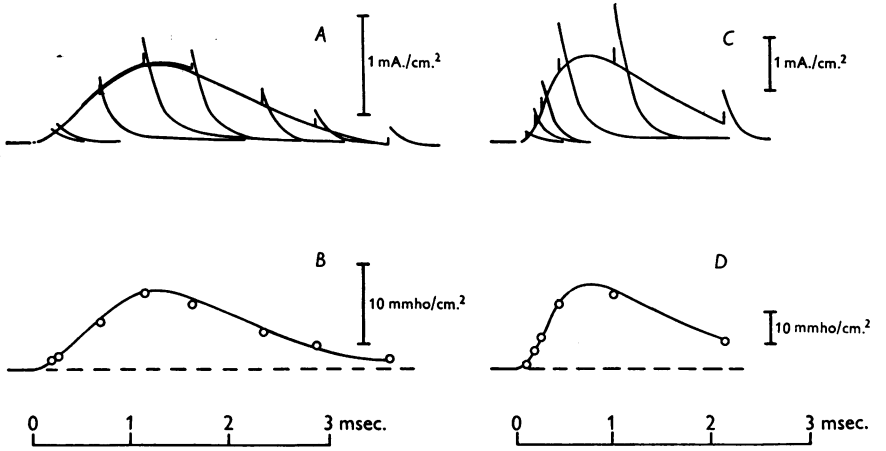

Fig. 10. *A*, time course of ionic currents associated with depolarizations of 32 mV. lasting from $t=0$ to times indicated by vertical strokes on tracings. Nerve in sea water. *B*, time course of sodium conductance. The circles were obtained by dividing the peak currents in *A* by 112 mV. and the continuous curve from the difference between the continuous curve in *A* and a similar curve in choline sea water (see text and legend to Fig. 4). *C*, same as *A* but employing depolarization of 51 mV. *D*, sodium conductance obtained from *C* by similar methods to those used for *B*. (The smooth curve is the same as that shown in Fig. 4.) Axon 17; temperature 6° C.; V_{Na} in sea water $= -112$ mV.; uncompensated feed-back.

depends on the fact that the inward current immediately after a pulse is proportional to the sodium conductance at the end of the preceding depolarization. The variation of inward current with pulse duration is illustrated by the tracings in Fig. 10*A*. The time course of the sodium conductance can be measured by determining the maximum ionic current associated with repolar-

ization and dividing this quantity by the difference between the resting potential and the sodium potential (about −112 mV. in this experiment). A series of points obtained by this method is shown in Fig. 10*B*. These may be compared with the smooth curve, which represents sodium conductance obtained by the method described in the preceding paper (subtraction of ionic current in choline from that in sea water). Good agreement was obtained, and also when other depolarizations were employed, for example *C* and *D* at −51 mV. The only occasions on which the two methods did not agree were those in which the sodium conductance was measured at long times, with a large depolarization. In these experiments the subtraction method sometimes gave an apparent negative conductance which we regarded as an error due to slight differences between the potassium currents in the two records. This conclusion was confirmed by the fact that the alternative method never showed a 'negative conductance' but only a residual positive conductance.

Experiments with relatively long depolarizations

The instantaneous relation between potassium current and membrane potential

In a previous paper (Hodgkin & Huxley, 1952) we gave reasons for thinking that potassium ions were largely responsible for carrying the maintained outward current associated with prolonged depolarization of the membrane. In order to investigate the instantaneous relation between potassium current and membrane potential it is necessary to employ depolarizations lasting for much longer periods than those used to study sodium current. Polarization effects made such experiments difficult at 5° C., but errors from this cause could be greatly reduced by working at 20° C. In this case the polarization effect occurred at the same rate but the potassium conductance rose in about one-fifth of the time required at 5° C.

A typical experiment with a nerve in choline sea water is illustrated by Fig. 11. Its general object is to measure the ionic currents associated with repolarization of the membrane when the potassium conductance is much greater than the sodium conductance. The amplitude of the first step was −84 mV. and its duration 0·63 msec., which is equivalent to about 4 msec. at 5° C. Under these conditions 90–95% of the outward current should be potassium current and only 5–10% should be sodium current (see Fig. 10 for an indication of the rate of fall of sodium conductance from its initial maximum). After the pulse, sodium current should be negligible since the nerve was in choline sea water (see Fig. 3).

The simplest record in Fig. 11 is *E*, in which the membrane potential was restored to its resting value at the end of the first step. The sequence of events was as follows. At $t=0$ the membrane was depolarized by 84 mV. and was held at this level until $t=0{\cdot}63$ msec. The current was outward during the whole period and consisted of a hump of sodium current followed by a rise of

potassium current which reached 1·83 mA./cm.^{2} at $t=0·63$ msec. At this moment the membrane potential was restored to its resting value. The sudden increase in potential was associated with a brief capacity current in an inward direction. This was followed by an outward current which declined exponentially to zero. A record at higher amplification (*e*) shows this 'tail' of outward current more clearly. The dots give the ionic current extrapolated to

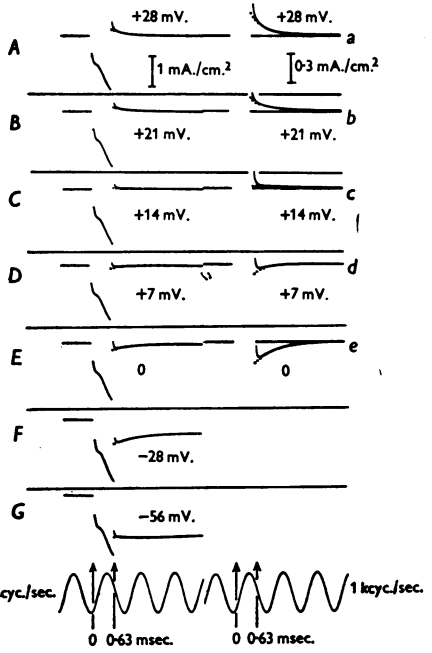

Fig. 11. Membrane currents associated with depolarization of 84 mV. followed by repolarization to value shown on each record. The duration of the first step was 0·63 msec. The second step lasted longer than these records. *A* to *G*, records at low amplification showing current during both steps. *a–e*, records at higher amplification showing only the current during the second step. The dots give the ionic current after correcting for capacity current. Axon 26 in choline sea water; temperature 20° C.; uncompensated feed-back.

$t=0·63$ msec. after correcting for the residual effect of the capacitative surge. The 'tail' of outward current can be explained by supposing that the equilibrium potential for potassium is about 12 mV. greater than the resting potential in choline sea water, and that the instantaneous value of the potassium conductance (g_K) is independent of V. At $t=0·63$ msec. the current is 1·83 mA./cm.^{2} when $V=-84$ mV., or 0·22 mA./cm.^{2} when $V=0$. Taking the potassium potential (V_K) as +12 mV. and neglecting the contribution of chloride and other ions it follows that the potassium conductance (g_K) was approximately the same in the two cases. Thus

$$g_K=I_K/(V-V_K), \qquad (2)$$

so that

$$g_K = \frac{-1{\cdot}83 \text{ mA./cm.}^2}{-96 \text{ mV.}} = 19 \text{ m.mho/cm.}^2 \quad \text{when } V = -84 \text{ mV.},$$

and

$$g_K = \frac{-0{\cdot}22 \text{ mA./cm.}^2}{-12 \text{ mV.}} = 18 \text{ m.mho/cm.}^2 \quad \text{when } V = 0.$$

As soon as the membrane potential is restored to its resting value the potassium conductance reverts exponentially to its resting level and therefore gives the tail of current seen in E and e. If this explanation is right, the exponential tail of current should disappear at $V = V_K$ and should be reversed in sign when $V > V_K$. Records a to d show that the current is inward for $V > 21$ mV. and is outward for $V < 7$ mV. There is practically no inward current at $V = 14$ mV. and 13 ± 1 mV. would seem to be a reasonable estimate of V_K.

This method of measuring the potassium potential depends on the assumption that potassium ions are the only charged particles responsible for the component of the current which varies with time after the end of the pulse. It is not affected by the fact that chloride and other ions may carry appreciable quantities of current, provided that the resistance to the motion of these ions is constant at any given value of membrane potential. The magnitude of the 'leak' due to chloride and other ions may be estimated from the current needed to maintain the membrane at the potassium potential. In the experiment illustrated by Fig. 11 this current was about 0·008 mA./cm.^{2} which is small compared with the maximum potassium current at $V = 0$ or $V = +28$ mV.

Fig. 12 was prepared from the records in Fig. 11 by essentially the same method as that used in studying the instantaneous relation between sodium current and membrane potential. Curve α gives the relation between current and voltage 0·63 msec. after the application of a single step of amplitude V_1. In curve A, V_1 was fixed at -84 mV. and the potential was changed suddenly to a new level V_2. The abscissa is V_2, while the ordinate is the ionic current immediately after the sudden change. The experimental points in A are seen to fall very close to a straight line which crosses curve α at the potassium potential ($+13$ mV.). In this experiment no measurements were made with $V_2 < V_1$ but records obtained with other fibres showed that the instantaneous current-voltage relation was linear for $V_2 < V_1$ as well as for $V_2 > V_1$.

In the experiment considered in the previous paragraphs the initial rise of potassium current was obscured by sodium current and the plateau was not reached because the pulse was kept short in order to reduce possible errors from the 'polarization effect'. A clearer picture of the sequence of events is provided by Fig. 13. In this experiment the amplitude of the pulse was -25 mV. and its duration nearly 5 msec. The polarization effect was not appreciable since the current density was relatively small. Sodium current was also small since the nerve was in choline sea water, and the depolarization

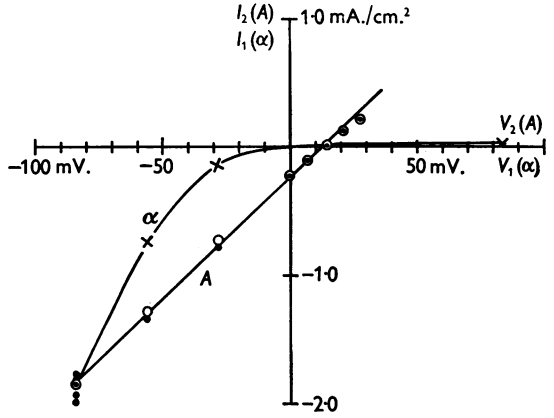

Fig. 12. Current-voltage relations during period of high potassium permeability. Line *A*, instantaneous current-voltage relation determined by changing membrane potential in two steps. The first step had a constant amplitude of −84 mV. and a constant duration of 0·63 msec. The abscissa (V_2) gives the amplitude of the second step in millivolts. The ordinate (I_2) is the ionic current density at the beginning of the second step. The dots are observed currents. Hollow circles are these currents multiplied by factors which equalize the currents at the end of the first step. Curve α and crosses, relation between current and membrane potential at 0·63 msec. after beginning of single step of amplitude V_1. Experimental details are as in Fig. 11.

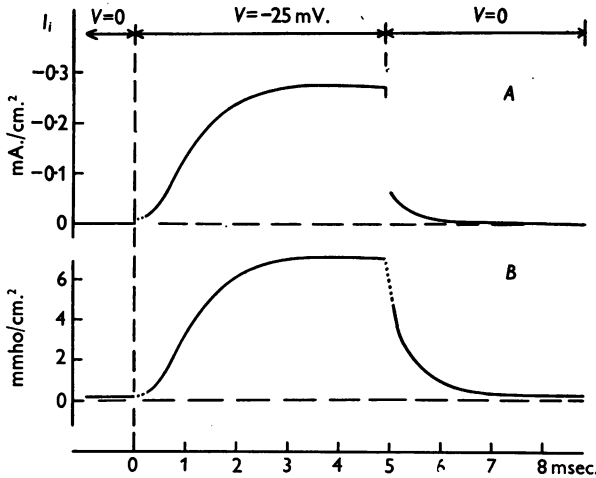

Fig. 13. *A*, ionic current associated with depolarization of 25 mV. lasting 4·9 msec. Axon 18 in choline sea water at a temperature of 21° C. The curve is a direct replot of the original current record except in the regions 0–0·3 msec. and 4·9–5·2 msec., where corrections for capacity current were made by the usual method. Outward current shown upward. *B*, potassium conductance estimated from *A* by the equation $g_K = I_K/(V - V_K)$, where V_K is 12 mV. and I_K is taken as the ionic current (I_i) minus a leakage current of 0·5 m.mho/cm.² × (V + 4 mV.).

was less than that at which a hump of outward sodium current first became appreciable. On the other hand, it was desirable to make a small correction for the leakage current due to ions other than sodium and potassium. The method of estimating this current at different voltages is indicated on p. 494. The experiment shows that whereas the potassium conductance rises with a marked delay it falls along an exponential type of curve which has no inflexion corresponding to that on the rising phase. This difference was present in all records except, possibly, those with very small depolarizations. It was also present in the curves calculated for the rise and fall of sodium conductance (e.g. Figs. 4, 5 and 8).

The rate constant determining the decline of potassium conductance

The experiments described in the preceding sections indicate that the potassium conductance returns to a low level when the membrane is repolarized to its resting value. The restoration of the condition of low conductance leads to a 'tail' of potassium current which can be fitted with reasonable accuracy by a curve of the form $\exp(-b_K t)$. Table 2 gives the values of the rate constant (b_K) determined by this method. It shows that b_K varies markedly with temperature and also to some extent with the amplitude of the step used to depolarize the axon. The second effect was particularly noticeable in axon 1 which was in poor condition and had a high potassium conductance in the resting state.

The effect of repolarizing the membrane to different levels is shown in Fig. 14. For $V_2 > -20$ mV. the rate constant increased with membrane potential but the relation is less steep than in the corresponding curve for sodium conductance (Fig. 9). Thus, changing V_2 from 0 to +40 mV. increases b_{Na} about 3·2-fold and b_K about 1·6-fold. Another important difference between the two processes is that b_{Na} is about 30 times greater than b_K at the resting potential.

The potassium potential

Table 3 summarizes a number of measurements of the potential at which potassium current reverses its direction. At 22° C. the apparent potassium potential is about 19 mV. higher than the resting potential if the axon is in sea water and about 13 mV. higher if it is in choline sea water. Corresponding figures at 6–11° C. are 13 mV. in sea water and 8 mV. in choline sea water. Since the resting potential is about 4 mV. higher in choline sea water (Hodgkin & Huxley, 1952) it seems likely that the absolute value of the potassium potential is unaffected by substituting choline for sodium ions. At 20° C. the absolute value of the potassium potential would be 80–85 mV. if the resting potential is taken as 60–65 mV. (Hodgkin & Huxley, 1952). This is nearly equal to the potential of 91 mV. estimated from chemical analyses

(Hodgkin, 1951). A similar conclusion applies to the results at 6–11° C. In squid fibres, cooling from 20 to 8° C. either has no effect or increases the resting potential by 1 or 2 mV. (Hodgkin & Katz, 1949). The observed

TABLE 2. Rate constant determining decline of potassium conductance following repolarization to resting potential

	Axon	Depolarization (mV.)	Temperature (° C.)	Rate constant (msec.$^{-1}$)	Rate constant at 6° C. (msec.$^{-1}$)	Average rate constant at 6° C. (msec.$^{-1}$)
A	1	6	23	1·2	0·14	
	1	13	23	1·3	0·15	
	1	21	23	1·3	0·16	
	15	13	11	0·36	0·19	
	15	20	11	0·35	0·19	
	17	10	6	0·20	0·20	
	18	6	22	1·5	0·20	
	18	13	22	1·6	0·22	
	20	21	6	0·17	0·17	0·17
	21	14	7	0·19	0·16	
	38*	10	5	0·12	0·13	
	39*	20	19	1·0	0·20	
	39*	10	19	0·83	0·16	
	39*	10	3	0·10	0·15	
	41*	20	4	0·10	0·12	
	41*	10	4	0·11	0·14	
B	1	36	23	1·5	0·18	
	1	54	23	1·8	0·22	
	18	50	22	2·0	0·27	
	18	63	22	1·7	0·23	0·22
	18	112	22	1·8	0·24	
	27	28	21	1·4	0·22	
	28	28	21	1·3	0·20	
C	15	13	11	0·49	0·26	
	17	10	6	0·21	0·21	
	18	6	22	1·6	0·21	0·23
	18	13	22	1·7	0·23	
	18	19	22	1·9	0·25	
D	18	25	22	2·0	0·27	
	18	50	22	2·1	0·28	
	18	63	22	2·1	0·28	
	23	84	21	1·8	0·28	0·28
	24	84	20	2·0	0·35	
	26	84	20	1·8	0·30	
	27	28	21	1·3	0·19	

Groups A and B in sea water; C and D in choline sea water. Groups A and C: depolarization less than 25 mV.; B and D: depolarization greater than 25 mV. An asterisk denotes the use of compensated feed-back. Rate constants at 6° C. are calculated for a Q_{10} of 3·5, which was found suitable for groups A and C.

potassium potential should therefore be taken as 75–80 mV. while the theoretical potassium potential would be reduced from 91 to 87 mV.

The effect of changing the external concentration of potassium on the potassium potential

Experimental determinations of V_K such as that illustrated by Fig. 11 were made in choline solutions containing different concentrations of potassium.

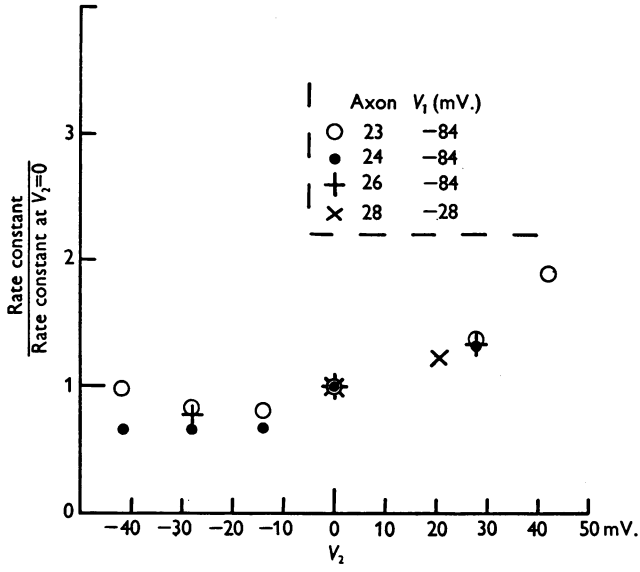

Fig. 14. Effect of membrane potential on the rate constant determining decline of potassium conductance. Abscissa (V_2): membrane potential during second step. Ordinate: relative value of rate constant.

TABLE 3. Apparent values of potassium potential

Axon	Medium	Temperature (°C.)	Potassium potential minus resting potential (mV.)	Average (mV.)
1	S	23	18	19
28	S	21	19	
15	S	11	14	11
20	S	6	10	
21	S	8	9	
18	C	22	12	13
23	C	21	14	
24	C	20	7	
26	C	20	13	
27	C	21	15	
28	C	21	16	
15	C	11	8	8
17	C	6	7	
20	0·7C:0·3S	6	8	
21	0·9C:0·1S	8	10	

S denotes sea water; C choline sea water. In axons 23–28 the potassium potential was found by the method illustrated by Fig. 12. In other cases it was taken as the potential at which the steady state current-voltage curve intersects the line joining the potassium currents before and after repolarization to the resting potential (e.g. line A and curve α intersect at 13 mV. in Fig. 12).

TABLE 4. Effect of potassium concentration on the apparent value of the potassium potential

Axon	Medium	Change in resting potential (ΔE_r) (mV.)	Change in applied potential at which I_K is zero (ΔV_K) (mV.)	Change in absolute membrane potential at which I_K is zero ($\Delta E_K = \Delta E_r + \Delta V_K$) (mV.)
27	A ($\frac{1}{2}$K)	+2	+6	+8
27	B (2K)	−3	−6	−9
28	B (2K)	−3	−7	−10
28	C (5K)	−13	−9	−22

Changes are given relative to the mean potentials observed in a 1K choline sea water before and after application of the test solution. The 1K choline sea water was identical with that described by Hodgkin & Huxley (1952) and contained choline at a concentration of 484 and potassium at 10 g.ions/kg. H_2O. The test solutions A, B, C and D were similar but contained potassium at concentrations of 5, 10, 20, 50 g.ions/kg. H_2O and correspondingly reduced concentrations of choline. Potentials are given as 'outside potential' minus 'inside potential'.

It was not possible to use a wide range of potassium concentrations, since squid axons tend to undergo irreversible changes if left in solutions containing high concentrations of potassium for any length of time. The results obtained with the two axons studied by this method are given in Table 4. They show that the potassium potential (E_K) is sensitive to the external concentration of potassium but that it changes by only about half the amount calculated for a concentration cell. Thus solutions *A*, *B*, *C* should give changes of +17, −17 and −41 mV. if E_K obeyed the ordinary equation for a concentration cell.

One possible explanation of this result is that potassium ions are not the only charged particles responsible for the delayed rise in conductance associated with depolarization (delayed rectification). Thus the discrepancy would be explained if choline or sodium, which are present in relatively high concentrations in the external solution, take part in the process with an affinity only 5% of that of potassium. This explanation might be consistent with the evidence which suggests that potassium ions are responsible for carrying most of the outward current through a depolarized membrane. For the concentration of potassium inside a fibre is about 10 times greater than that of sodium and the internal concentration of choline is almost certainly negligible. The participation of chloride ions in the process responsible for delayed rectification can probably be eliminated since one experiment showed that replacing all the choline chloride and two-thirds of the magnesium chloride in the choline sea water by dextrose gave an apparent *increase* of 3 mV. in the 'potassium potential'. The magnitude of the change was less certain in this experiment, since the solution employed gave a junction potential of 5–7 mV. which had to be allowed for in estimating the shift in resting potential. But it was clear that any change in E_K was small compared with the *reduction* of 45 mV. expected on the hypothesis that delayed rectification is entirely due to chloride ions.

Another way of accounting for the relatively small changes seen in Table 4 is to suppose that the potassium concentration in the immediate vicinity of the surface membrane is not the same as that in the external solution. Isolated cephalopod axons leak potassium ions at a fairly high rate and these must diffuse through layers of connective tissue and other structures between the excitable membrane and the external solution. This leakage is likely to increase in potassium-deficient solutions and to decrease in potassium-rich solutions. Hence the changes in effective potassium concentration might be less than those in Table 4. A related possibility is that the potassium concentration may be raised locally by the large outward currents used in these

experiments. This hypothesis is of interest since it might account for the slow polarization effect which is not otherwise explained except in terms of a complicated polarization process at the internal electrode. In a former paper (Hodgkin *et al.* 1952) we obtained evidence of an external layer with a resistance of about 3 Ω.cm.^{2}. The transient change in potassium concentration due to current cannot be calculated without knowing the thickness of this layer. The steady change due to leakage might be large enough to explain the deviations in Table 4, if the leakage of potassium had been several times greater than that found by Steinbach & Spiegelman (1943).

It may be asked why effects similar to those discussed in the preceding paragraph do not upset the relation between the external sodium concentration and V_{Na}. The answer, probably, is that similar effects are present but that they are small because the sodium concentration in sea water is 45 times greater than that of potassium. Changes in concentration due to current would also be smaller in the case of sodium because the sodium currents are of relatively short duration.

The contribution of ions other than sodium and potassium

The experimental results described in this series of papers point to the existence of special mechanisms which allow first sodium and then potassium to cross the membrane at a high rate when it is depolarized. In addition it is likely that charge can be carried through the membrane by other means. Steinbach's (1941) experiments suggest that chloride ions can cross the membrane and there is probably a small leakage of sodium, potassium and choline through cut branches

TABLE 5. Tentative values of leakage conductance and 'equilibrium' potential for leakage current. Five nerves in choline sea water at 6–22° C.

	Average	Range
Leakage conductance (g_l) (m.mho/cm.^{2})	0·26	0·13 to 0·50
Equilibrium potential for leakage current (V_l) (mV.)	−11	−4 to −22
Resting potassium conductance $(g_K)_r$ (m.mho/cm.^{2})	0·23	0·12 to 0·39
Equilibrium potential for potassium (V_K)	+10	+7 to +13

or through parts of the membrane other than those concerned with the selective system. All these minor currents may be thought of as contributing towards a leakage current (I_l) which has a conductance (g_l) and an apparent equilibrium potential (V_l) at which I_l is zero. In this leakage current we should probably also include ions transferred by metabolism against concentration gradients. So many processes may contribute towards a leakage current that measurement of its properties is unlikely to give useful information about the nature of the charged particles on which it depends. Nevertheless, a knowledge of the approximate magnitude of g_l and V_l is important since it is needed for any calculation of threshold or electrical stability. Various methods of measurement were tried but only the simplest will be considered since the orders of magnitude of g_l and V_l were unaffected by the precise method employed. In the experiment of Fig. 11 the steady current needed to maintain the membrane at the potassium potential (+13 mV.) was 8 μA./cm.^{2}. According to our definitions this inward current must have been almost entirely leakage current, for the nerve was in choline sea water and $I_K = 0$ when $V = V_K$. Hence

$$(13 \text{ mV.} - V_l)\, g_l = 8 \ \mu\text{A./cm.}^2.$$

In order to estimate g_l we make use of the fact that the inward current associated with $V = +84$ mV. was not appreciably affected by a fourfold change of potassium concentration (from 5 to 20 mM.). We therefore assume that the potassium conductance was reduced to a negligible value at this membrane potential and that the inward current of 24 μA./cm.^{2} was entirely leakage current. Hence

$$(84 \text{ mV.} - V_l)\, g_l = 24 \ \mu\text{A./cm.}^2.$$

From these two equations we find a value of −22 mV. for V_l and one of 0·23 m.mho/cm.^{2} for g_l. An estimate of the resting value of g_K may also be obtained by this method. At the resting potential in choline sea water

$$V_l g_l + V_K (g_K)_r = 0.$$

Hence

$$(g_K)_r = 0{\cdot}39 \text{ m.mho/cm.}^2.$$

Tentative values obtained by this type of method are given in Table 5.

DISCUSSION

At this stage all that will be attempted by way of a discussion is a brief comparison of the processes underlying the changes in sodium and potassium conductance. The main points of resemblance are: (1) both sodium and potassium conductances rise along an inflected curve when the membrane is depolarized and fall without any appreciable inflexion when the membrane is repolarized; (2) the rate of rise of conductance increases continuously as the membrane potential is reduced whereas the rate of fall associated with repolarization increases continuously as the membrane potential is raised; (3) the rates at which the conductances rise or fall have high temperature coefficients whereas the absolute values attained depend only slightly on temperature; (4) the instantaneous relation between sodium or potassium current and membrane potential normally consists of a straight line with zero current at the sodium or potassium potential.

The main differences are: (1) the rise and fall of sodium conductance occurs 10–30 times faster than the corresponding rates for potassium; (2) the variation of peak conductance with membrane potential is greater for sodium than for potassium; (3) if the axon is held in the depolarized condition the potassium conductance is maintained but the sodium conductance declines to a low level after reaching its peak.

SUMMARY

1. Repolarization of the giant axon of *Loligo* during the period of high sodium permeability is associated with a large inward current which declines rapidly along an approximately exponential curve.

2. The 'tail' of inward current disappears if sodium ions are removed from the external medium.

3. These results are explained quantitatively by supposing that the sodium conductance is a continuous function of time which rises when the membrane is depolarized and falls when it is repolarized.

4. For nerves in sea water the instantaneous relation between sodium current and membrane potential is a straight line passing through zero current about 110 mV. below the resting potential.

5. The rate at which sodium conductance is reduced when the fibre is repolarized increases markedly with membrane potential.

6. The time course of the sodium conductance during a voltage clamp can be calculated from the variation of the 'tail' of inward current with the duration of depolarization. The curves obtained by this method agree with those described in previous paper.

7. Repolarization of the membrane during the period of high potassium permeability is associated with a 'tail' of current which is outward at the

resting potential and inward above a critical potential about 10–20 mV. above the resting potential.

8. The instantaneous relation between potassium current and membrane potential is a straight line passing through zero at 10–20 mV. above the resting potential.

9. These results suggest that the potassium conductance is a continuous function of time which rises when the nerve is depolarized and falls when it is repolarized.

10. The rate at which the potassium conductance is reduced on repolarization increases with membrane potential.

11. The critical potential at which the 'potassium current' appears to reverse in sign varies with external potassium concentration but less steeply than the theoretical potential of a potassium electrode.

REFERENCES

HODGKIN, A. L. (1951). The ionic basis of electrical activity in nerve and muscle. *Biol. Rev.* **26**, 339–409.

HODGKIN, A. L. & HUXLEY, A. F. (1952). Currents carried by sodium and potassium ions through the membrane of the giant axon of *Loligo*. *J. Physiol.* **116**, 449–272.

HODGKIN, A. L., HUXLEY, A. F. & KATZ, B. (1952). Measurement of current-voltage relations in the membrane of the giant axon of *Loligo*. *J. Physiol.* **116**, 424–448.

HODGKIN, A. L. & KATZ, B. (1949). The effect of temperature on the electrical activity of the giant axon of the squid. *J. Physiol.* **109**, 240–249.

STEINBACH, H. B. (1941). Chloride in the giant axons of the squid. *J. cell. comp. Physiol.* **17**, 57–64.

STEINBACH, H. B. & SPIEGELMAN, S. (1943). The sodium and potassium balance in squid nerve axoplasm. *J. cell. comp. Physiol.* **22**, 187–196.

J. Physiol. (1952) 116, 497–506

THE DUAL EFFECT OF MEMBRANE POTENTIAL ON SODIUM CONDUCTANCE IN THE GIANT AXON OF *LOLIGO*

By A. L. HODGKIN and A. F. HUXLEY

From the Laboratory of the Marine Biological Association, Plymouth, and the Physiological Laboratory, University of Cambridge

(*Received* 24 *October* 1951)

This paper contains a further account of the electrical properties of the giant axon of *Loligo*. It deals with the 'inactivation' process which gradually reduces sodium permeability after it has undergone the initial rise associated with depolarization. Experiments described previously (Hodgkin & Huxley, 1952*a*, *b*) show that the sodium conductance always declines from its initial maximum, but they leave a number of important points unresolved. Thus they give no information about the rate at which repolarization restores the ability of the membrane to respond with its characteristic increase of sodium conductance. Nor do they provide much quantitative evidence about the influence of membrane potential on the process responsible for inactivation. These are the main problems with which this paper is concerned. The experimental method needs no special description, since it was essentially the same as that used previously (Hodgkin, Huxley & Katz, 1952; Hodgkin & Huxley, 1952*b*).

RESULTS

The influence of a small change in membrane potential on the ability of the membrane to undergo its increase in sodium permeability is illustrated by Fig. 1. In this experiment the membrane potential was changed in two steps. The amplitude of the first step was −8 mV. and its duration varied between 0 and 50 msec. This step will be called the conditioning voltage (V_1). It was followed by a second step called the test voltage (V_2) which was kept at a constant amplitude of −44 mV.

Record *A* gives the current observed with the test voltage alone. *B–F* show the effect of preceding this by a conditioning pulse of varying duration. Although the depolarization of 8 mV. was not associated with any appreciable inward current it greatly altered the subsequent response of the nerve. Thus, if the conditioning voltage lasted longer than 20 msec., it reduced the inward

current during the test pulse by about 40%. At intermediate durations the inward current decreased along a smooth exponential curve with a time constant of about 7 msec. The outward current, on the other hand, evidently behaved in a different manner; for it may be seen to approach a final level which was independent of the duration of the conditioning step. This is consistent with the observation that depolarization is associated with a maintained increase in potassium conductance (Hodgkin & Huxley, 1952*a*).

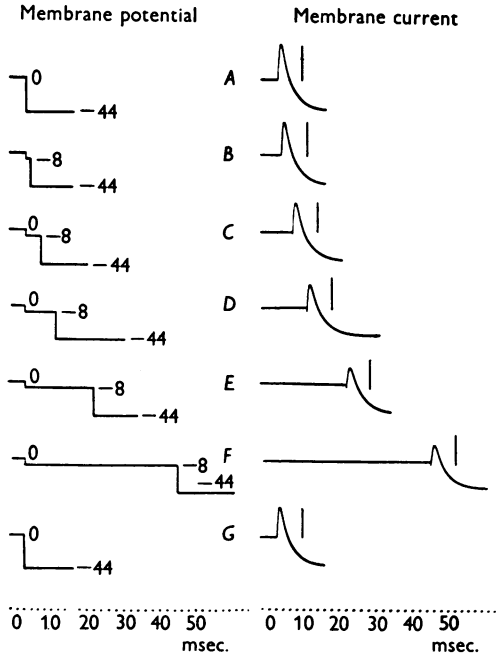

Fig. 1. Development of 'inactivation' during constant depolarization of 8 mV. Left-hand column: time course of membrane potential (the numbers show the displacement of the membrane potential from its resting value in mV.). Right-hand column: time course of membrane current density. Inward current is shown as an upward deflexion. (The vertical lines show the 'sodium current' expected in the absence of a conditioning step; they vary between 1·03 mA./cm.^{2} in *A* and 0·87 mA./cm.^{2} in *G*). Axon 38; compensated feed-back; temperature 5° C.

Fig. 2 illustrates the converse process of raising the membrane potential before applying the test pulse. In this case the conditioning voltage improved the state of the nerve for the inward current increased by about 70% if the first step lasted longer than 15 msec. This finding is not altogether surprising, for the resting potential of isolated squid axons is less than that of other excitable cells (Hodgkin, 1951) and is probably lower than that in the living animal.

A convenient way of expressing these results is to plot the amplitude of the sodium current during the test pulse against the duration of the conditioning

pulse. For this purpose we used the simple method of measurement illustrated by Fig. 3 (inset). This procedure avoids the error introduced by variations of potassium conductance during the first step and should give reasonable results for $V > -15$ mV. With larger depolarizations both the method of measurement and the interpretation of the results become somewhat doubtful, since there may be appreciable sodium current during the conditioning period. Two

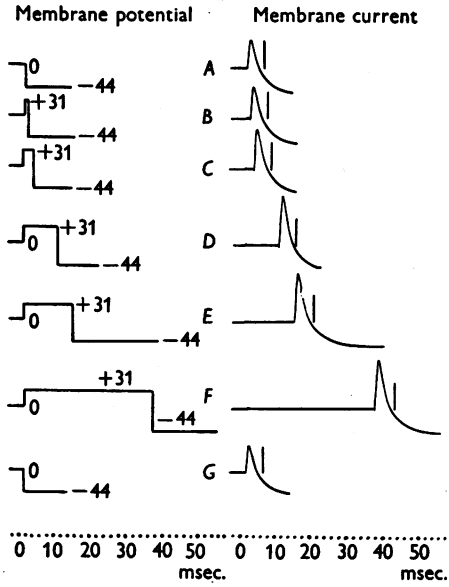

Fig. 2. Removal of 'inactivation' at membrane potential of +31 mV. Experimental details are as in Fig. 1. The vertical lines show the 'sodium current' with no conditioning step; they vary between 0·82 mA./cm.^{2} in *A* and 0·75 mA./cm.^{2} in *G*.

of the curves in Fig. 3 were obtained from the families of records illustrated in Figs. 1 and 2. The other two were determined from similar families obtained on the same axon. All four curves show that inactivation developed or was removed in an approximately exponential manner with a time constant which varied with membrane potential and had a maximum near $V = 0$. They also indicate that inactivation tended to a definite steady level at any particular membrane potential. Values of the exponential time-constant (τ_h) of the inactivation process are given in Table 1.

The influence of membrane potential on the steady level of inactivation is illustrated by the records in Fig. 4. In this experiment the conditioning step lasted long enough to allow inactivation to attain its final level at all voltages. Its amplitude was varied between +46 and −29 mV., while that of the test step was again kept constant at −44 mV. The effect of a small progressive change was allowed for in calculating the vertical lines on each record. These give the inward current expected in the absence of a conditioning step and

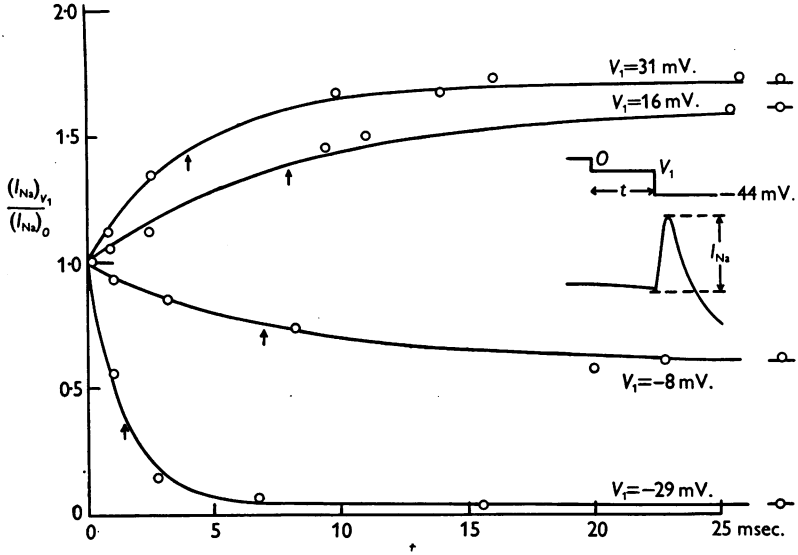

Fig. 3. Time course of inactivation at four different membrane potentials. Abscissa: duration of conditioning step. Ordinate: circles, sodium current (measured as inset) relative to normal sodium current; smooth curve, $y = y_\infty - (y_\infty - 1)\exp(-t/\tau_h)$, where y_∞ is the ordinate at $t = \infty$ and τ_h is the time constant (shown by arrows). Experimental details as in Figs. 1 and 2.

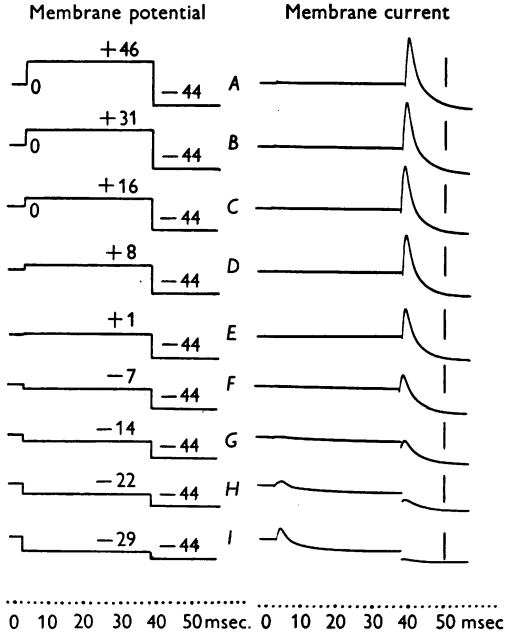

Fig. 4. Influence of membrane potential on 'inactivation' in the steady state. Experimental details are as in Fig. 1. The vertical lines show the sodium current with no conditioning step; they vary between 0·74 mA./cm.^{2} in *A* and 0·70 mA./cm.^{2} in *I*.

were obtained by interpolating between records made with the test step alone. The conditioning voltage clearly had a marked influence on the inward current during the second step, for the amplitude of the sodium current varied between 1·3 mA./cm.^{2} with $V_1 = +46$ mV. and about 0·03 mA./cm.^{2} with $V_1 = -29$ mV.

The quantitative relation between the sodium current during the test pulse and the membrane potential during the conditioning period is given in Fig. 5.

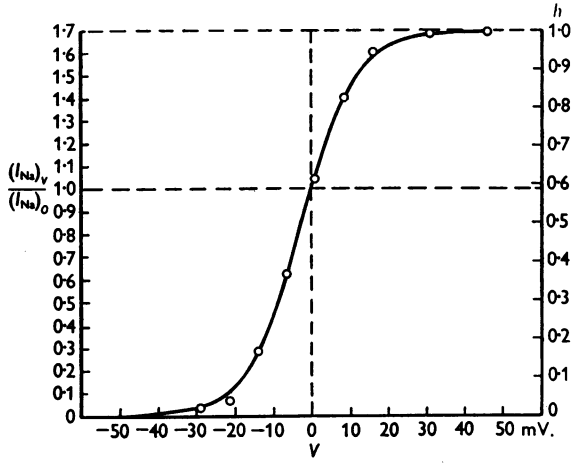

Fig. 5. Influence of membrane potential on 'inactivation' in the steady state. Abscissa: displacement of membrane potential from its resting value during conditioning step. Ordinate: circles, sodium current during test step relative to sodium current in unconditioned test step (left-hand scale) or relative to maximum sodium current (right-hand scale). The smooth curve was drawn according to equation 1 with a value of −2·5 mV. for V_h. This graph is based on the records illustrated in Fig. 4. Sodium currents were determined in the manner shown in Fig. 3.

This shows that the two variables are related by a smooth symmetrical curve which has a definite limiting value at large membrane potentials. In discussing this curve it is convenient to adopt the following nomenclature. We shall denote the ability of the nerve to undergo a change in sodium permeability by a variable, h, which covers a range from 0 to 1 and is proportional to the ordinate in Fig. 5. In these terms $(1-h)$ is a measure of inactivation, while h is the fraction of the sodium-carrying system which is not inactivated and is therefore rapidly available for carrying sodium ions when the membrane is depolarized. If these definitions are adopted we may say that inactivation is almost complete when $V < -20$ mV. and is almost absent when $V > 30$ mV. At the resting potential h is about 0·6 which implies that inactivation is 40% complete.

The smooth curve in Fig. 5 was calculated from the equation

$$(h)_{\text{steady state}} = \frac{1}{1+\exp(V_h - V)/7}, \qquad (1)$$

where V is expressed in millivolts and V_h is the value of V at which $h = \frac{1}{2}$ in the steady state. The same equation gave a satisfactory fit in all experiments but there was some variation in the value of V_h. Five experiments with three fresh fibres gave resting values of h between 0·55 and 0·62. In these cases V_h varied between $-1{\cdot}5$ and $-3{\cdot}5$ mV. On the other hand, two experiments with a fibre which had been used for some time gave a resting h of only about 0·25; V_h was then $+7{\cdot}5$ mV. Since the resting potential was found to decline by 10–15 mV. during the course of a long experiment it is reasonable to suppose that the change in V_h arose solely from this cause and that the relation between h and the absolute membrane potential was independent of the condition of the fibre.

In a former paper we examined the relation between the concentration of sodium ions in the external medium and the sodium current through the membrane (Hodgkin & Huxley, 1952*a*). The results were reasonably close to those predicted by the 'independence principle' except that the currents were 20–60% too large in the sodium-deficient solutions. This effect was attributed to the small increase in resting potential associated with the substitution of choline ions for sodium ions. This explanation now seems very reasonable. The resting potential probably increased by about 4 mV. in choline sea water and this would raise h from 0·6 to 0·73 in a fresh fibre and from 0·25 to 0·37 in a fibre which had been used for some time.

The quantitative results obtained in this series of experiments are summarized in Table 1. Most of the experiments were made at 3–7° C. but a temperature of 19° C. was used on one occasion. The results suggest that temperature has little effect on the equilibrium relation between h and V, but greatly alters the rate at which this equilibrium is attained. The Q_{10} of the rate constants cannot be stated with certainty but is clearly of the order of 3.

Two-pulse experiment

This section deals with a single experiment which gave an independent measurement of the time constant of inactivation.

Two pulses of amplitude -44 mV. and duration 1·8 msec. were applied to the membrane. Fig. 6*A* is a record obtained with the second pulse alone. The ionic current was inward and reached a maximum of about 0·25 mA./cm.^{2}. As in all other records, the inward current was not maintained but declined as a result of inactivation. Restoration of the normal membrane potential was associated with a tail of inward current due to the rapid fall of sodium conductance (see Hodgkin & Huxley, 1952*b*). When two pulses were applied in quick succession the effect of the first was similar to that in *A*, but the inward current during the second was reduced to about one half (record *B*). A gradual recovery to the normal level is shown in records *C*–*G*.

The curve in Fig. 7 was obtained by estimating sodium current in the manner

TABLE 1. Experiments with conditioning voltage

Axon	Temperature (° C.)	Variable	Displacement of membrane potential (mV.) −29	−22	−14	−8	−7	0	9	16	31	46
38	5	h* (steady	0·02	0·04	0·17	—	0·37	0·59	0·82	0·94	0·99	1·00
39	19	state)	0·02	0·04	0·09	—	0·28	0·55	0·83	0·94	0·98	0·99
39†	3		0·01	0·03	0·04	—	0·11	0·26	0·50	0·69	0·93	0·99
38	5	h‡ (steady	0·02	—	—	0·43	—	0·58	—	0·92	0·99	—
39	19	state)	0·03	—	—	0·40	—	0·61	—	0·94	—	—
39†	3		—	—	—	—	—	0·22	—	0·75	0·93	—
37	3		—	0·04	—	0·34	—	0·55	0·81	0·96	—	—
38	5	τ_h‡ (msec.)	1·5	—	—	7	—	[8–10]	—	8	4	—
39	19		0·35	—	—	1·5	—	[1·7–2·1]	—	1·8	—	—
39†	3		—	—	—	—	—	—	—	13	7	—
37	3		—	3	—	6	—	[8–10]	9	7	—	—
38	6	τ_h§ (msec.)	1·3	—	—	6	—	[7–9]	—	7	3·6	—
39	6		1·5	—	—	6	—	[7–9]	—	8	—	—
39†	6		—	—	—	—	—	—	—	9	5	—
37	6		—	2·2	—	4	—	[6–7]	7	5	—	—

Two-pulse experiment

Axon 31 at 4·5° C. $\tau_h = 1{\cdot}8$ msec. at $V = -44$ mV. $\tau_h = 12$ msec. at $V = 0$

Axon 31 at 6° C. τ_h§ $= 1{\cdot}5$ msec. at $V = -44$ mV. τ_h§ $= 10$ msec. at $V = 0$

* Measurements made by methods illustrated in Figs. 4 and 5.

† The axon had been used for some time and was in poor condition when these measurements were made.

‡ Methods illustrated in Figs. 1–3.

§ Calculated from above assuming Q_{10} of 3.

[ ] Interpolated.

h is the fraction of the sodium system which is rapidly available, $(1 - h)$ is the fraction inactivated.

τ_h determines the rate at which h approaches its steady state.

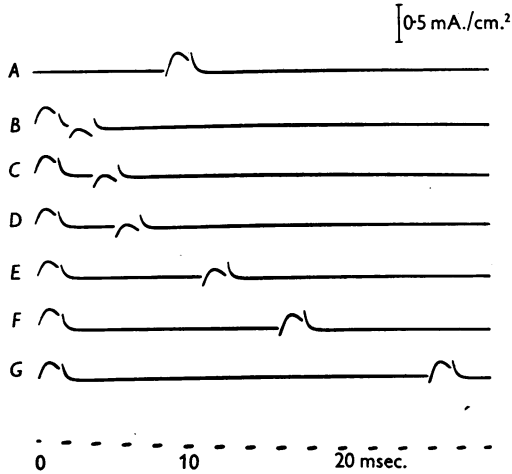

Fig. 6. Membrane currents associated with two square waves applied in succession. The amplitude of each square wave was −44 mV. and the duration 1·8 msec. Record *A* shows the second square wave alone, *B–G* both square waves at various intervals. Axon 31; uncompensated feed-back; temperature 4·5° C.

shown in Fig. 3 and plotting this against the interval between the two pulses. It will be seen that recovery from inactivation took place in an approximately exponential manner with a time constant of about 12 msec. A similar curve and a similar time constant were obtained by plotting

$$\left(\frac{dI_{Na}}{dt}\right)_{max.} \quad \text{instead of} \quad (I_{Na})_{max.}.$$

This time constant is clearly of the same order as that given by the method using weak conditioning voltages (see Table 1). An estimate of the inactivation time constant at -44 mV. may be obtained by extrapolating the curve in Fig. 7 to zero time. This indicates that the available fraction of the sodium-carrying system was reduced to 0·37 at the end of a pulse of amplitude -44 mV. and duration 1·8 msec. Hence the inactivation time constant at -44 mV. is about 1·8 msec., which is of the same order as the values obtained with large depolarizations by the first method (Table 1). It is also in satisfactory agreement with the time constant obtained by fitting a curve to the variation of sodium conductance during a maintained depolarization of 40–50 mV. (Hodgkin & Huxley, 1952*c*).

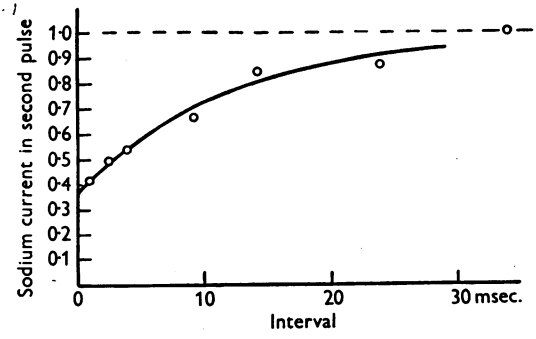

Fig. 7. Recovery from inactivation. Abscissa: interval between end of first pulse and beginning of second pulse. Ordinate: sodium current in second pulse measured as shown in Fig. 3 and expressed as a fraction of the sodium current in an unconditioned pulse. The circles are experimental points derived from the records in Fig. 6. The smooth curve is drawn according to the expression $1-0{\cdot}63 \exp(-t/\tau_h)$, where $\tau_h = 12$ msec.

The two-pulse experiment is interesting because it emphasizes the difference between the rapid fall of sodium conductance associated with repolarization and the slower decline during a maintained depolarization. Both events lead to a decrease in sodium current, but the underlying mechanisms are clearly different. In the first case it must be supposed that repolarization converts active membrane into resting membrane; in the second that prolonged depolarization turns it into a refractory or inactivated condition from which it recovers at a relatively slow rate when the fibre is repolarized. It cannot be argued that repolarization reduces sodium conductance by making the active

membrane refractory. If this were so, one would expect that the inward current during the second pulse would be reduced to zero at short intervals, instead of to 37 % as in Fig. 7. The reduction to 37 % is clearly associated with the incomplete decline of sodium conductance during the first pulse and not with the rapid and complete decline due to repolarization at the end of the first pulse.

DISCUSSION

The experimental evidence in this paper and in those which precede it (Hodgkin & Huxley, 1952*a*, *b*) suggests that the membrane potential has two distinct influences on the system which allows sodium ions to flow through the membrane. The early effects of changes in membrane potential are a rapid increase in sodium conductance when the fibre is depolarized and a rapid decrease when it is repolarized. The late effects are a slow onset of a refractory or inactive condition during a maintained depolarization and a slow recovery following repolarization. A membrane in the refractory or inactive condition resembles one in the resting state in having a low sodium conductance. It differs in that it cannot undergo an increase in sodium conductance if the fibre is depolarized. The difference allows inactivation to be measured by methods such as those described in this paper. The results show that both the final level of inactivation and the rate at which this level is approached are greatly influenced by membrane potential. At high membrane potentials inactivation appears to be absent, at low membrane potentials it approaches completion with a time constant of about 1·5 msec. at 6° C. This conclusion is clearly consistent with former evidence which suggests that the sodium conductance declines to a low level with a time constant of 1–2 msec. during a large and maintained depolarization (Hodgkin & Huxley, 1952*a*). Both sets of experiments may be summarized by stating that changes in sodium conductance are transient over a wide range of membrane potentials.

The persistence of inactivation after a depolarization is clearly connected with the existence of a refractory state and with accommodation. It is not the only factor concerned, since the persistence of the raised potassium conductance will also help to hold the membrane potential at a positive value and will therefore tend to make the fibre inexcitable. The relative importance of the two processes can only be judged by numerical analysis of the type described in the final paper of this series (Hodgkin & Huxley, 1952*c*).

SUMMARY

1. Small changes in the membrane potential of the giant axon of *Loligo* are associated with large alterations in the ability of the surface membrane to undergo its characteristic increase in sodium conductance.

2. A steady depolarization of 10 mV. reduces the sodium current associated with a sudden depolarization of 45 mV. by about 60 %. A steady rise of 10 mV.

increases the sodium current associated with subsequent depolarization by about 50%.

3. These effects are described by stating that depolarization gradually inactivates the system which enables sodium ions to cross the membrane.

4. In the steady state, inactivation appears to be almost complete if the membrane potential is reduced by 30 mV. and is almost absent if it is increased by 30 mV. Between these limits the amount of inactivation is determined by a smooth symmetrical curve and is about 40% complete in a resting fibre at the beginning of an experiment.

5. At 6° C. the time constant of the inactivation process is about 10 msec. with $V=0$, about 1·5 msec. with $V=-30$ mV. and about 5 msec. at $V=+30$ mV.

REFERENCES

HODGKIN, A. L. (1951). The ionic basis of electrical activity in nerve and muscle. *Biol. Rev.* **26**, 339–409.

HODGKIN, A. L. & HUXLEY, A. F. (1952*a*). Currents carried by sodium and potassium ions through the membrane of the giant axon of *Loligo*. *J. Physiol.* **116**, 449–472.

HODGKIN, A. L. & HUXLEY, A. F. (1952*b*). The components of membrane conductance in the giant axon of *Loligo*. *J. Physiol.* **116**, 473–496.

HODGKIN, A. L. & HUXLEY, A. F. (1952*c*). A quantitative description of membrane current and its application to conduction and excitation in nerve. *J. Physiol.* (in the press).

HODGKIN, A. L., HUXLEY, A. F. & KATZ, B. (1952). Measurement of current-voltage relations in the membrane of the giant axon of *Loligo*. *J. Physiol.* **116**, 424–448.

J. Physiol. (1952) 117, 500–544

A QUANTITATIVE DESCRIPTION OF MEMBRANE CURRENT AND ITS APPLICATION TO CONDUCTION AND EXCITATION IN NERVE

By A. L. HODGKIN and A. F. HUXLEY

From the Physiological Laboratory, University of Cambridge

(*Received* 10 *March* 1952)

This article concludes a series of papers concerned with the flow of electric current through the surface membrane of a giant nerve fibre (Hodgkin, Huxley & Katz, 1952; Hodgkin & Huxley, 1952*a–c*). Its general object is to discuss the results of the preceding papers (Part I), to put them into mathematical form (Part II) and to show that they will account for conduction and excitation in quantitative terms (Part III).

PART I. DISCUSSION OF EXPERIMENTAL RESULTS

The results described in the preceding papers suggest that the electrical behaviour of the membrane may be represented by the network shown in Fig. 1. Current can be carried through the membrane either by charging the membrane capacity or by movement of ions through the resistances in parallel with the capacity. The ionic current is divided into components carried by sodium and potassium ions (I_{Na} and I_K), and a small 'leakage current' (I_l) made up by chloride and other ions. Each component of the ionic current is determined by a driving force which may conveniently be measured as an electrical potential difference and a permeability coefficient which has the dimensions of a conductance. Thus the sodium current (I_{Na}) is equal to the sodium conductance (g_{Na}) multiplied by the difference between the membrane potential (E) and the equilibrium potential for the sodium ion (E_{Na}). Similar equations apply to I_K and I_l and are collected on p. 505.

Our experiments suggest that g_{Na} and g_K are functions of time and membrane potential, but that E_{Na}, E_K, E_l, C_M and $\bar{g}_l$ may be taken as constant. The influence of membrane potential on permeability can be summarized by stating: first, that depolarization causes a transient increase in sodium conductance and a slower but maintained increase in potassium conductance; secondly, that these changes are graded and that they can be reversed by repolarizing the membrane. In order to decide whether these effects are sufficient to account for complicated phenomena such as the action potential and refractory period, it is necessary to obtain expressions relating

the sodium and potassium conductances to time and membrane potential. Before attempting this we shall consider briefly what types of physical system are likely to be consistent with the observed changes in permeability.

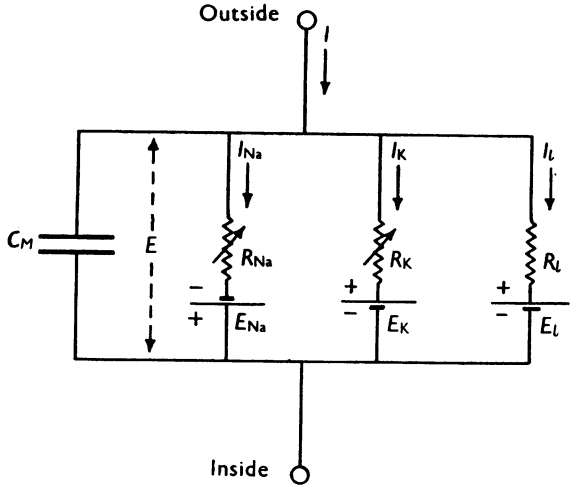

Fig. 1. Electrical circuit representing membrane. $R_{Na}=1/g_{Na}$; $R_K=1/g_K$; $R_l=1/\bar{g}_l$. R_{Na} and R_K vary with time and membrane potential; the other components are constant.

The nature of the permeability changes

At present the thickness and composition of the excitable membrane are unknown. Our experiments are therefore unlikely to give any certain information about the nature of the molecular events underlying changes in permeability. The object of this section is to show that certain types of theory are excluded by our experiments and that others are consistent with them.

The first point which emerges is that the changes in permeability appear to depend on membrane potential and not on membrane current. At a fixed depolarization the sodium current follows a time course whose form is independent of the current through the membrane. If the sodium concentration is such that $E_{Na}<E$, the sodium current is inward; if it is reduced until $E_{Na}>E$ the current changes in sign but still appears to follow the same time course. Further support for the view that membrane potential is the variable controlling permeability is provided by the observation that restoration of the normal membrane potential causes the sodium or potassium conductance to decline to a low value at any stage of the response.

The dependence of g_{Na} and g_K on membrane potential suggests that the permeability changes arise from the effect of the electric field on the distribution or orientation of molecules with a charge or dipole moment. By this we do not mean to exclude chemical reactions, for the rate at which these occur might depend on the position of a charged substrate or catalyst. All that is intended is that small changes in membrane potential would be most unlikely

to cause large alterations in the state of a membrane which was composed entirely of electrically neutral molecules.

The next question to consider is how changes in the distribution of a charged particle might affect the ease with which sodium ions cross the membrane. Here we can do little more than reject a suggestion which formed the original basis of our experiments (Hodgkin, Huxley & Katz, 1949). According to this view, sodium ions do not cross the membrane in ionic form but in combination with a lipoid soluble carrier which bears a large negative charge and which can combine with one sodium ion but no more. Since both combined and uncombined carrier molecules bear a negative charge they are attracted to the outside of the membrane in the resting state. Depolarization allows the carrier molecules to move, so that sodium current increases as the membrane potential is reduced. The steady state relation between sodium current and voltage could be calculated for this system and was found to agree reasonably with the observed curve at 0·2 msec after the onset of a sudden depolarization. This was encouraging, but the analogy breaks down if it is pursued further. In the model the first effect of depolarization is a movement of negatively charged molecules from the outside to the inside of the membrane. This gives an initial outward current, and an inward current does not occur until combined carriers lose sodium to the internal solution and return to the outside of the membrane. In our original treatment the initial outward current was reduced to vanishingly small proportions by assuming a low density of carriers and a high rate of movement and combination. Since we now know that the sodium current takes an appreciable time to reach its maximum, it is necessary to suppose that there are more carriers and that they react or move more slowly. This means that any inward current should be preceded by a large outward current. Our experiments show no sign of a component large enough to be consistent with the model. This invalidates the detailed mechanism assumed for the permeability change but it does not exclude the more general possibility that sodium ions cross the membrane in combination with a lipoid soluble carrier.

A different form of hypothesis is to suppose that sodium movement depends on the distribution of charged particles which do not act as carriers in the usual sense, but which allow sodium to pass through the membrane when they occupy particular sites in the membrane. On this view the rate of movement of the activating particles determines the rate at which the sodium conductance approaches its maximum but has little effect on the magnitude of the conductance. It is therefore reasonable to find that temperature has a large effect on the rate of rise of sodium conductance but a relatively small effect on its maximum value. In terms of this hypothesis one might explain the transient nature of the rise in sodium conductance by supposing that the activating particles undergo a chemical change after moving from the position which they occupy when the membrane potential is high. An alternative is to

attribute the decline of sodium conductance to the relatively slow movement of another particle which blocks the flow of sodium ions when it reaches a certain position in the membrane.

Much of what has been said about the changes in sodium permeability applies equally to the mechanism underlying the change in potassium permeability. In this case one might suppose that there is a completely separate system which differs from the sodium system in the following respects: (1) the activating molecules have an affinity for potassium but not for sodium; (2) they move more slowly; (3) they are not blocked or inactivated. An alternative hypothesis is that only one system is present but that its selectivity changes soon after the membrane is depolarized. A situation of this kind would arise if inactivation of the particles selective for sodium converted them into particles selective for potassium. However, this hypothesis cannot be applied in a simple form since the potassium conductance rises too slowly for a direct conversion from a state of sodium permeability to one of potassium permeability.

One of the most striking properties of the membrane is the extreme steepness of the relation between ionic conductance and membrane potential. Thus g_{Na} may be increased e-fold by a reduction of only 4 mV, while the corresponding figure for g_K is 5–6 mV (Hodgkin & Huxley, 1952*a*, figs. 9, 10). In order to illustrate the possible meaning of this result we shall suppose that a charged molecule which has some special affinity for sodium may rest either on the inside or the outside of the membrane but is present in negligible concentrations elsewhere. We shall also suppose that the sodium conductance is proportional to the number of such molecules on the inside of the membrane but is independent of the number on the outside. From Boltzmann's principle the proportion P_i of the molecules on the inside of the membrane is related to the proportion on the outside, P_o, by

$$\frac{P_i}{P_o} = \exp[(w + zeE)/kT],$$

where E is the potential difference between the outside and the inside of the membrane, w is the work required to move the molecule from the inside to the outside of the membrane when $E = 0$, e is the absolute value of the electronic charge, z is the valency of the molecule (i.e. the number of positive electronic charges on it), k is Boltzmann's constant and T is the absolute temperature. Since we have assumed that $P_i + P_o = 1$ the expression for P_i is

$$P_i = 1 \Big/ \left[1 + \exp - \left(\frac{w + zeE}{kT}\right)\right].$$

For negative values of z and with E sufficiently large and positive this gives

$$P_i = \text{constant} \times \exp[zeE/kT].$$

In order to explain our results z must be about -6 since $\frac{kT}{e}\left(=\frac{RT}{F}\right)$ is 25 mV at room temperature and $g_{Na} \propto \exp -E/4$ for E large. This suggests that the particle whose distribution changes must bear six negative electronic charges, or, if a similar theory is developed in terms of the orientation of a long molecule with a dipole moment, it must have at least three negative charges on one end and three positive charges on the other. A different but related approach is to suppose that sodium movement depends on the presence of six singly charged molecules at a particular site near the inside of the membrane. The proportion of the time that each of the charged molecules spends at the inside is determined by $\exp -E/25$ so that the proportion of sites at which all six are at the inside is $\exp -E/4{\cdot}17$. This suggestion may be given plausibility but not mathematical simplicity by imagining that a number of charges form a bridge or chain which allows sodium ions to flow through the membrane when it is depolarized. Details of the mechanism will probably not be settled for some time, but it seems difficult to escape the conclusion that the changes in ionic permeability depend on the movement of some component of the membrane which behaves as though it had a large charge or dipole moment. If such components exist it is necessary to suppose that their density is relatively low and that a number of sodium ions cross the membrane at a single active patch. Unless this were true one would expect the increase in sodium permeability to be accompanied by an outward current comparable in magnitude to the current carried by sodium ions. For movement of any charged particle in the membrane should contribute to the total current and the effect would be particularly marked with a molecule, or aggregate, bearing a large charge. As was mentioned earlier, there is no evidence from our experiments of any current associated with the change in sodium permeability, apart from the contribution of the sodium ion itself. We cannot set a definite upper limit to this hypothetical current, but it could hardly have been more than a few per cent of the maximum sodium current without producing a conspicuous effect at the sodium potential.

PART II. MATHEMATICAL DESCRIPTION OF MEMBRANE CURRENT DURING A VOLTAGE CLAMP

Total membrane current

The first step in our analysis is to divide the total membrane current into a capacity current and an ionic current. Thus

$$I = C_M \frac{dV}{dt} + I_i, \tag{1}$$

where

I is the total membrane current density (inward current positive);
I_i is the ionic current density (inward current positive);
V is the displacement of the membrane potential from its resting value (depolarization negative);
C_M is the membrane capacity per unit area (assumed constant);
t is time.

The justification for this equation is that it is the simplest which can be used and that it gives values for the membrane capacity which are independent of the magnitude or sign of V and are little affected by the time course of V (see, for example, table 1 of Hodgkin *et al.* 1952). Evidence that the capacity current and ionic current are in parallel (as suggested by eqn. (1)) is provided by the similarity between ionic currents measured with $\frac{dV}{dt}=0$ and those calculated from $-C_M \frac{dV}{dt}$ with $I=0$ (Hodgkin *et al.* 1952).

The only major reservation which must be made about eqn. (1) is that it takes no account of dielectric loss in the membrane. There is no simple way of estimating the error introduced by this approximation, but it is not thought to be large since the time course of the capacitative surge was reasonably close to that calculated for a perfect condenser (Hodgkin *et al.* 1952).

The ionic current

A further subdivision of the membrane current can be made by splitting the ionic current into components carried by sodium ions (I_{Na}), potassium ions (I_K) and other ions (I_l):

$$I_i = I_{Na} + I_K + I_l. \tag{2}$$

The individual ionic currents

In the third paper of this series (Hodgkin & Huxley, 1952*b*), we showed that the ionic permeability of the membrane could be satisfactorily expressed in terms of ionic conductances (g_{Na}, g_K and $\bar{g}_l$). The individual ionic currents are obtained from these by the relations

$$I_{Na} = g_{Na}(E - E_{Na}),$$
$$I_K = g_K(E - E_K),$$
$$I_l = \bar{g}_l(E - E_l),$$

where E_{Na} and E_K are the equilibrium potentials for the sodium and potassium ions. E_l is the potential at which the 'leakage current' due to chloride and other ions is zero. For practical application it is convenient to write these equations in the form

$$I_{Na} = g_{Na}(V - V_{Na}), \tag{3}$$
$$I_K = g_K(V - V_K), \tag{4}$$
$$I_l = \bar{g}_l(V - V_l), \tag{5}$$

where

$$V = E - E_r,$$
$$V_{Na} = E_{Na} - E_r,$$
$$V_K = E_K - E_r,$$
$$V_l = E_l - E_r,$$

and E_r is the absolute value of the resting potential. V, V_{Na}, V_K and V_l can then be measured directly as displacements from the resting potential.

The ionic conductances

The discussion in Part I shows that there is little hope of calculating the time course of the sodium and potassium conductances from first principles. Our object here is to find equations which describe the conductances with reasonable accuracy and are sufficiently simple for theoretical calculation of the action potential and refractory period. For the sake of illustration we shall try to provide a physical basis for the equations, but must emphasize that the interpretation given is unlikely to provide a correct picture of the membrane.

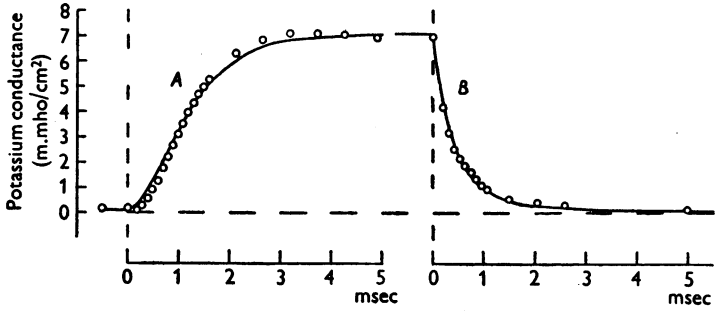

Fig. 2. *A*, rise of potassium conductance associated with depolarization of 25 mV; *B*, fall of potassium conductance associated with repolarization to the resting potential. Circles: experimental points replotted from Hodgkin & Huxley (1952*b*, Fig. 13). The last point of *A* is the same as the first point in *B*. Axon 18, 21° C in choline sea water. The smooth curve is drawn according to eqn. (11) with the following parameters:

	Curve *A* ($V = -25$ mV)	Curve *B* ($V = 0$)
g_{K0}	0·09 m.mho/cm²	7·06 m.mho/cm²
$g_{K\infty}$	7·06 m.mho/cm²	0·09 m.mho/cm²
τ_n	0·75 msec	1·1 msec

At the outset there is the difficulty that both sodium and potassium conductances increase with a delay when the axon is depolarized but fall with no appreciable inflexion when it is repolarized. This is illustrated by the circles in Fig. 2, which shows the change in potassium conductance associated with a depolarization of 25 mV lasting 4·9 msec. If g_K is used as a variable the end of the record can be fitted by a first-order equation but a third- or fourth-order equation is needed to describe the beginning. A useful simplification is

achieved by supposing that g_K is proportional to the fourth power of a variable which obeys a first-order equation. In this case the rise of potassium conductance from zero to a finite value is described by $(1-\exp(-t))^4$, while the fall is given by $\exp(-4t)$. The rise in conductance therefore shows a marked inflexion, while the fall is a simple exponential. A similar assumption using a cube instead of a fourth power describes the initial rise of sodium conductance, but a term representing inactivation must be included to cover the behaviour at long times.

The potassium conductance

The formal assumptions used to describe the potassium conductance are:

$$g_K = \bar{g}_K n^4, \tag{6}$$

$$\frac{dn}{dt} = \alpha_n (1-n) - \beta_n n, \tag{7}$$

where $\bar{g}_K$ is a constant with the dimensions of conductance/cm^2, α_n and β_n are rate constants which vary with voltage but not with time and have dimensions of [time]$^{-1}$, n is a dimensionless variable which can vary between 0 and 1.

These equations may be given a physical basis if we assume that potassium ions can only cross the membrane when four similar particles occupy a certain region of the membrane. n represents the proportion of the particles in a certain position (for example at the inside of the membrane) and $1-n$ represents the proportion that are somewhere else (for example at the outside of the membrane). α_n determines the rate of transfer from outside to inside, while β_n determines the transfer in the opposite direction. If the particle has a negative charge α_n should increase and β_n should decrease when the membrane is depolarized.

Application of these equations will be discussed in terms of the family of curves in Fig. 3. Here the circles are experimental observations of the rise of potassium conductance associated with depolarization, while the smooth curves are theoretical solutions of eqns. (6) and (7).

In the resting state, defined by $V=0$, n has a resting value given by

$$n_0 = \frac{\alpha_{n0}}{\alpha_{n0}+\beta_{n0}}.$$

If V is changed suddenly α_n and β_n instantly take up values appropriate to the new voltage. The solution of (7) which satisfies the boundary condition that $n=n_0$ when $t=0$ is

$$n = n_\infty - (n_\infty - n_0)\exp(-t/\tau_n), \tag{8}$$

where

$$n_\infty = \alpha_n/(\alpha_n+\beta_n), \tag{9}$$

and

$$\tau_n = 1/(\alpha_n+\beta_n). \tag{10}$$

From eqn. (6) this may be transformed into a form suitable for comparison with the experimental results, i.e.

$$g_K = \{(g_{K\infty})^{\frac{1}{4}} - [(g_{K\infty})^{\frac{1}{4}} - (g_{K0})^{\frac{1}{4}}] \exp(-t/\tau_n)\}^4, \quad (11)$$

where $g_{K\infty}$ is the value which the conductance finally attains and g_{K0} is the conductance at $t=0$. The smooth curves in Fig. 3 were calculated from

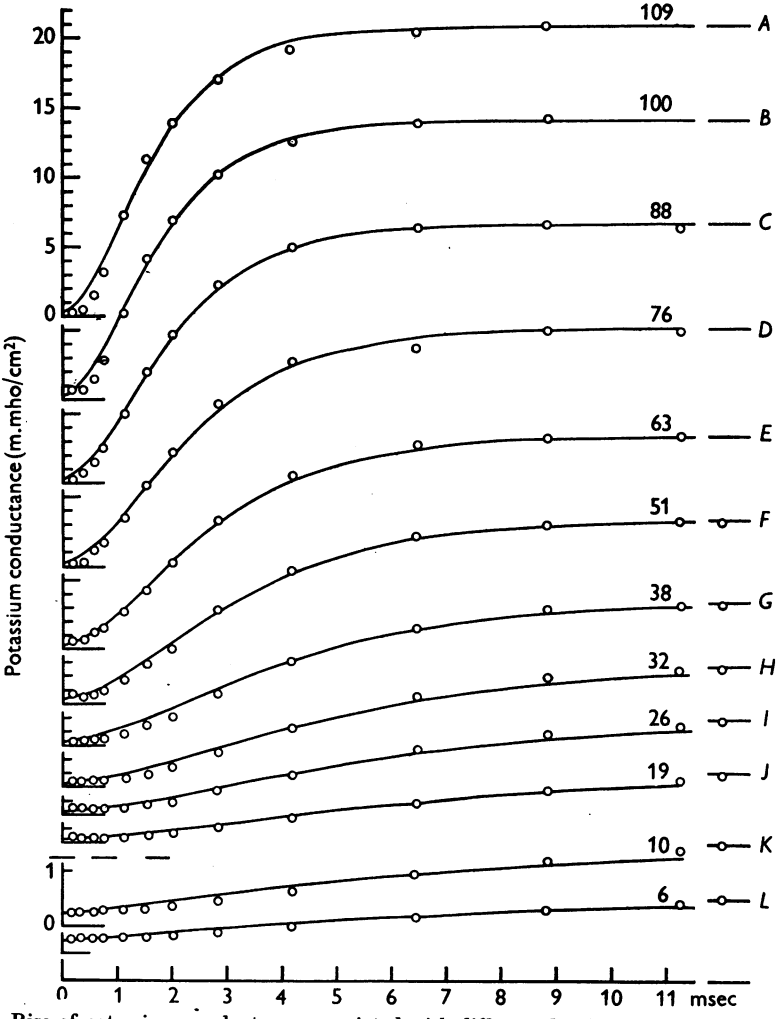

Fig. 3. Rise of potassium conductance associated with different depolarizations. The circles are experimental points obtained on axon 17, temperature 6–7° C, using observations in sea water and choline sea water (see Hodgkin & Huxley, 1952*a*). The smooth curves were drawn from eqn. (11) with $g_{K0}=0{\cdot}24$ m.mho/cm² and other parameters as shown in Table 1. The time scale applies to all records. The ordinate scale is the same in the upper ten curves (*A* to *J*) and is increased fourfold in the lower two curves (*K* and *L*). The number on each curve gives the depolarization in mV.

eqn. (11) with a value of τ_n chosen to give the best fit. It will be seen that there is reasonable agreement between theoretical and experimental curves, except that the latter show more initial delay. Better agreement might have been obtained with a fifth or sixth power, but the improvement was not considered to be worth the additional complication.

The rate constants α_n and β_n. At large depolarizations $g_{K\infty}$ seems to approach an asymptote about 20–50% greater than the conductance at −100 mV.

TABLE 1. Analysis of curves in Fig. 3

Curve	V (mV) (1)	$g_{K\infty}$ (m.mho/cm²) (2)	n_∞ (3)	τ_n (msec) (4)	α_n (msec^{-1}) (5)	β_n (msec^{-1}) (6)
—	$(-\infty)$	(24·31)	(1·000)	—	—	—
A	−109	20·70	0·961	1·05	0·915	0·037
B	−100	20·00	0·953	1·10	0·866	0·043
C	− 88	18·60	0·935	1·25	0·748	0·052
D	− 76	17·00	0·915	1·50	0·610	0·057
E	− 63	15·30	0·891	1·70	0·524	0·064
F	− 51	13·27	0·859	2·05	0·419	0·069
G	− 38	10·29	0·806	2·60	0·310	0·075
H	− 32	8·62	0·772	3·20	0·241	0·071
I	− 26	6·84	0·728	3·80	0·192	0·072
J	− 19	5·00	0·674	4·50	0·150	0·072
K	− 10	1·47	0·496	5·25	0·095	0·096
L	− 6	0·98	0·448	5·25	0·085	0·105
—	(0)	(0·24)	(0·315)	—	—	—

Col. 1 shows depolarization in mV; col. 2, final potassium conductance; col. 3, $n_\infty = (g_{K\infty}/\bar{g}_K)^{\frac{1}{4}}$; col. 4, time constant used to compute curve; col. 5, $\alpha_n = n_\infty/\tau_n$; col. 6, $\beta_n = (1 - n_\infty)/\tau_n$. The figure of 24·31 was chosen for $\bar{g}_K$ because it made the asymptotic value of n_∞ 5% greater than the value at −100 mV.

For the purpose of calculation we assume that $n = 1$ at the asymptote which is taken as about 20% greater than the value of $g_{K\infty}$ at $V = -100$ mV. These assumptions are somewhat arbitrary, but should introduce little error since we are not concerned with the behaviour of g_K at depolarizations greater than about 110 mV. In the experiment illustrated by Fig. 3, $g_{K\infty} = 20$ m.mho/cm² at $V = -100$ mV. $\bar{g}_K$ was therefore chosen to be near 24 m.mho/cm². This value was used to calculate n_∞ at various voltages by means of eqn. (6). α_n and β_n could then be obtained from the following relations which are derived from eqns. (9) and (10):

$$\alpha_n = n_\infty/\tau_n,$$

$$\beta_n = (1 - n_\infty)/\tau_n.$$

The results of analysing the curves in Fig. 3 by this method are shown in Table 1.

An estimate of the resting values of α_n and β_n could be obtained from the decline in potassium conductance associated with repolarization. The procedure was essentially the same but the results were approximate because the

resting value of the potassium conductance was not known with any accuracy when the membrane potential was high. Fig. 2 illustrates an experiment in which the membrane potential was restored to its resting value after a depolarization of 25 mV. It will be seen that both the rise and fall of the potassium conductance agree reasonably with theoretical curves calculated from eqn. (11) after an appropriate choice of parameters. The rate constants derived from these parameters were (in msec^{-1}): $\alpha_n = 0{\cdot}21$, $\beta_n = 0{\cdot}70$ when $V = 0$ and $\alpha_n = 0{\cdot}90$, $\beta_n = 0{\cdot}43$ when $V = -25$ mV.

In order to find functions connecting α_n and β_n with membrane potential we collected all our measurements and plotted them against V, as in Fig. 4. Differences in temperature were allowed for by adopting a temperature coefficient of 3 (Hodgkin *et al.* 1952) and scaling to 6° C. The effect of replacing sodium by choline on the resting potential was taken into account by displacing the origin for values in choline sea water by +4 mV. The continuous curves, which are clearly a good fit to the experimental data, were calculated from the following expressions:

$$\alpha_n = 0{\cdot}01\,(V+10)\Big/\left[\exp\frac{V+10}{10}-1\right], \tag{12}$$

$$\beta_n = 0{\cdot}125\exp(V/80), \tag{13}$$

where α_n and β_n are given in reciprocal msec and V is the displacement of the membrane potential from its resting value in mV.

These expressions should also give a satisfactory formula for the steady potassium conductance ($g_{K\infty}$) at any membrane potential (V), for this relation is implicit in the measurement of α_n and β_n. This is illustrated by Fig. 5, in which the abscissa is the membrane potential and the ordinate is $(g_{K\infty}/\bar{g}_K)^{\frac{1}{4}}$. The smooth curve was calculated from eqn. (9) with α_n and β_n substituted from eqns. (12) and (13).

Fig. 4 shows that β_n is small compared to α_n over most of the range; we therefore do not attach much weight to the curve relating β_n to V and have used the simplest expression which gave a reasonable fit. The function for α_n was chosen for two reasons. First, it is one of the simplest which fits the experimental results and, secondly, it bears a close resemblance to the equation derived by Goldman (1943) for the movements of a charged particle in a constant field. Our equations can therefore be given a qualitative physical basis if it is supposed that the variation of α and β with membrane potential arises from the effect of the electric field on the movement of a negatively charged particle which rests on the outside of the membrane when V is large and positive, and on the inside when it is large and negative. The analogy cannot be pressed since α and β are not symmetrical about $E = 0$, as they should be if Goldman's theory held in a simple form. Better agreement might

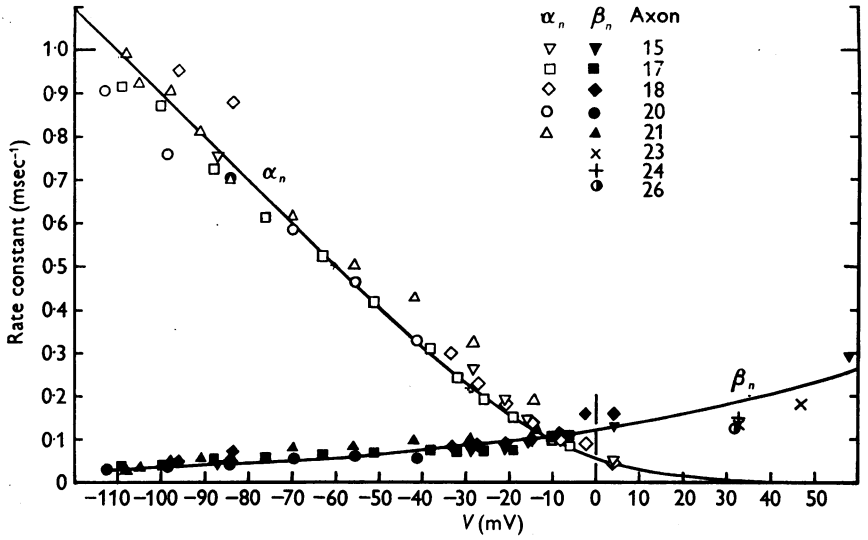

Fig. 4. Abscissa: membrane potential minus resting potential in sea water. Ordinate: rate constants determining rise (α_n) or fall (β_n) of potassium conductance at 6° C. The resting potential was assumed to be 4 mV higher in choline sea water than in ordinary sea water. Temperature differences were allowed for by assuming a Q_{10} of 3. All values for $V < 0$ were obtained by the method illustrated by Fig. 3 and Table 1; those for $V > 0$ were obtained from the decline of potassium conductance associated with an increase of membrane potential or from repolarization to the resting potential in choline sea water (e.g. Fig. 2). Axons 17–21 at 6–11° C, the remainder at about 20° C. The smooth curves were drawn from eqns. (12) and (13).

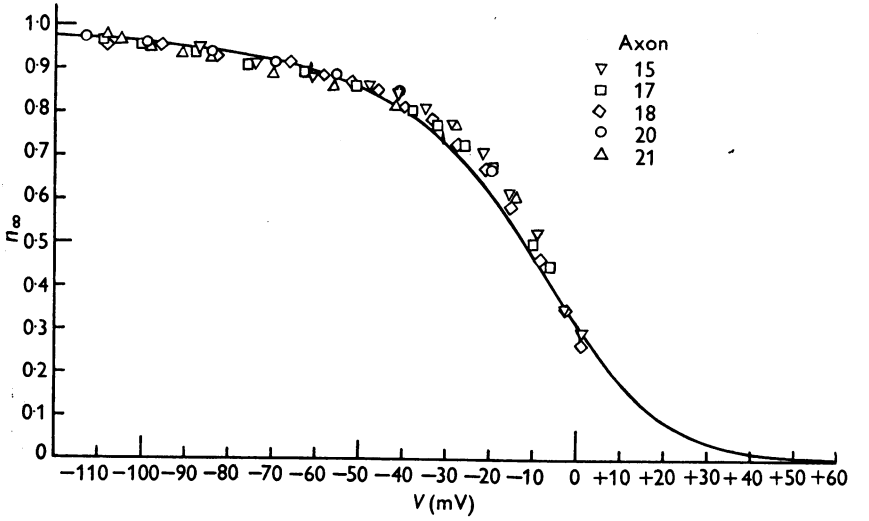

Fig. 5. Abscissa: membrane potential minus resting potential in sea water. Ordinate: experimental measurements of n_∞ calculated from the steady potassium conductance by the relation $n_\infty = \sqrt[4]{(g_{K\infty}/\bar{g}_K)}$, where $\bar{g}_K$ is the 'maximum' potassium conductance. The smooth curve is drawn according to eqn. (9).

be obtained by postulating some asymmetry in the structure of the membrane, but this assumption was regarded as too speculative for profitable consideration.

The sodium conductance

There are at least two general methods of describing the transient changes in sodium conductance. First, we might assume that the sodium conductance is determined by a variable which obeys a second-order differential equation. Secondly, we might suppose that it is determined by two variables, each of which obeys a first-order equation. These two alternatives correspond roughly to the two general types of mechanism mentioned in connexion with the nature of inactivation (pp. 502–503). The second alternative was chosen since it was simpler to apply to the experimental results.

The formal assumptions made are:

$$g_{Na} = m^3 h \bar{g}_{Na}, \tag{14}$$

$$\frac{dm}{dt} = \alpha_m (1-m) - \beta_m m, \tag{15}$$

$$\frac{dh}{dt} = \alpha_h (1-h) - \beta_h h, \tag{16}$$

where $\bar{g}_{Na}$ is a constant and the α's and β's are functions of V but not of t.

These equations may be given a physical basis if sodium conductance is assumed to be proportional to the number of sites on the inside of the membrane which are occupied simultaneously by three activating molecules but are not blocked by an inactivating molecule. m then represents the proportion of activating molecules on the inside and $1-m$ the proportion on the outside; h is the proportion of inactivating molecules on the outside and $1-h$ the proportion on the inside. α_m or β_h and β_m or α_h represent the transfer rate constants in the two directions.

Application of these equations will be discussed first in terms of the family of curves in Fig. 6. Here the circles are experimental estimates of the rise and fall of sodium conductance during a voltage clamp, while the smooth curves were calculated from eqns. (14)–(16).

The solutions of eqns. (15) and (16) which satisfy the boundary conditions $m = m_0$ and $h = h_0$ at $t = 0$ are

$$m = m_\infty - (m_\infty - m_0) \exp(-t/\tau_m), \tag{17}$$

$$h = h_\infty - (h_\infty - h_0) \exp(-t/\tau_h), \tag{18}$$

where $m_\infty = \alpha_m/(\alpha_m + \beta_m)$ and $\tau_m = 1/(\alpha_m + \beta_m)$,

$h_\infty = \alpha_h/(\alpha_h + \beta_h)$ and $\tau_h = 1/(\alpha_h + \beta_h)$.

In the resting state the sodium conductance is very small compared with the value attained during a large depolarization. We therefore neglect m_0 if the

depolarization is greater than 30 mV. Further, inactivation is very nearly complete if $V < -30$ mV so that h_∞ may also be neglected. The expression for the sodium conductance then becomes

$$g_{Na} = g'_{Na}\,[1-\exp(-t/\tau_m)]^3 \exp(-t/\tau_h), \tag{19}$$

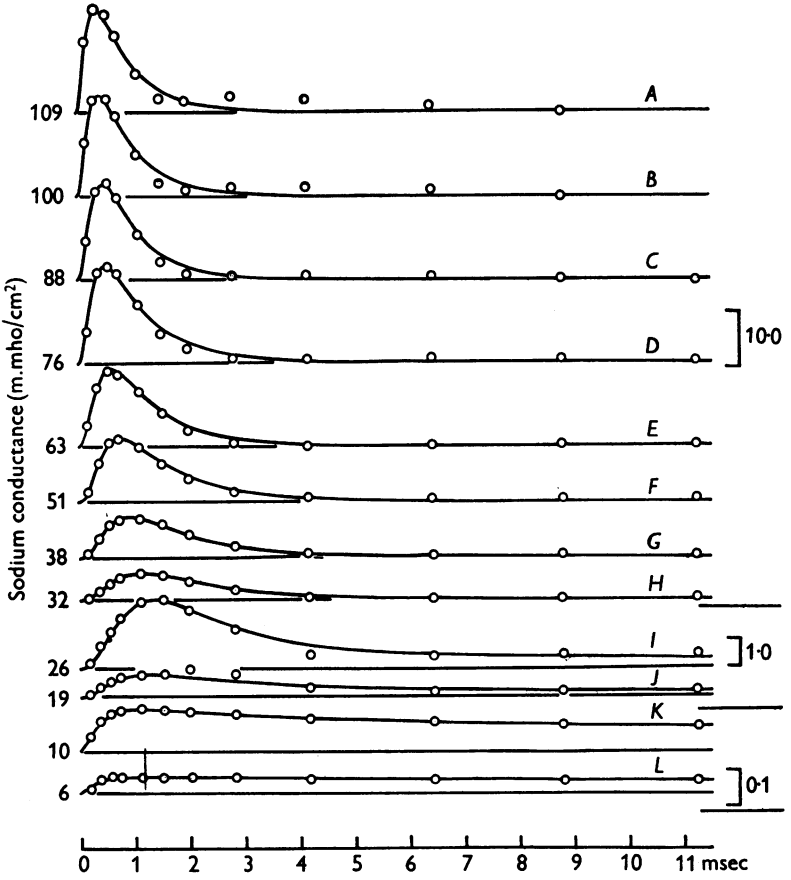

Fig. 6. Changes of sodium conductance associated with different depolarizations. The circles are experimental estimates of sodium conductance obtained on axon 17, temperature 6–7° C (cf. Fig. 3). The smooth curves are theoretical curves with parameters shown in Table 2; *A* to *H* drawn from eqn. 19, *I* to *L* from 14, 17, 18 with $\bar{g}_{Na} = 70{\cdot}7$ m.mho/cm². The ordinate scales on the right are given in m.mho/cm². The numbers on the left show the depolarization in mV. The time scale applies to all curves.

where $g'_{Na} = \bar{g}_{Na} m_\infty^3 h_0$ and is the value which the sodium conductance would attain if h remained at its resting level (h_0). Eqn. (19) was fitted to an experimental curve by plotting the latter on double log paper and comparing it with a similar plot of a family of theoretical curves drawn with different ratios of τ_m to τ_h. Curves *A* to *H* in Fig. 6 were obtained by this method and gave the

TABLE 2. Analysis of curves in Fig. 6

Curve	V (mV)	g'_{Na} (m.mho/cm²)	m_∞	τ_m (msec)	α_m (msec^{-1})	β_m (msec^{-1})	τ_h (msec)	h_∞	α_h (msec^{-1})	β_h (msec^{-1})
—	(−∞)	(42·9)	(1·00)	—	—	—	—	—	—	—
A	−109	40·3	0·980	0·140	7·0	(0·14)	0·67	(0)	(0)	1·50
B	−100	42·6	0·997	0·160	6·2	(0·02)	0·67	(0)	(0)	1·50
C	− 88	46·8	1·029	0·200	5·15	(−0·14)	0·67	(0)	(0)	1·50
D	− 76	39·5	0·975	0·189	5·15	0·13	0·84	(0)	(0)	1·19
E	− 63	38·2	0·963	0·252	3·82	0·15	0·84	(0)	(0)	1·19
F	− 51	30·7	0·895	0·318	2·82	0·33	1·06	(0)	(0)	0·94
G	− 38	20·0	0·778	0·382	2·03	0·58	1·27	(0)	(0)	0·79
H	− 32	15·3	0·709	0·520	1·36	0·56	1·33	(0)	(0)	0·75
I	− 26	7·90	0·569	0·600	0·95	0·72	(1·50)	(0·029)	(0·02)	(0·65)
J	− 19	1·44	0·323	0·400	0·81	1·69	(2·30)	(0·069)	(0·03)	(0·40)
K	− 10	0·13	0·145	0·220	0·66	3·9	(5·52)	(0·263)	(0·05)	(0·13)
L	− 6	0·046	0·103	0·200	0·51	4·5	(6·73)	(0·388)	(0·06)	(0·09)
—	(0)	(0·0033)	(0·042)	—	—	—	—	(0·608)	—	—

Values enclosed in brackets were not plotted in Figs. 7–10 either because they were too small to be reliable or because they were not independent measurements obtained in this experiment.

values of g'_{Na}, τ_m and τ_h shown in Table 2. Curves *I* to *L* were obtained from eqns. (17) and (18) assuming that h_∞ and τ_h had values calculated from experiments described in a previous paper (Hodgkin & Huxley, 1952 *c*).

The rate constants α_m and β_m. Having fitted theoretical curves to the experimental points, α_m and β_m were found by a procedure similar to that used with α_n and β_n, i.e.

$$\alpha_m = m_\infty/\tau_m, \quad \beta_m = (1-m_\infty)/\tau_m,$$

the value of m_∞ being obtained from $\sqrt[3]{g'_{Na}}$ on the basis that m_∞ approaches unity at large depolarizations.

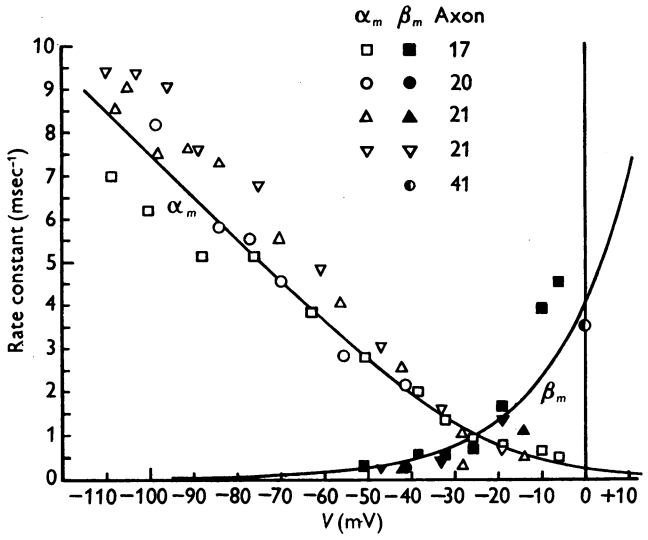

Fig. 7. Abscissa: membrane potential minus resting potential in sea water. Ordinate: rate constants (α_m and β_m) determining initial changes in sodium conductance at 6° C. All values for $V<0$ were obtained by the method illustrated by Fig. 6 and Table 2; the value at $V=0$ was obtained from the decline in sodium conductance associated with repolarization to the resting potential. The temperature varied between 3 and 11° C and was allowed for by assuming a Q_{10} of 3. The smooth curves were drawn from eqns. (20) and (21).

Values of α_m and β_m were collected from different experiments, reduced to a temperature of 6° C by adopting a Q_{10} of 3 and plotted in the manner shown in Fig. 7. The point for $V=0$ was obtained from what we regard as the most reliable estimate of the rate constant determining the decline of sodium conductance when the membrane is repolarized (Hodgkin & Huxley, 1952*b*, table 1, axon 41). The smooth curves in Fig. 7 were drawn according to the equations:

$$\alpha_m = 0{\cdot}1\,(V+25)\Big/\left(\exp\frac{V+25}{10}-1\right), \tag{20}$$

$$\beta_m = 4\exp(V/18), \tag{21}$$

where α_m and β_m are expressed in msec^{-1} and V is in mV.

Fig. 8 illustrates the relation between m_∞ and V. The symbols are experimental estimates and the smooth curve was calculated from the equation

$$m_\infty = \alpha_m/(\alpha_m + \beta_m), \tag{22}$$

where α_m and β_m have the values given by eqns. (20) and (21).

The rate constants α_h and β_h. The rate constants for the inactivation process were calculated from the expressions

$$\alpha_h = h_\infty/\tau_h,$$
$$\beta_h = (1-h_\infty)/\tau_h.$$

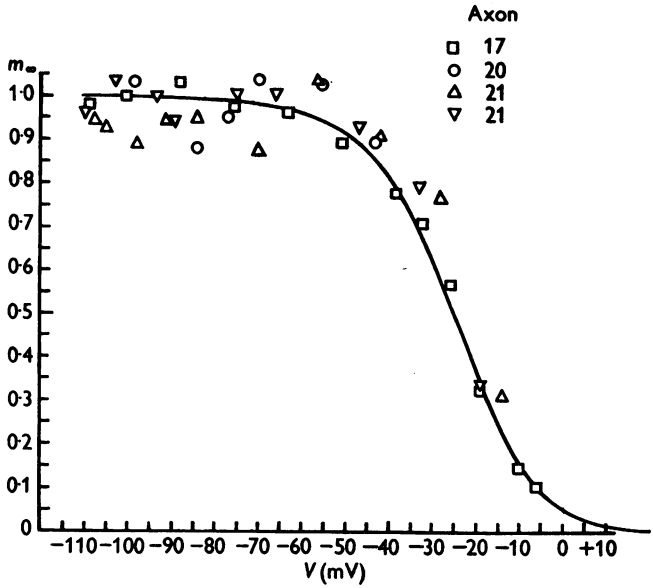

Fig. 8. Abscissa: membrane potential minus resting potential in sea water. Ordinate: m_∞ obtained by fitting curves to observed changes in sodium conductance at different depolarizations (e.g. Fig. 6 and Table 2). The smooth curve is drawn according to eqn. (22). The experimental points are proportional to the cube root of the sodium conductance which would have been obtained if there were no inactivation.

Values obtained by these equations are plotted against membrane potential in Fig. 9. The points for $V < -30$ mV were derived from the analysis described in this paper (e.g. Table 2), while those for $V > -30$ mV were obtained from the results given in a previous paper (Hodgkin & Huxley, 1952 *c*). A temperature coefficient of 3 was assumed and differences in resting potential were allowed for by taking the origin at a potential corresponding to $h_\infty = 0{\cdot}6$.

The smooth curves in this figure were calculated from the expressions

$$\alpha_h = 0{\cdot}07 \exp(V/20), \tag{23}$$

and

$$\beta_h = 1\Big/\left(\exp\frac{V+30}{10}+1\right). \tag{24}$$

The steady state relation between h_∞ and V is shown in Fig. 10. The smooth curve is calculated from the relation

$$h_\infty = \alpha_h/(\alpha_h + \beta_h), \tag{25}$$

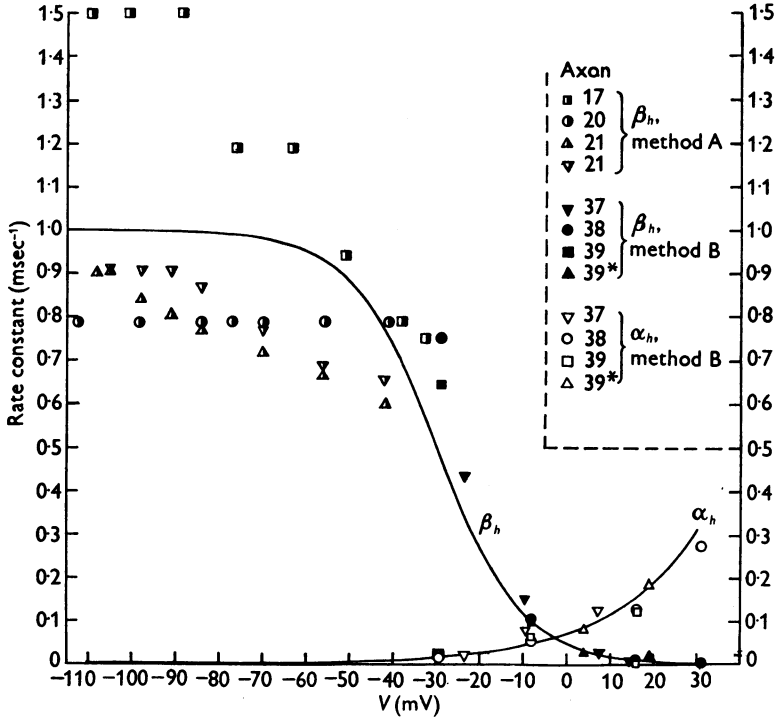

Fig. 9. Rate constants of inactivation (α_h and β_h) as functions of membrane potential (V). The smooth curves were calculated from eqns. (23) and (24). The experimental values of α_h and β_h were obtained from data such as those in Table 2 of this paper (method A) or from the values of τ_h and h_∞ given in Table 1 of Hodgkin & Huxley (1952*c*) (method B). Temperature differences were allowed for by scaling with a Q_{10} of 3. Axon 39 was at 19° C; all others at 3–9° C. The values for axons 37 and 39* were displaced by −1·5 and −12 mV in order to give $h_\infty = 0{\cdot}6$ at $V = 0$.

with α_h and β_h given by eqns. (23) and (24). If $V > -30$ mV this expression approximates to the simple expression used in a previous paper (Hodgkin & Huxley, 1952 *c*), i.e.

$$h_\infty = 1\Big/\left(1 + \exp\frac{V_h - V}{7}\right),$$

where V_h is about −2 and is the potential at which $h_\infty = 0{\cdot}5$. This equation is the same as that giving the effect of a potential difference on the proportion of negatively charged particles on the outside of a membrane to the total number of such particles on both sides of the membrane (see p. 503). It is therefore consistent with the suggestion that inactivation might be due to the

movement of a negatively charged particle which blocks the flow of sodium ions when it reaches the inside of the membrane. This is encouraging, but it must be mentioned that a physical theory of this kind does not lead to satisfactory functions for α_h and β_h without further *ad hoc* assumptions.

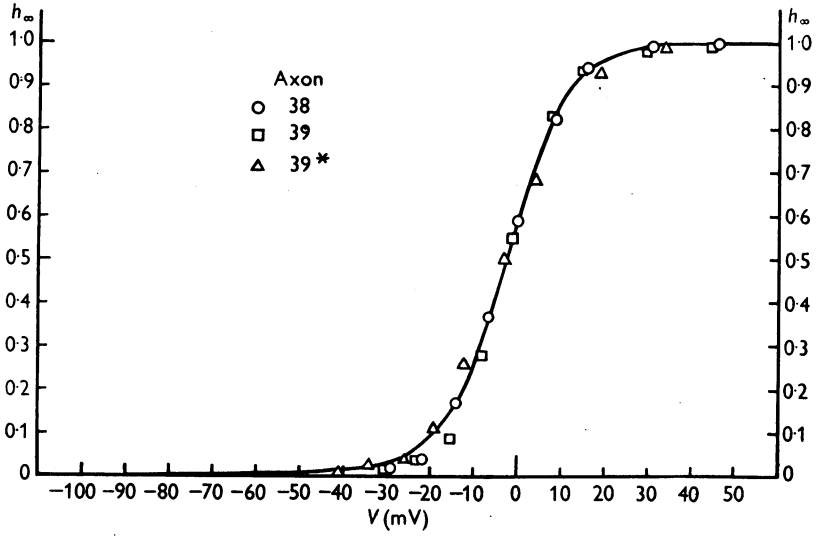

Fig. 10. Steady state relation between h and V. The smooth curve is drawn according to eqn. (25). The experimental points are those given in Table 1 of Hodgkin & Huxley (1952*c*). Axon 38 (5° C) as measured. Axon 39 (19° C) displaced −1·5 mV. Axon 39* (3° C, fibre in derelict state) displaced −12 mV. The curve gives the fraction of the sodium-carrying system which is readily available, as a function of membrane potential, in the steady state.

PART III. RECONSTRUCTION OF NERVE BEHAVIOUR

The remainder of this paper will be devoted to calculations of the electrical behaviour of a model nerve whose properties are defined by the equations which were fitted in Part II to the voltage clamp records described in the earlier papers of this series.

Summary of equations and parameters

We may first collect the equations which give the total membrane current I as a function of time and voltage. These are:

$$I = C_M \frac{dV}{dt} + \bar{g}_K n^4 (V - V_K) + \bar{g}_{Na} m^3 h (V - V_{Na}) + \bar{g}_l (V - V_l), \tag{26}$$

where

$$dn/dt = \alpha_n (1 - n) - \beta_n n, \tag{7}$$

$$dm/dt = \alpha_m (1 - m) - \beta_m m, \tag{15}$$

$$dh/dt = \alpha_h (1 - h) - \beta_h h, \tag{16}$$

and

$$\alpha_n = 0{\cdot}01\,(V+10)\Big/\left(\exp\frac{V+10}{10}-1\right), \tag{12}$$

$$\beta_n = 0{\cdot}125\exp(V/80), \tag{13}$$

$$\alpha_m = 0{\cdot}1\,(V+25)\Big/\left(\exp\frac{V+25}{10}-1\right), \tag{20}$$

$$\beta_m = 4\exp(V/18), \tag{21}$$

$$\alpha_h = 0{\cdot}07\exp(V/20), \tag{23}$$

$$\beta_h = 1\Big/\left(\exp\frac{V+30}{10}+1\right). \tag{24}$$

Equation (26) is derived simply from eqns. (1)–(6) and (14) in Part II. The four terms on the right-hand side give respectively the capacity current, the current carried by K ions, the current carried by Na ions and the leak current, for 1 cm^2 of membrane. These four components are in parallel and add up to give the total current density through the membrane I. The conductances to K and Na are given by the constants $\bar{g}_K$ and $\bar{g}_{Na}$, together with the dimensionless quantities n, m and h, whose variation with time after a change of membrane potential is determined by the three subsidiary equations (7), (15) and (16). The α's and β's in these equations depend only on the instantaneous value of the membrane potential, and are given by the remaining six equations.

Potentials are given in mV, current density in μA/cm^2, conductances in m.mho/cm^2, capacity in μF/cm^2, and time in msec. The expressions for the α's and β's are appropriate to a temperature of 6·3° C; for other temperatures they must be scaled with a Q_{10} of 3.

The constants in eqn. (26) are taken as independent of temperature. The values chosen are given in Table 3, column 2, and may be compared with the experimental values in columns 3 and 4.

Membrane currents during a voltage clamp

Before applying eqn. (26) to the action potential it is well to check that it predicts correctly the total current during a voltage clamp. At constant voltage $dV/dt=0$ and the coefficients α and β are constant. The solution is then obtained directly in terms of the expressions already given for n, m and h (eqns. (8), (17) and (18)). The total ionic current was computed from these for a number of different voltages and is compared with a series of experimental curves in Fig. 11. The only important difference is that the theoretical current has too little delay at the sodium potential; this reflects the inability of our equations to account fully for the delay in the rise of g_K (p. 509).

'Membrane' and propagated action potentials

By a 'membrane' action potential is meant one in which the membrane potential is uniform, at each instant, over the whole of the length of fibre

TABLE 3

Constant (1)	Value chosen (2)	Experimental values: Mean (3)	Experimental values: Range (4)	Reference (5)
C_M (μF/cm^2)	1·0	0·91	0·8 to 1·5	Table 1, Hodgkin *et al.* (1952)
V_{Na} (mV)	−115	−109	−95 to −119	p. 455, Hodgkin & Huxley (1952*a*)
V_K (mV)	+ 12	+ 11	+ 9 to + 14	Table 3, values for low temperature in sea water, Hodgkin & Huxley (1952*b*)
V_l (mV)	−10·613*	− 11	− 4 to − 22	Table 5, Hodgkin & Huxley (1952*b*)
$\bar{g}_{Na}$ (m.mho/cm^2)	120	80	65 to 90	Fully analysed results, Table 2† } Hodgkin & Huxley (1952*a*)
		160	120 to 260	Fresh fibres, p. 465† } Hodgkin & Huxley (1952*a*)
$\bar{g}_K$ (m.mho/cm^2)	36	34	26 to 49	p. 463, Hodgkin & Huxley (1952*a*)
$\bar{g}_l$ (m.mho/cm^2)	0·3	0·26	0·13 to 0·50	Table 5, Hodgkin & Huxley (1952*b*)

* Exact value chosen to make the total ionic current zero at the resting potential ($V = 0$).

† The experimental values for $\bar{g}_{Na}$ were obtained by multiplying the peak sodium conductances by factors derived from the values chosen for α_m, β_m, α_h, and β_h.

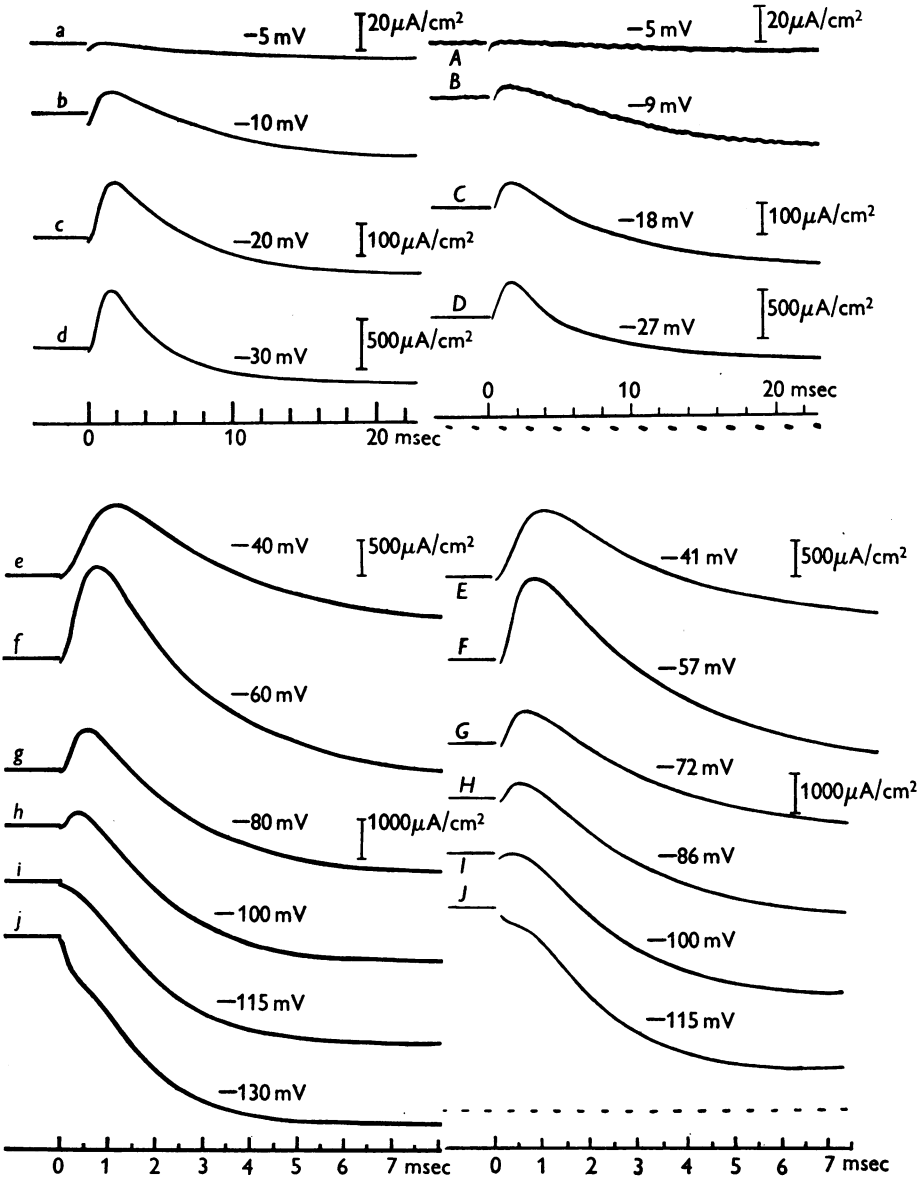

Fig. 11. Left-hand column: time course of membrane current during voltage clamp, calculated for temperature of 4° C from eqn. (26) and subsidiaries and plotted on the same scale as the experimental curves in the right-hand column. Right-hand column: observed time course of membrane currents during voltage clamp. Axon 31 at 4° C; compensated feedback. The time scale changes between *d*, *D* and *e*, *E*. The current scale changes after *b*, *B*; *c*, *C*; *d*, *D* and *f*, *F*.

considered. There is no current along the axis cylinder and the net membrane current must therefore always be zero, except during the stimulus. If the stimulus is a short shock at $t=0$, the form of the action potential should be given by solving eqn. (26) with $I=0$ and the initial conditions that $V=V_0$ and m, n and h have their resting steady state values, when $t=0$.

The situation is more complicated in a propagated action potential. The fact that the local circuit currents have to be provided by the net membrane current leads to the well-known relation

$$i=\frac{1}{r_1+r_2}\frac{\partial^2 V}{\partial x^2}, \tag{27}$$

where i is the membrane current per unit length, r_1 and r_2 are the external and internal resistances per unit length, and x is distance along the fibre. For an axon surrounded by a large volume of conducting fluid, r_1 is negligible compared with r_2. Hence

$$i=\frac{1}{r_2}\frac{\partial^2 V}{\partial x^2},$$

or

$$I=\frac{a}{2R_2}\frac{\partial^2 V}{\partial x^2}, \tag{28}$$

where I is the membrane current density, a is the radius of the fibre and R_2 is the specific resistance of the axoplasm. Inserting this relation in eqn. (26), we have

$$\frac{a}{2R_2}\frac{\partial^2 V}{\partial x^2}=C_M\frac{\partial V}{\partial t}+\bar{g}_K n^4(V-V_K)+\bar{g}_{Na}m^3h(V-V_{Na})+\bar{g}_l(V-V_l), \tag{29}$$

the subsidiary equations being unchanged.

Equation (29) is a partial differential equation, and it is not practicable to solve it as it stands. During steady propagation, however, the curve of V against time at any one position is similar in shape to that of V against distance at any one time, and it follows that

$$\frac{\partial^2 V}{\partial x^2}=\frac{1}{\theta^2}\frac{\partial^2 V}{\partial t^2},$$

where θ is the velocity of conduction. Hence

$$\frac{a}{2R_2\theta^2}\frac{d^2V}{dt^2}=C_M\frac{dV}{dt}+\bar{g}_K n^4(V-V_K)+\bar{g}_{Na}m^3h(V-V_{Na})+\bar{g}_l(V-V_l). \tag{30}$$

This is an ordinary differential equation and can be solved numerically, but the procedure is still complicated by the fact that θ is not known in advance. It is necessary to guess a value of θ, insert it in eqn. (30) and carry out the numerical solution starting from the resting state at the foot of the action potential. It is then found that V goes off towards either $+\infty$ or $-\infty$, according as the guessed θ was too small or too large. A new value of θ is

then chosen and the procedure repeated, and so on. The correct value brings V back to zero (the resting condition) when the action potential is over.

The solutions which go towards $\pm\infty$ correspond to action potentials travelling slower than normal under a travelling anode or faster than normal under a travelling cathode. We suspect that a system which tends to $-\infty$ for all values of θ after an initial negative displacement of V is one which is incapable of propagating an action potential.

NUMERICAL METHODS

Membrane action potentials

Integration procedure. The equations to be solved are the four simultaneous first-order equations (26), (7), (15), and (16) (p. 518). After slight rearrangement (which will be omitted in this description) these were integrated by the method of Hartree (1932–3). Denoting the beginning and end of a step by t_0 and t_1 ($=t_0+\delta t$) the procedure for each step was as follows:

(1) Estimate V_1 from V_0 and its backward differences.

(2) Estimate n_1 from n_0 and its backward differences.

(3) Calculate $(\mathrm{d}n/\mathrm{d}t)_1$ from eqn. 7 using the estimated n_1 and the values of α_n and β_n appropriate to the estimated V_1.

(4) Calculate n_1 from the equation

$$n_1-n_0=\frac{\delta t}{2}\left\{\left(\frac{\mathrm{d}n}{\mathrm{d}t}\right)_0+\left(\frac{\mathrm{d}n}{\mathrm{d}t}\right)_1-\frac{1}{12}\left[\Delta^2\left(\frac{\mathrm{d}n}{\mathrm{d}t}\right)_0+\Delta^2\left(\frac{\mathrm{d}n}{\mathrm{d}t}\right)_1\right]\right\};$$

$\Delta^2(\mathrm{d}n/\mathrm{d}t)$ is the second difference of $\mathrm{d}n/\mathrm{d}t$; its value at t_1 has to be estimated.

(5) If this value of n_1 differs from that estimated in (2), repeat (3) and (4) using the new n_1. If necessary, repeat again until successive values of n_1 are the same.

(6) Find m_1 and h_1 by procedures analogous to steps (2)–(5).

(7) Calculate $\bar{g}_K n_1^4$ and $\bar{g}_{Na} m_1^3 h_1$.

(8) Calculate $(\mathrm{d}V/\mathrm{d}t)_1$ from eqn. 26 using the values found in (7) and the originally estimated V_1.

(9) Calculate a corrected V_1 by procedures analogous to steps (4) and (5). This result never differed enough from the original estimated value to necessitate repeating the whole procedure from step (3) onwards.

The step value had to be very small initially (since there are no differences at $t=0$) and it also had to be changed repeatedly during a run, because the differences became unmanageable if it was too large. It varied between about 0·01 msec at the beginning of a run or 0·02 msec during the rising phase of the action potential, and 1 msec during the small oscillations which follow the spike.

Accuracy. The last digit retained in V corresponded to microvolts. Sufficient digits were kept in the other variables for the resulting errors in the change of V at each step to be only occasionally as large as 1 μV. It is difficult to estimate the degree to which the errors at successive steps accumulate, but we are confident that the overall errors are not large enough to be detected in the illustrations of this paper.

Temperature differences. In calculating the action potential it was convenient to use tables giving the α's and β's at intervals of 1 mV. The tabulated values were appropriate to a fibre at 6·3° C. To obtain the action potential at some other temperature T' °C the direct method would be to multiply all α's and β's by a factor $\phi=3^{(T'-6\cdot3)/10}$, this being correct for a Q_{10} of 3. Inspection of eqn. 26 shows that the same result is achieved by calculating the action potential at 6·3° C with a membrane capacity of ϕC_M μF/cm^2, the unit of time being $1/\phi$ msec. This method was adopted since it saved recalculating the tables.

Propagated action potential

Equations. The main equation for a propagated action potential is eqn. (30). Introducing a quantity $K = 2R_2\theta^2 C_M/a$, this becomes

$$\frac{d^2V}{dt^2} = K\left\{\frac{dV}{dt} + \frac{1}{C_M}[\bar{g}_K n^4(V - V_K) + \bar{g}_{Na} m^3 h(V - V_{Na}) + \bar{g}_l(V - V_l)]\right\}. \quad (31)$$

The subsidiary equations (7), (15) and (16), and the α's and β's, are the same as for the membrane equation.

Integration procedure. Steps (1)–(7) were the same as for the membrane action potential. After that the procedure was as follows:

(8) Estimate $(dV/dt)_1$ from $(dV/dt)_0$ and its backward differences.

(9) Calculate $(d^2V/dt^2)_1$ from eqn. (31), using the values found in (7) and the estimated values of V_1 and $(dV/dt)_1$.

(10) Calculate a corrected $(dV/dt)_1$ by procedures analogous to steps (4) and (5).

(11) Calculate a corrected V_1 by a procedure analogous to step (4), using the corrected $(dV/dt)_1$.

(12) If necessary, repeat (9)–(11) using the new V_1 and $(dV/dt)_1$, until successive values of V_1 agree.

Starting conditions. In practice it is necessary to start with V deviating from zero by a finite amount (0·1 mV was used). The first few values of V, and hence the differences, were obtained as follows. Neglecting the changes in g_K and g_{Na}, eqn. (31) is

$$\frac{d^2V}{dt^2} = K\left\{\frac{dV}{dt} + \frac{g_0}{C_M}V\right\},$$

where g_0 is the resting conductance of the membrane. The solution of this equation is $V = V_0 e^{\mu t}$, where μ is a solution of

$$\mu^2 - K\mu - Kg_0/C_M = 0. \quad (32)$$

When K has been chosen, μ can thus be found and hence V_1, V_2, etc. ($V_0 e^{\mu t_1}$, $V_0 e^{\mu t_2}$, etc.).

After several runs had been calculated, so that K was known within fairly narrow limits, time was saved by starting new runs not from near $V = 0$ but from a set of values interpolated between corresponding points on a run which had gone towards $+\infty$ and another which had gone towards $-\infty$.

Choice of K. The value of K chosen for the first run makes no difference to the final result, but the nearer it is to the correct value the fewer runs will need to be evaluated. The starting value was found by inserting in eqn. (32) a value of μ found by measuring the foot of an observed action potential.

Calculation of falling phase. The procedure outlined above is satisfactory for the rising phase and peak of the action potential but becomes excessively tedious in the falling phase and the oscillations which follow the spike. A different method, which for other reasons is not applicable in the earlier phases, was therefore employed. The solution was continued as a membrane action potential, and the value of d^2V/dt^2 calculated at each step from the differences of dV/dt. From these it was possible to derive an estimate of the values (denoted by z) that d^2V/dt^2 would have taken in a propagated action potential. The membrane solution was then re-calculated using the following equation instead of eqn. (31):

$$\frac{dV}{dt} = -\frac{1}{C_M}\{\bar{g}_K n^4(V - V_K) + \bar{g}_{Na} m^3 h(V - V_{Na}) + \bar{g}_l(V - V_l)\} + \frac{z}{K}. \quad (33)$$

This was repeated until the z's assumed for a particular run agreed with the d^2V/dt^2's derived from the same run. When this is the case, eqn. (33) is identical with eqn. (31), the main equation for the propagated action potential.

RESULTS

Membrane action potentials

Form of action potential at 6° C. Three calculated membrane action potentials, with different strengths of stimulus, are shown in the upper part of Fig. 12. Only one, in which the initial displacement of membrane potential was 15 mV, is complete; in the other two the calculation was not carried beyond the middle of the falling phase because of the labour involved and because the solution

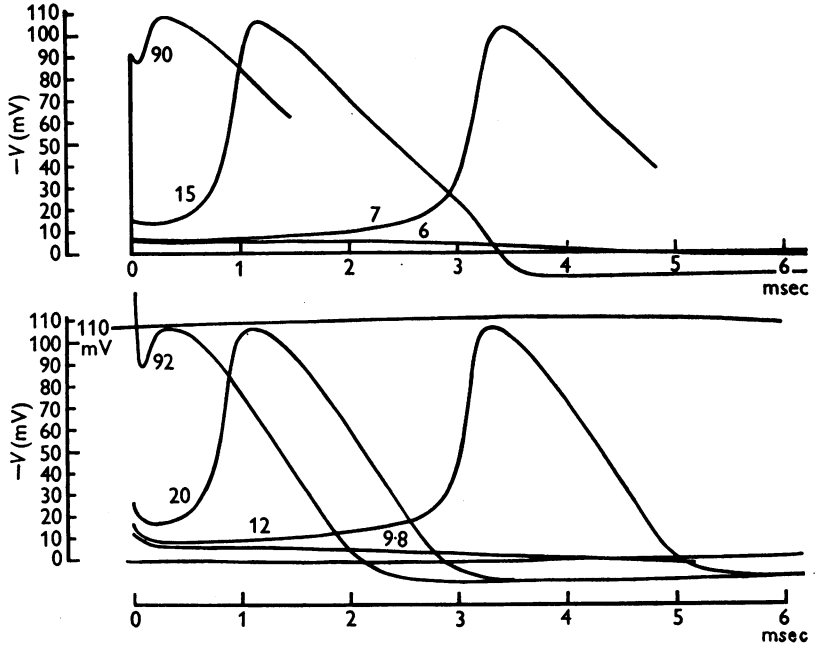

Fig. 12. Upper family: solutions of eqn. (26) for initial depolarizations of 90, 15, 7 and 6 mV (calculated for 6° C). Lower family: tracings of membrane action potentials recorded at 6° C from axon 17. The numbers attached to the curves give the shock strength in mμcoulomb/cm². The vertical and horizontal scales are the same in both families (apart from the slight curvature indicated by the 110 mV calibration line). In this and all subsequent figures depolarizations (or negative displacements of V) are plotted upwards.

had become almost identical with the 15 mV action potential, apart from the displacement in time. One solution for a stimulus just below threshold is also shown.

The lower half of Fig. 12 shows a corresponding series of experimental membrane action potentials. It will be seen that the general agreement is good, as regards amplitude, form and time-scale. The calculated action potentials do, however, differ from the experimental in the following respects: (1) The drop during the first 0·1 msec is smaller. (2) The peaks are sharper.

(3) There is a small hump in the lower part of the falling phase. (4) The ending of the falling phase is too sharp. The extent to which these differences are the result of known shortcomings in our formulation will be discussed on pp. 542–3.

The positive phase of the calculated action potential has approximately the correct form and duration, as may be seen from Fig. 13 in which a pair of curves are plotted on a slower time scale.

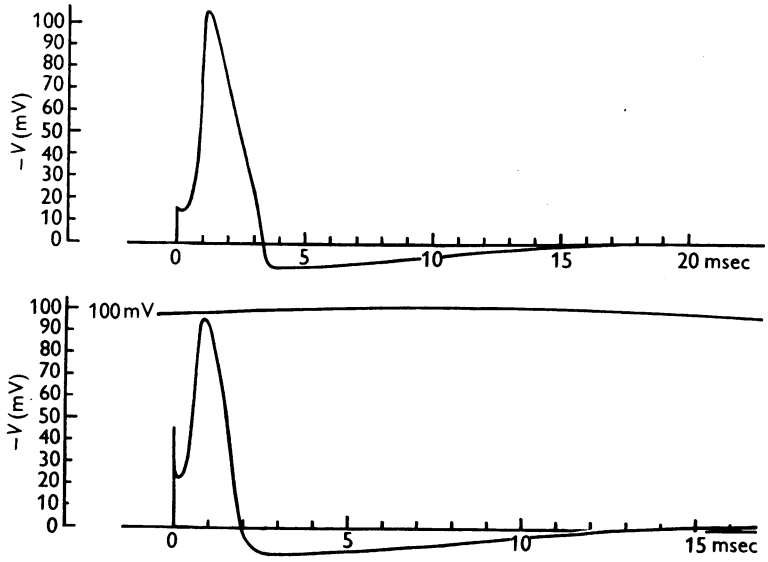

Fig. 13. Upper curve: solution of eqn. (26) for initial depolarization of 15 mV, calculated for 6° C. Lower curve: tracing of membrane action potential recorded at 9·1° C (axon 14). The vertical scales are the same in both curves (apart from curvature in the lower record). The horizontal scales differ by a factor appropriate to the temperature difference.

Certain measurements of these and other calculated action potentials are collected in Table 4.

Form of action potential at 18·5° C. Fig. 14 shows a comparison between a calculated membrane action potential at 18·5° C and an experimental one at 20·5° C. The same differences can be seen as at the low temperature, but, except for the initial drop, they are less marked. In both the calculated and the experimental case, the rise of temperature has greatly reduced the duration of the spike, the difference being more marked in the falling than in the rising phase (Table 4), as was shown in propagated action potentials by Hodgkin & Katz (1949).

The durations of both falling phase and positive phase are reduced at the higher temperature by factors which are not far short of that (3·84) by which the rate constants of the permeability changes are raised ($Q_{10} = 3{\cdot}0$). This is the justification for the differences in time scale between the upper and lower parts in Figs. 13 and 14.

TABLE 4. Characteristics of calculated action potentials

Type of action potential	Temperature (°C)	Stimulus	Spike height (mV)	Amplitude of positive phase (mV)	Peak conductance (m.mho/cm²)	Duration of rising phase, 20 mV to peak (msec)	Duration of falling phase, peak to $V=0$ (msec)	Duration of positive phase (msec)	Interval from peak of potential to peak of conductance (msec)	Max. rate of rise (V/sec)
Propagated	18·5	—	90·5	9·7	32·6	0·252	0·67	5·20	−0·016	431
Membrane	18·5	15 mV depolarization	96·8	10·5	30·7	0·275	0·61	5·09	+0·012	564
Membrane	6·3	100 mV depolarization	108·8	—	45·5	—	—	—	+0·16	—
Membrane	6·3	90 mV depolarization	108·5	—	44·8	—	—	—	+0·15	—
Membrane	6·3	15 mV depolarization	105·4	11·2	37·0	0·59	2·21	14·15	+0·15	311
Membrane	6·3	7 mV depolarization	102·1	—	33·4	0·62	—	—	+0·16	277
Membrane	6·3	Anode break	112·1	11·2	53·4	0·50	2·54	14·4	+0·14	414

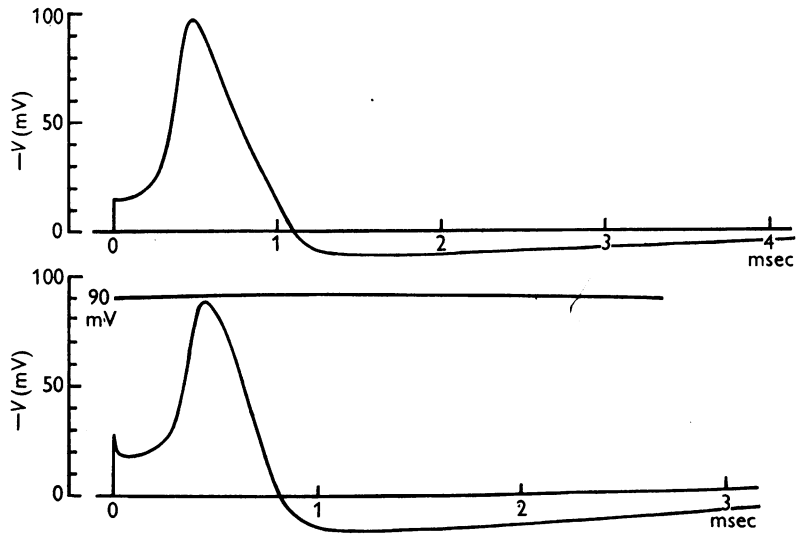

Fig. 14. Upper curve: solution of eqn. (26) for initial depolarization of 15 mV, calculated for 18·5° C. Lower curve: tracing of membrane action potential recorded at 20·5° C (axon 11). Vertical scales are similar. Horizontal scales differ by a factor appropriate to the temperature difference.

Propagated action potential

Form of propagated action potential. Fig. 15 compares the calculated propagated action potential, at 18·5° C, with experimental records on both fast and slow time bases. As in the case of the membrane action potential, the only differences are in certain details of the form of the spike.

Velocity of conduction. The value of the constant K that was found to be needed in the equation for the propagated action potential (eqn. 31) was 10·47 msec^{-1}. This constant, which depends only on properties of the membrane,

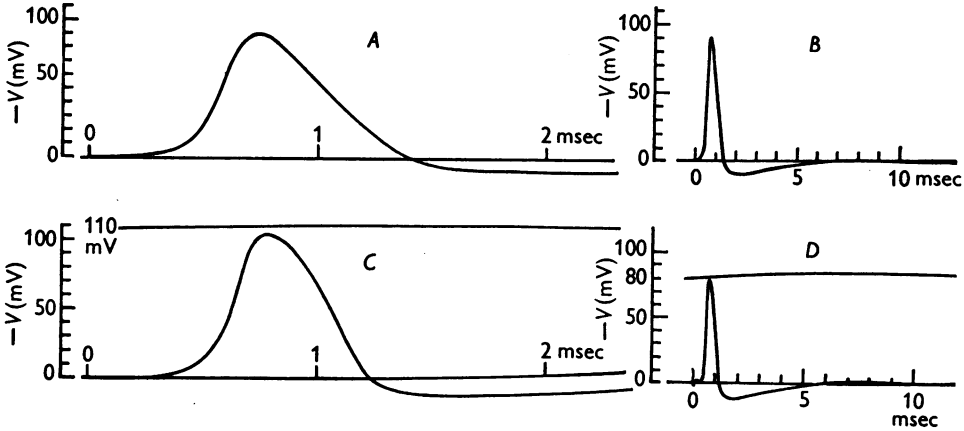

Fig. 15. *A*, solution of eqn. (31) calculated for K of 10·47 msec^{-1} and temperature of 18·5° C. *B*, same solution plotted on slower time scale. *C*, tracing of propagated action potential on same vertical and horizontal scales as *A*. Temperature 18·5° C. *D*, tracing of propagated action potential from another axon on approximately the same vertical and horizontal scales as *B*. Temperature 19·2° C. This axon had been used for several hours; its spike was initially 100 mV.

determines the conduction velocity in conjunction with the constants of the nerve fibre considered as a cable. The relation is given by the definition of K (p. 524), from which

$$\theta = \sqrt{(Ka/2R_2C_M)}, \tag{34}$$

where θ = conduction velocity, a = radius of axis cylinder, R_2 = specific resistance of axoplasm, and C_M = capacity per unit area of membrane.

The propagated action potential was calculated for the temperature at which the record C of Fig. 15 was obtained, and with the value of C_M (1·0 μF/cm^2) that was measured on the fibre from which that record was made. Since θ, a and R_2 were also measured on that fibre, a direct comparison between calculated and observed velocities is possible. The values of a and R_2 were 238 μ and 35·4 Ω. cm respectively. Hence the calculated conduction velocity is

$$(10470 \times 0{\cdot}0238/2 \times 35{\cdot}4 \times 10^{-6})^{\frac{1}{2}} \text{ cm/sec} = 18{\cdot}8 \text{ m/sec}.$$

The velocity found experimentally in this fibre was 21·2 m/sec.

Impedance changes

Time course of conductance change. Cole & Curtis (1939) showed that the impedance of the membrane fell during a spike, and that the fall was due to a great increase in the conductance which is in parallel with the membrane capacity. An effect of this kind is to be expected on our formulation, since the entry of Na^+ which causes the rising phase, and the loss of K^+ which causes the falling phase, are consequent on increases in the conductance of the membrane to currents carried by these ions. These component conductances are evaluated during the calculation, and the total conductance is obtained by adding them and the constant 'leak conductance', $\bar{g}_l$.

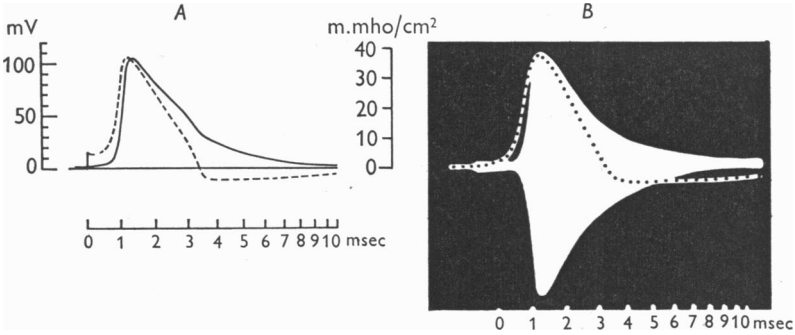

Fig. 16. *A*, solution of eqn. (26) for initial depolarization of 15 mV at a temperature of 6° C. The broken curve shows the membrane action potential in mV; the continuous curve shows the total membrane conductance ($g_{Na}+g_K+\bar{g}_l$) as a function of time. *B*, records of propagated action potential (dotted curve) and conductance change reproduced from Cole & Curtis (1939). The time scales are the same in *A* and *B*.

Fig. 16*A* shows the membrane potential and conductance in a calculated membrane action potential. For comparison, Fig. 16*B* shows superposed records of potential and impedance bridge output (proportional to conductance change), taken from Cole & Curtis's paper. The time scale is the same in *B* as in *A*, and the curves have been drawn with the same peak height. It will be seen that the main features of Cole & Curtis's record are reproduced in the calculated curve. Thus (1) the main rise in conductance begins later than the rise of potential; (2) the conductance does not fall to its resting value until late in the positive phase; and (3) the peak of the conductance change occurs at nearly the same time as the peak of potential. The exact time relation between the peaks depends on the conditions, as can be seen from Table 4.

We chose a membrane action potential for the comparison in Fig. 16 because the spike duration shows that the experimental records were obtained at about 6° C, and our propagated action potential was calculated for 18·5° C. The conductance during the latter is plotted together with the potential in Fig. 17. The same features are seen as in the membrane action potential, the delay

between the rise of potential and the rise of conductance being even more marked.

Absolute value of peak conductance. The agreement between the height of the conductance peak in Fig. 16*A* and the half-amplitude of the bridge output in Fig. 16*B* is due simply to the choice of scale. Nevertheless, our calculated action potentials agree well with Cole & Curtis's results in this respect. These authors found that the average membrane resistance at the peak of the impedance change was 25 $\Omega.cm^2$, corresponding to a conductance of 40 m.mho/cm^2. The peak conductances in our calculated action potentials ranged from 31 to 53 m.mho/cm^2 according to the conditions, as shown in Table 4.

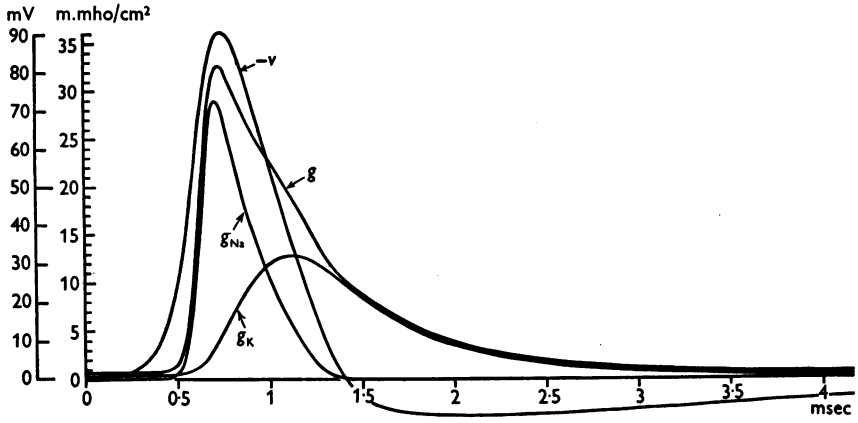

Fig. 17. Numerical solution of eqn. (31) showing components of membrane conductance (g) during propagated action potential ($-V$). Details of the analysis are as in Fig. 15.

Components of conductance change. The manner in which the conductances to Na^+ and K^+ contribute to the change in total conductance is shown in Fig. 17 for the calculated propagated action potential. The rapid rise is due almost entirely to sodium conductance, but after the peak the potassium conductance takes a progressively larger share until, by the beginning of the positive phase, the sodium conductance has become negligible. The tail of raised conductance that falls away gradually during the positive phase is due solely to potassium conductance, the small constant leak conductance being of course present throughout.

Ionic movements

Time course of ionic currents. The time course of the components of membrane current carried by sodium and potassium ions during the calculated propagated spike is shown in Fig. 18 *C*. The total ionic current contains also a small contribution from 'leak current' which is not plotted separately.

Two courses are open to current which is carried into the axis cylinder by ions crossing the membrane: it may leave the axis cylinder again by altering

the charge on the membrane capacity, or it may turn either way along the axis cylinder making a net contribution, I, to the local circuit current. The magnitudes of these two terms during steady propagation are $-C_M\,\mathrm{d}V/\mathrm{d}t$ and $(C_M/K)\,\mathrm{d}^2V/\mathrm{d}t^2$ respectively, and the manner in which the ionic current is divided between them at the different stages of the spike is shown in Fig. 18*B*. It will be seen that the ionic current is very small until the potential is well beyond the threshold level, which is shown by Fig. 12*A* to be about 6 mV.

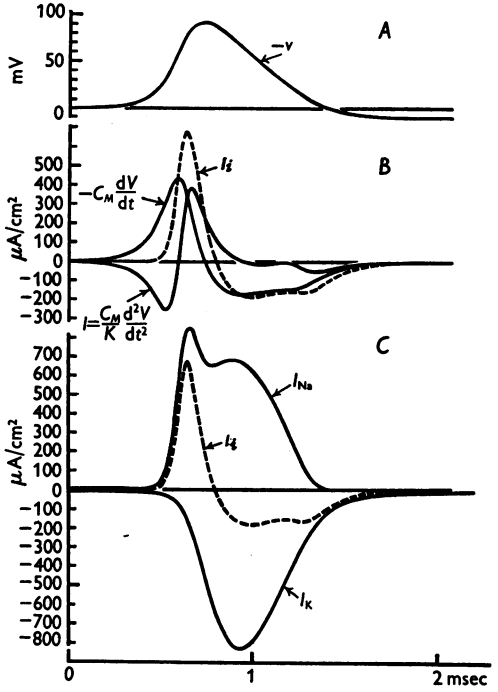

Fig. 18. Numerical solution of eqn. (31) showing components of membrane current during propagated action potential. *A*, membrane potential $(-V)$. *B*, ionic current (I_i), capacity current $\left(-C_M\frac{\mathrm{d}V}{\mathrm{d}t}\right)$ and total membrane current $\left(I=\frac{C_M}{K}\frac{\mathrm{d}^2V}{\mathrm{d}t^2}\right)$. *C*, ionic current (I_i), sodium current (I_{Na}) and potassium current (I_K). The time scale applies to all the curves. Details of the analysis are as in Fig. 15.

During this period the current for charging the membrane capacity comes almost entirely from local circuits. The fact that the ionic current does not become appreciable as soon as the threshold depolarization is passed is due partly to the smallness of the currents reached in any circumstances near the threshold, and partly to the delay with which sodium conductance rises when the potential is lowered.

Total movements of ions. The total entry of sodium and loss of potassium can be obtained by integrating the corresponding ionic currents over the whole

impulse. This has been done for the four complete action potentials that we calculated, and the results are given in Table 5. It will be seen that the results at 18·5° C are in good agreement with the values found experimentally by Keynes (1951) and Keynes & Lewis (1951), which were obtained at comparable temperatures.

Ionic fluxes. The flux in either direction of an ion can be obtained from the net current and the equilibrium potential for that ion, if the independence principle (Hodgkin & Huxley, 1952*a*) is assumed to hold. Thus the outward flux of sodium ions is $I_{Na}/(\exp(V-V_{Na})F/RT-1)$, and the inward flux of potassium ions is $-I_K/(\exp(V_K-V)F/RT-1)$. These two quantities were evaluated at each step of the calculated action potentials, and integrated over the whole impulse. The integrated flux in the opposite direction is given in each case by adding the total net movement. The results are given in Table 5, where they can be compared with the results obtained with radioactive tracers by Keynes (1951) on *Sepia* axons. It will be seen that our theory predicts too little exchange of Na and too much exchange of K during an impulse. This discrepancy will be discussed later.

Refractory period

Time course of inactivation and delayed rectification. According to our theory, there are two changes resulting from the depolarization during a spike which make the membrane unable to respond to another stimulus until a certain time has elapsed. These are 'inactivation', which reduces the level to which

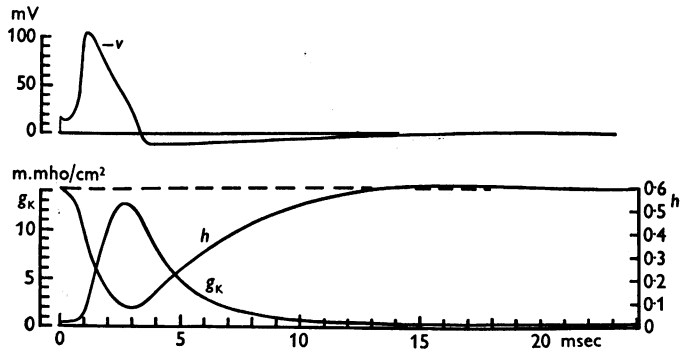

Fig. 19. Numerical solution of eqn. (26) for initial depolarization of 15 mV and temperature of 6° C. Upper curve: membrane potential, as in Fig. 13. Lower curves show time course of g_K and h during action potential and refractory period.

the sodium conductance can be raised by a depolarization, and the delayed rise in potassium conductance, which tends to hold the membrane potential near to the equilibrium value for potassium ions. These two effects are shown in Fig. 19 for the calculated membrane action potential at 6° C. Both curves reach their normal levels again near the end of the positive phase, and finally

TABLE 5. Ionic movements during an impulse. All values are expressed in $\mu\mu$mole/cm^2 and represent the excess over the corresponding movement in the resting state. In the theoretical cases the integration is taken as far as the 3rd intersection with the base line after the spike; it is begun in case (1) when $V = 0{\cdot}1$ mV; (2) and (3) at the stimulus; (4) when $V = 0$ before the spike. Experimental data from Keynes (1951) for row 6 and from Keynes & Lewis (1951) for rows 5 and 7.

	Type of action potential	Temp. (° C)	Stimulus (mV)	Sodium			Potassium		
				Influx	Outflux	Net entry	Influx	Outflux	Net loss
Theoretical (*Loligo*):									
1	Propagated	18·5	—	5·42	1·09	4·33	1·72	5·98	4·26
2	Membrane	18·5	15	5·01	1·02	3·99	1·71	5·78	4·07
3	Membrane	6·3	15	19·30	4·84	14·46	6·17	20·49	14·32
4	Membrane	6·3	Anode break	26·61	9·45	17·16	6·64	23·41	16·77
Experimental:									
5	Propagated (*Loligo*)	22	—	—	—	3·5	—	—	3·0
6	Propagated (*Sepia*)	14	—	10·3	6·6	3·7	0·39	4·7	4·3
7	Propagated (*Sepia*)	22	—	—	—	3·8	—	—	3·6

settle down after a heavily damped oscillation of small amplitude which is not seen in the figure.

Responses to stimuli during positive phase. We calculated the responses of the membrane when it was suddenly depolarized by 90 mV at various times during the positive phase of the membrane action potential at 6° C. These are shown by the upper curves in Fig. 20. After the earliest stimulus the

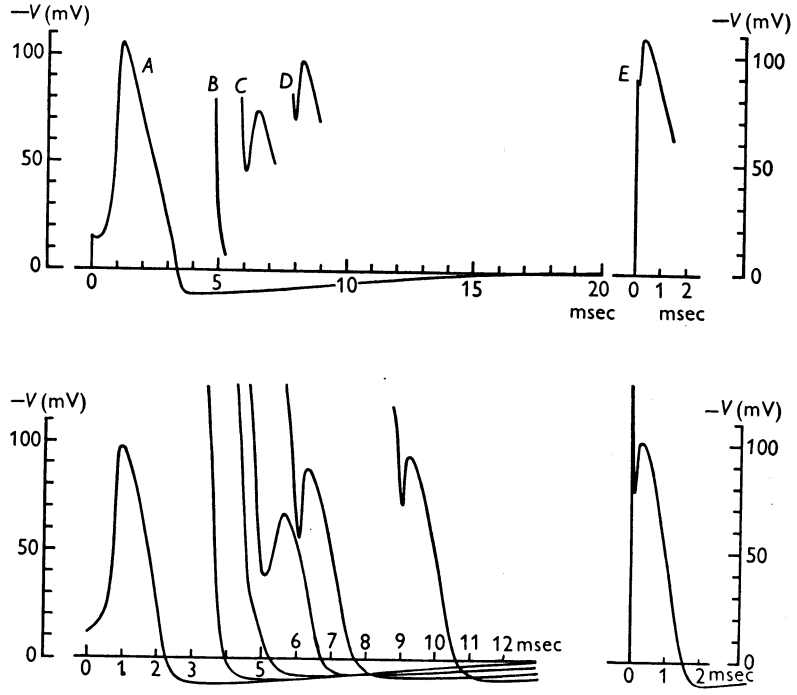

Fig. 20. Theoretical basis of refractory period. Upper curves: numerical solutions of eqn. (26) for temperature of 6° C. Curve *A* gives the response to 15 mμcoulomb/cm^2 applied instantaneously at $t=0$. Curve *E* gives the response to 90 mμcoulomb/cm^2 again applied in the resting state. Curves *B* to *D* show effect of applying 90 mμcoulomb/cm^2 at various times after curve *A*. Lower curves: a similar experiment with an actual nerve, temperature 9° C. The voltage scales are the same throughout. The time scales differ by a factor appropriate to the temperature difference.

membrane potential falls again with hardly a sign of activity, and the membrane can be said to be in the 'absolute refractory period'. The later stimuli produce action potentials of increasing amplitude, but still smaller than the control; these are in the 'relative refractory period'. Corresponding experimental curves are shown in the lower part of Fig. 20. The agreement is good, as regards both the duration of the absolute refractory period and the changes in shape of the spike as recovery progresses.

Excitation

Our calculations of excitation processes were all made for the case where the membrane potential is uniform over the whole area considered, and not for the case of local stimulation of a whole nerve. There were two reasons for this: first, that such data from the squid giant fibre as we had for comparison were obtained by uniform stimulation of the membrane with the long electrode; and, secondly, that calculations for the whole nerve case would have been extremely laborious since the main equation is then a partial differential equation.

Threshold. The curves in Figs. 12 and 21 show that the theoretical 'membrane' has a definite threshold when stimulated by a sudden displacement of membrane potential. Since the initial fall after the stimulus is much less marked in these than in the experimental curves, it is relevant to compare the lowest point reached in a just threshold curve, rather than the magnitude of the original displacement. In the calculated series this is about 6 mV and in the experimental about 8 mV. This agreement is satisfactory, especially as the value for the calculated series must depend critically on such things as the leak conductance, whose value was not very well determined experimentally.

The agreement might have been somewhat less good if the comparison had been made at a higher temperature. The calculated value would have been much the same, but the experimental value in the series at 23° C shown in Fig. 8 of Hodgkin *et al.* (1952) is about 15 mV. However, this fibre had been stored for 5 hr before use and was therefore not in exactly the same state as those on which our measurements were based.

Subthreshold responses. When the displacement of membrane potential was less than the threshold for setting up a spike, characteristic subthreshold responses were seen. One such response is shown in Fig. 12, while several are plotted on a larger scale in Fig. 21*B*. Fig. 21*A* shows for comparison the corresponding calculated responses of our model. The only appreciable differences, in the size of the initial fall and in the threshold level, have been mentioned already in other connexions.

During the positive phase which follows each calculated subthreshold response, the potassium conductance is raised and there is a higher degree of 'inactivation' than in the resting state. The threshold must therefore be raised in the same way as it is during the relative refractory period following a spike. This agrees with the experimental findings of Pumphrey, Schmitt & Young (1940).

Anode break excitation. Our axons with the long electrode in place often gave anode break responses at the end of a period during which current was made to flow inward through the membrane. The corresponding response of out theoretical model was calculated for the case in which a current sufficient

to bring the membrane potential to 30 mV above the resting potential was suddenly stopped after passing for a time long compared with all the time-constants of the membrane. To do this, eqn. (26) was solved with $I=0$ and the initial conditions that $V=+30$ mV, and m, n and h have their steady state values for $V=+30$ mV, when $t=0$. The calculation was made for a temperature

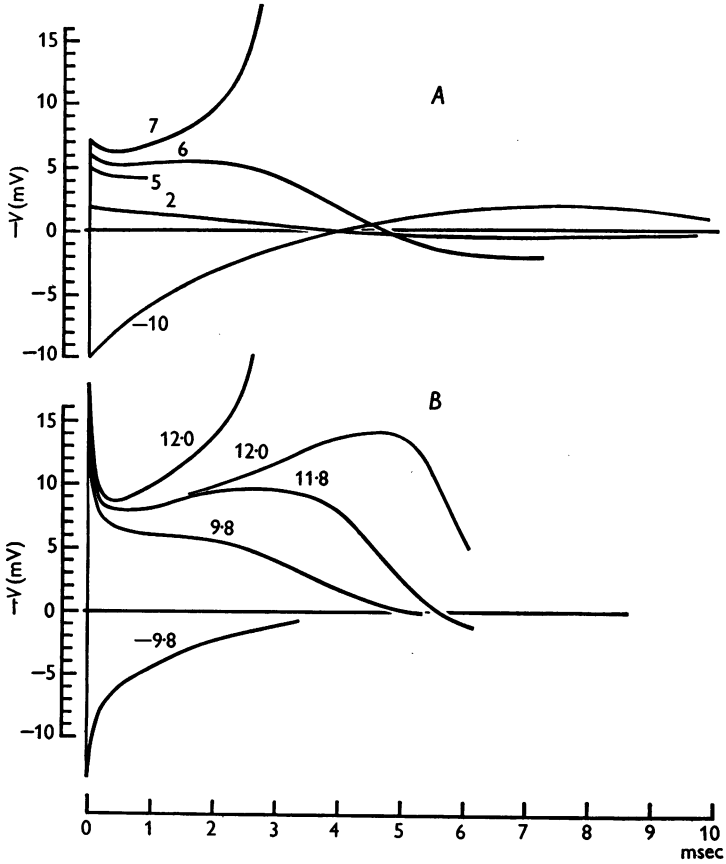

Fig. 21. *A*, numerical solutions of eqn. (26) for 6° C. The numbers attached to the curves give the initial depolarization in mV (also the quantity of charge applied in mμcoulomb/cm²). *B*, response of nerve membrane at 6° C to short shocks; the numbers show the charge applied in mμcoulomb/cm². The curves have been replotted from records taken at low amplification and a relatively high time-base speed.

of 6·3° C. A spike resulted, and the time course of membrane potential is plotted in Fig. 22*A*. A tracing of an experimental anode break response is shown in Fig. 22*B*; the temperature is 18·5° C, no record near 6° being available. It will be seen that there is good general agreement. (The oscillations after the positive phase in Fig. 22*B* are exceptionally large; the response of

this axon to a small constant current was also unusually oscillatory as shown in Fig. 23.)

The basis of the anode break excitation is that anodal polarization decreases the potassium conductance and removes inactivation. These effects persist for an appreciable time so that the membrane potential reaches its resting value with a reduced outward potassium current and an increased inward sodium current. The total ionic current is therefore inward at $V=0$ and the membrane undergoes a depolarization which rapidly becomes regenerative.

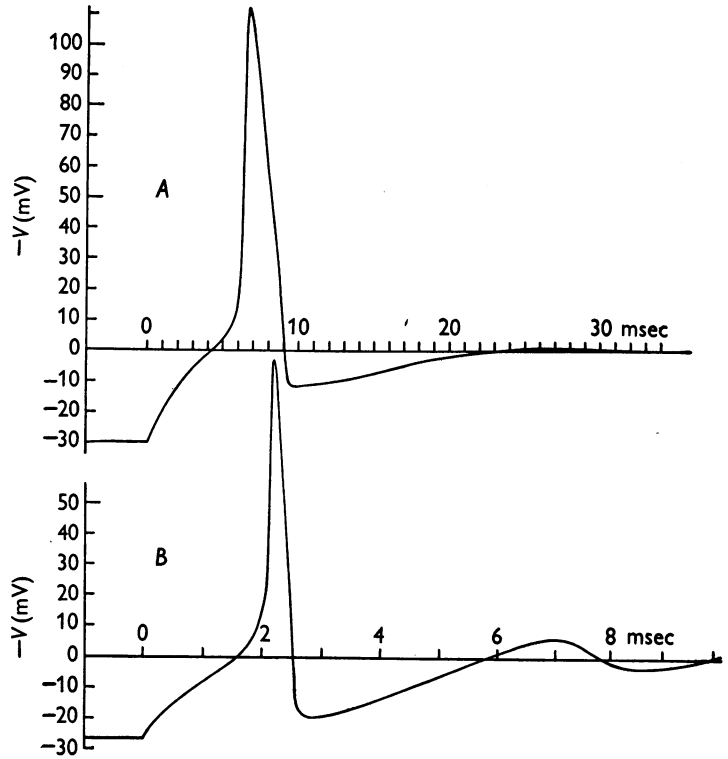

Fig. 22. Theoretical basis of anode break excitation. *A*, numerical solution of eqn. (26) for boundary condition $-V=-30$ mV for $t<0$; temperature 6° C. *B*, anode break excitation following sudden cessation of external current which had raised the membrane potential by 26·5 mV; giant axon with long electrode at 18·5° C. Time scales differ by a factor appropriate to the temperature difference.

Accommodation. No measurements of accommodation were made nor did we make any corresponding calculations for our model. It is clear, however, that the model will show 'accommodation' in appropriate cases. This may be shown in two ways. First, during the passage of a constant cathodal current through the membrane, the potassium conductance and the degree of inactivation will rise, both factors raising the threshold. Secondly, the steady state

ionic current at all strengths of depolarization is outward (Fig. 11), so that an applied cathodal current which rises sufficiently slowly will never evoke a regenerative response from the membrane, and excitation will not occur.

Oscillations

In all the calculated action potentials and subthreshold responses the membrane potential finally returns to its resting value with a heavily damped oscillation. This is well seen after subthreshold stimuli in Figs. 21 *A* and 24, but the action potentials are not plotted on a slow enough time base or with a large enough vertical scale to show the oscillations which follow the positive phase.

The corresponding oscillatory behaviour of the real nerve could be seen after a spike or a subthreshold short shock, but was best studied by passing a small constant current through the membrane and recording the changes of membrane potential that resulted. The current was supplied by the long internal electrode so that the whole area of membrane was subjected to a uniform current density. It was found that when the current was very weak the potential changes resulting from inward current (anodal) were almost exactly similar to those resulting from an equal outward current, but with opposite sign. This is shown in Fig. 23 *B* and *C*, where the potential changes are about ± 1 mV. This symmetry with weak currents is to be expected from our equations, since they can be reduced to a linear form when the displacements of all the variables from their resting values are small. Thus, neglecting products, squares and higher powers of δV, δm, δn and δh, the deviations of V, m, n and h from their resting values (0, m_0, n_0 and h_0 respectively), eqn. (26) (p. 518) becomes

$$\delta I = C_M \frac{\mathrm{d}\delta V}{\mathrm{d}t} + \bar{g}_K n_0^4 \delta V - 4\bar{g}_K n_0^3 V_K \delta n + \bar{g}_{Na} m_0^3 h_0 \delta V - 3\bar{g}_{Na} m_0^2 h_0 V_{Na} \delta m - \bar{g}_{Na} m_0^3 V_{Na} \delta h + \bar{g}_l \delta V. \quad (35)$$

Similarly, eqn. (7) (p. 518) becomes

$$\frac{\mathrm{d}\delta n}{\mathrm{d}t} = \frac{\partial \alpha_n}{\partial V}\delta V - (\alpha_n + \beta_n)\,\delta n - n_0 \frac{\partial(\alpha_n + \beta_n)}{\partial V}\delta V,$$

or

$$(p + \alpha_n + \beta_n)\,\delta n = \left\{\frac{\partial \alpha_n}{\partial V} - n_0 \frac{\partial(\alpha_n + \beta_n)}{\partial V}\right\}\delta V, \quad (36)$$

where p represents $\mathrm{d}/\mathrm{d}t$, the operation of differentiating with respect to time.

The quantity δn can be eliminated between eqns. (35) and (36). This process is repeated for δm and δh, yielding a fourth-order linear differential equation with constant coefficients for δV. This can be solved by standard methods for any particular time course of the applied current density δI.

Fig. 23*A* shows the response of the membrane to a constant current pulse calculated in this way. The constants in the equations are chosen to be appropriate to a temperature of 18·5° C so as to make the result comparable with the tracings of experimental records shown in *B* and *C*. It will be seen that the calculated curve agrees well with the records in *B*, while those in *C*, obtained from another axon, are much less heavily damped and show a higher

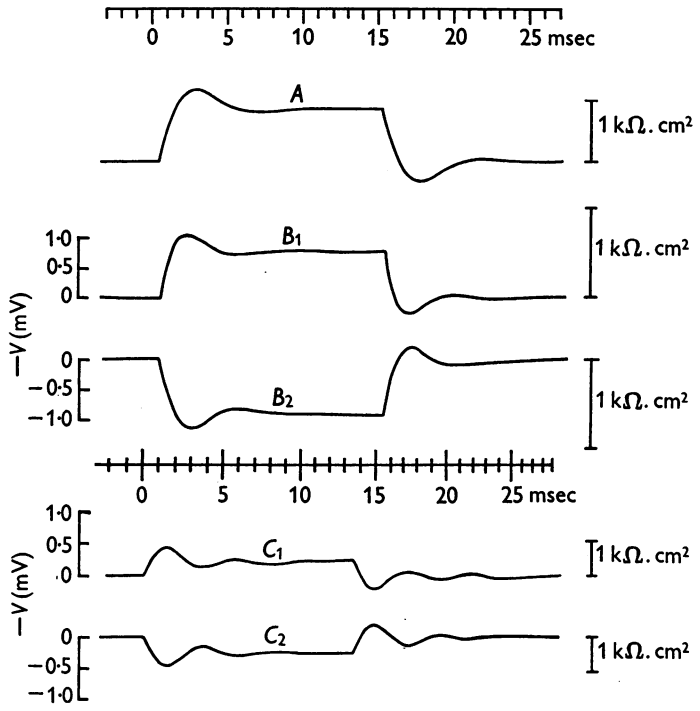

Fig. 23. *A*, solution of eqn. (35) for small constant current pulse; temperature 18·5° C; linear approximation. The curve shows $\delta V/\delta I$ (plotted upwards) as a function of time. *B*, changes in membrane potential associated with application of weak constant currents of duration 15 msec and strength $\pm 1{\cdot}49\,\mu$A/cm². B_1, cathodic current; B_2, anodic current. Depolarization is shown upward. Temperature 19° C. *C*, similar records from another fibre enlarged to have same time scale. Current strengths are $\pm 0{\cdot}55\,\mu$A/cm². Temperature 18° C. The response is unusually oscillatory.

frequency of oscillation. A fair degree of variability is to be expected in these respects since both frequency and damping depend on the values of the components of the resting conductance. Of these, g_{Na} and g_K depend critically on the resting potential, while $\bar{g}_l$ is very variable from one fibre to another.

Both theory and experiment indicate a greater degree of oscillatory behaviour than is usually seen in a cephalopod nerve in a medium of normal ionic composition. We believe that this is largely a direct result of using the long internal

electrode. If current is applied to a whole nerve through a point electrode, neighbouring points on the membrane will have different membrane potentials and the resulting currents in the axis cylinder will increase the damping.

The linear solution for the behaviour of the theoretical membrane at small displacements provided a convenient check on our step-by-step numerical procedure. The response of the membrane at 6·3° C to a small short shock was calculated by this means and compared with the step-by-step solution for an initial depolarization of the membrane by 2 mV. The results are plotted in Fig. 24. The agreement is very close, the step-by-step solution deviating in the direction that would be expected to result from its finite amplitude (cf. Fig. 21).

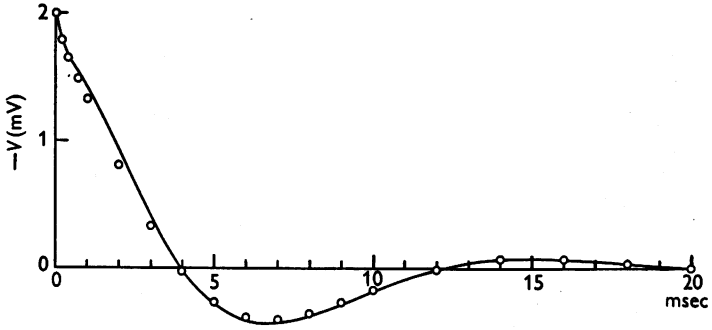

Fig. 24. Comparison of step-by-step solution and linear approximation. Eqn. (26), temperature 6° C; initial displacement of $-V=2$ mV. Continuous line: step-by-step solution. Circles: linear approximation with same initial displacement.

As pointed out by Cole (1941), the process underlying oscillations in membrane potential must be closely connected with the inductive reactance observed with alternating currents. In our theoretical model the inductance is due partly to the inactivation process and partly to the change in potassium conductance, the latter being somewhat more important. For small displacements of the resting potential the variations in potassium current in 1 cm^2 of membrane are identical with those in a circuit containing a resistance of 820 Ω in series with an inductance which is shunted by a resistance of 1900 Ω. The value of the inductance is 0·39 H at 25° C, which is of the same order as the 0·2 H found by Cole & Baker (1941). The calculated inductance increases 3-fold for a 10° C fall in temperature and decreases rapidly as the membrane potential is increased; it disappears at the potassium potential and is replaced by a capacity for $E > E_K$.

DISCUSSION

The results presented here show that the equations derived in Part II of this paper predict with fair accuracy many of the electrical properties of the squid giant axon: the form, duration and amplitude of spike, both 'membrane'

and propagated; the conduction velocity; the impedance changes during the spike; the refractory period; ionic exchanges; subthreshold responses; and oscillations. In addition, they account at least qualitatively for many of the phenomena of excitation, including anode break excitation and accommodation. This is a satisfactory degree of agreement, since the equations and constants were derived entirely from 'voltage clamp' records, without any adjustment to make them fit the phenomena to which they were subsequently applied. Indeed any such adjustment would be extremely difficult, because in most cases it is impossible to tell in advance what effect a given change in one of the equations will have on the final solution.

The agreement must not be taken as evidence that our equations are anything more than an empirical description of the time-course of the changes in permeability to sodium and potassium. An equally satisfactory description of the voltage clamp data could no doubt have been achieved with equations of very different form, which would probably have been equally successful in predicting the electrical behaviour of the membrane. It was pointed out in Part II of this paper that certain features of our equations were capable of a physical interpretation, but the success of the equations is no evidence in favour of the mechanism of permeability change that we tentatively had in mind when formulating them.

The point that we do consider to be established is that fairly simple permeability changes in response to alterations in membrane potential, of the kind deduced from the voltage clamp results, are a sufficient explanation of the wide range of phenomena that have been fitted by solutions of the equations.

Range of applicability of the equations

The range of phenomena to which our equations are relevant is limited in two respects: in the first place, they cover only the short-term responses of the membrane, and in the second, they apply in their present form only to the isolated squid giant axon.

Slow changes. A nerve fibre whose membrane was described by our equations would run down gradually, since even in the resting state potassium leaves and sodium enters the axis cylinder, and both processes are accelerated by activity. This is no defect in describing the isolated squid giant axon, which does in fact run down in this way, but some additional process must take place in a nerve in the living animal to maintain the ionic gradients which are the immediate source of the energy used in impulse conduction.

After-potentials. Our equations give no account of after-potentials, apart from the positive phase and subsequent oscillations.

Conditions of isolated giant axon. There are many reasons for supposing that the resting potential of the squid giant axon is considerably lower after isolation than when it is intact in the living animal. Further evidence for this view

is provided by the observation (Hodgkin & Huxley, 1952*c*) that the maximum inward current that the membrane can pass on depolarization is increased by previously raising the resting potential by 10–20 mV by means of anodally directed current. Our equations could easily be modified to increase the resting potential (e.g. by reducing the leak conductance and adding a small outward current representing metabolic extrusion of sodium ions). We have not made any calculations for such a case, but certain qualitative results are evident from inspection of other solutions. If, for instance, the resting potential were raised (by 12 mV) to the potassium potential, the positive phase and subsequent oscillations after the spike would disappear, the rate of rise of the spike would be increased, the exchange of internal and external sodium in a spike would be increased, the membrane would not be oscillatory unless depolarized, and accommodation and the tendency to give anode break responses would be greatly reduced. Several of these phenomena have been observed when the resting potential of frog nerve is raised (Lòrente de Nó, 1947), but no corresponding information exists about the squid giant axon.

Applicability to other tissues. The similarity of the effects of changing the concentrations of sodium and potassium on the resting and action potentials of many excitable tissues (Hodgkin, 1951) suggests that the basic mechanism of conduction may be the same as implied by our equations, but the great differences in the shape of action potentials show that even if equations of the same form as ours are applicable in other cases, some at least of the parameters must have very different values.

Differences between calculated and observed behaviour

In the Results section, a number of points were noted on which the calculated behaviour of our model did not agree with the experimental results. We shall now discuss the extent to which these discrepancies can be attributed to known shortcomings in our equations. Two such shortcomings were pointed out in Part II of this paper, and were accepted for the sake of keeping the equations simple. One was that the membrane capacity was assumed to behave as a 'perfect' condenser (phase angle 90°; p. 505), and the other was that the equations governing the potassium conductance do not give as much delay in the conductance rise on depolarization (e.g. to the sodium potential) as was observed in voltage clamps (p. 509).

The assumption of a perfect capacity probably accounts for the fact that the initial fall in potential after application of a short shock is much less marked in the calculated than in the experimental curves (Figs. 12 and 21). Some of the initial drop in the experimental curves may also be due to end-effects, the guard system being designed for the voltage clamp procedure but not for stimulation by short shocks.

The inadequacy of the delay in the rise of potassium conductance has several effects. In the first place the falling phase of the spike develops too early, reducing the spike amplitude slightly and making the peak too pointed in shape (p. 525). In the membrane action potentials these effects become more marked the smaller the stimulus, since the potassium conductance begins to rise during the latent period. This causes the spike amplitude to decrease more in the calculated than in the experimental curves (Fig. 12).

The low calculated value for the exchange of internal and external sodium ions is probably due to this cause. Most of the sodium exchange occurs near the peak of the spike, when the potential is close to the sodium potential. The early rise of potassium conductance prevents the potential from getting as close to the sodium potential, and from staying there for as long a time, as it should.

A check on these points is provided by the 'anode break' action potential. Until the break of the applied current, the quantity n has the steady state value appropriate to $V = +30$ mV, i.e. it is much smaller than in the usual resting condition. This greatly increases the delay in the rise of potassium conductance when the membrane is depolarized. It was found that the spike height was greater (Table 4), the peak was more rounded, and the exchange of internal and external sodium was greater (Table 5), than in an action potential which followed a cathodal short shock.

The other important respect in which the model results disagreed with the experimental was that the calculated exchange of internal and external potassium ions per impulse was too large. This exchange took place largely during the positive phase, when the potential is close to the potassium potential and the potassium conductance is still fairly high. We have no satisfactory explanation for this discrepancy, but it is probably connected with the fact that the value of the potassium potential was less strongly affected by changes in external potassium concentration than is required by the Nernst equation.

SUMMARY

1. The voltage clamp data obtained previously are used to find equations which describe the changes in sodium and potassium conductance associated with an alteration of membrane potential. The parameters in these equations were determined by fitting solutions to the experimental curves relating sodium or potassium conductance to time at various membrane potentials.

2. The equations, given on pp. 518–19, were used to predict the quantitative behaviour of a model nerve under a variety of conditions which corresponded to those in actual experiments. Good agreement was obtained in the following cases:

(*a*) The form, amplitude and threshold of an action potential under zero membrane current at two temperatures.

(*b*) The form, amplitude and velocity of a propagated action potential.

(*c*) The form and amplitude of the impedance changes associated with an action potential.

(*d*) The total inward movement of sodium ions and the total outward movement of potassium ions associated with an impulse.

(*e*) The threshold and response during the refractory period.

(*f*) The existence and form of subthreshold responses.

(*g*) The existence and form of an anode break response.

(*h*) The properties of the subthreshold oscillations seen in cephalopod axons.

3. The theory also predicts that a direct current will not excite if it rises sufficiently slowly.

4. Of the minor defects the only one for which there is no fairly simple explanation is that the calculated exchange of potassium ions is higher than that found in *Sepia* axons.

5. It is concluded that the responses of an isolated giant axon of *Loligo* to electrical stimuli are due to reversible alterations in sodium and potassium permeability arising from changes in membrane potential.

REFERENCES

COLE, K. S. (1941). Rectification and inductance in the squid giant axon. *J. gen. Physiol.* **25**, 29–51.

COLE, K. S. & BAKER, R. F. (1941). Longitudinal impedance of the squid giant axon. *J. gen. Physiol.* **24**, 771–788.

COLE, K. S. & CURTIS, H. J. (1939). Electric impedance of the squid giant axon during activity. *J. gen. Physiol.* **22**, 649–670.

GOLDMAN, D. E. (1943). Potential, impedance, and rectification in membranes. *J. gen. Physiol.* **27**, 37–60.

HARTREE, D. R. (1932–3). A practical method for the numerical solution of differential equations. *Mem. Manchr lit. phil. Soc.* **77**, 91–107.

HODGKIN, A. L. (1951). The ionic basis of electrical activity in nerve and muscle. *Biol. Rev.* **26**, 339–409.

HODGKIN, A. L. & HUXLEY, A. F. (1952*a*). Currents carried by sodium and potassium ions through the membrane of the giant axon of *Loligo*. *J. Physiol.* **116**, 449–472.

HODGKIN, A. L. & HUXLEY, A. F. (1952*b*). The components of membrane conductance in the giant axon of *Loligo*. *J. Physiol.* **116**, 473–496.

HODGKIN, A. L. & HUXLEY, A. F. (1952*c*). The dual effect of membrane potential on sodium conductance in the giant axon of *Loligo*. *J. Physiol.* **116**, 497–506.

HODGKIN, A. L., HUXLEY, A. F. & KATZ, B. (1949). Ionic currents underlying activity in the giant axon of the squid. *Arch. Sci. physiol.* **3**, 129–150.

HODGKIN, A. L., HUXLEY, A. F. & KATZ, B. (1952). Measurement of current-voltage relations in the membrane of the giant axon of *Loligo*. *J. Physiol.* **116**, 424–448.

HODGKIN, A. L. & KATZ, B. (1949). The effect of temperature on the electrical activity of the giant axon of the squid. *J. Physiol.* **109**, 240–249.

KEYNES, R. D. (1951). The ionic movements during nervous activity. *J. Physiol.* **114**, 119–150.

KEYNES, R. D. & LEWIS, P. R. (1951). The sodium and potassium content of cephalopod nerve fibres. *J. Physiol.* **114**, 151–182.

LORENTE DE NÓ, R. (1947). A study of nerve physiology. *Stud. Rockefeller Inst. med. Res.* **131**, **132**.

PUMPHREY, R. J., SCHMITT, O. H. & YOUNG, J. Z. (1940). Correlation of local excitability with local physiological response in the giant axon of the squid (*Loligo*). *J. Physiol.* **98**, 47–72.